



# Discovery of Selective Ligands for the Modulation of NMDA Receptors

Klara Peltomaa

Master thesis in Organic Chemistry, 45hp, 2024
Department of Chemistry, Lund University

Supervisor: Professor Rasmus P. Clausen & Postdoc Yasaman Doroudian, Department of Drug Design and Pharmacology, University of Copenhagen.

Examiner: Professor Ulf J. Nilsson, Department of Chemistry, Lund University.

Date: 24 January 2024

# Popular science summary

How can a drug enter the body and magically fulfill its intended purpose? To be able to understand this, one must understand what the drug is targeting in the body. The target in this thesis is a specific receptor. Receptors can be located in the brain and can be associated as a communicator. They receive information and distribute it to the rest of the body. However, the question of how remains.

Think of it in three steps. Firstly, the drug must be able to reach the intended receptor. Secondly, the drug needs to do this without being decomposed on the way and lastly, it needs to fit inside the binding pocket of the receptor and activate or deactivate it. All these steps are used in theory, when synthesizing a potential drug. These different pieces are all needed to finish the puzzle. If one piece is missing, the puzzle can’t be completed.

The first puzzle piece can be described as going out to find chanterelles in the forest. It is raining and it is dark, therefore one needs an umbrella and a flashlight to be able to go outside in the first place. After reaching the forest, one walks and walks not knowing exactly where to go but eventually, after covering enough ground, a trail of chanterelles leads you to the right spot. The same is for the drug. It enters the body and is designed in a way for it to be able to reach its intended receptor. It then makes its way around the bloodstream until it finally finds that one receptor that it fits into.

The second puzzle piece can be described as a game of hide and seek. If one does not try to run away and hide when the person is counting, one will be easily found. If one tries to hide behind a small tree, it will take longer to be found but still not long enough to be the winner. Instead, if one disguises oneself with military clothing and hides in a bush one will be hard to find. The drug's journey within the body is similar. During its course of finding its intended receptor, there are obstacles on the way trying to degrade this foreign object in the body and get rid of it. However, the drug can be modified in such a way that it takes longer for it to be degraded and even be disguised to be in the body long enough to find its intended target.

The last puzzle piece can be described as turning on a flashlight. To turn the flashlight on it needs to have a specific battery inserted. The battery needs to be of the right size and needs to be put in the right direction for the circuit to be complete and turn the light on. It is the same for the drug. It needs to be of the right size and to fit in a specific direction to be able to either activate or deactivate the receptor depending on its intent.

Building this puzzle is a difficult task because the puzzle does not come with instructions, and it does not come in a box with designated pieces. These pieces need to be handmade, and the instructions need to be written along the way. However, with one piece at a time, it is making its way to completion. In this thesis, 12 new compounds have successfully been made with the purpose to gain further understanding of how the molecule-protein interactions work in this specific receptor system.

# Abstract

**Keywords: NMDA receptors, potential drugs.**

NMDA receptors are part of the family iGluRs that regulate the flow of positive ions, such as $Na^+$, $K^+$ and $Ca^{2+}$, by ligand gating. Upon activation with Glutamate, the channel opens, and a flowthrough of ions occurs. NMDA receptors are unique in that they require the co-agonist glycine for activation and that they exhibit voltage-dependent ion flow due to $Mg^{2+}$ blockade. The NMDA receptors have three subtypes, GluN1, GluN2 and GluN3 which in turn have subunits of their own. The NMDA receptors are constructed with two GluN1 subunits together with two GluN2 and/or GluN3 subunits. The GluN1/2 receptors are more important from a physiological perspective; thus, these receptors are the focus of this thesis, specifically GluN1/2A and GluN1/2B.

The NMDA receptors are known for their role in excitotoxicity, which make them important targets for potential drugs against e.g. Parkinson's disease and Huntignson's disease. It has been proven difficult in making potent drugs for the NMDA receptors due to the high risk of side effects. The reason for this is that the different subtypes of the NMDA receptors are similar in structure but also that they are widely spread across the brain, thus targeting only one receptor is challenging.

TCN213 is a scaffold that is selective for the GluN1/2A receptor with sufficient potency, binding at the interface, and able to cross the blood brain barrier. However, research on improving its potency and metabolism is ongoing. Different amide bioisostere analogues of the TCN213 scaffold have been synthesized to explore the amide part of this scaffold and study its importance in TCN213s activity. Important information of non-conserved amino acids between the subtypes GluN1/2A and GluN1/2B, specifically a switch from valine 267 to phenylalanine 262 respectively, have highlighted the theory behind the synthesis of the GluN1/2B analogues. Different synthetic approaches have been used to synthesize potential NAMs for the GluN1/2A and GluN1/2B receptors. However, their activity is yet to be determined.

# Acknowledgement

I would like to thank Professor Rasmus P. Clausen for letting me do my master thesis project in his research group, and to Yasaman Doroudian for helping me along the way. I would also like to thank Professor Ulf J. Nilsson for participating throughout the thesis and answering any questions one might have. Lastly, I would also like to acknowledge the members of lab 304 and the members of Rasmus P. Clausen's research group for the support I got through my practical work in the lab.

# Table of contents

# List of abbreviations

ABD - Agonist Binding Domain

AMPA - α-amino-3-hydroxy-5-methyl-4-isoxazole-propionate

Ana. HPLC - Analytical High Performance Liquid Chromatography

Aq. - Aqueous

ATD - Amino-Terminal Domain

CNS - Central Nervous System

CTD - Carboxy Terminal Domain

CuAAC - Copper catalyzed azide-alkyne cycloaddition

CV - Column volume

DAD - Diode Array Detector

DMAP - 4-Dimethylaminopyridine

EC50 - Effective concentration

EDG - Electron Donating Group

EPSC - Excitatory Postsynaptic Current

Eq. - Equivalent

ESI - Electron Spray Ionization

EWG - Electron Withdrawing Group

GluN - N-methyl-D-aspartate glutamate receptor

Hz - Hertz

iGluRs - Ionotropic Glutamate Receptors

LCMS - Liquid Chromatography Mass Spectrometry

NA - Not Applicable

NAM - Negative Allosteric Modulator

NMDA - N-methyl-D-aspartate

NMR - Nuclear magnetic resonance

O/N - Overnight

PAM - Positive Allosteric Modulator

Ppm - Parts per million

Prep. HPLC - Preoperative High Performance Liquid Chromatography

SAR - Structure-activity relationship

SN2 - Nucleophilic substitution reaction

TLC - Thin-layer chromatography

TMD - Transmembrane Domain

UPLCMS - Ultra Performance Liquid Chromatography Mass Spectrometry

UV-light - UltraViolet light

# Introduction

## General introduction

Ionotropic glutamate receptors (iGluRs) are ligand gated ion channels that regulate the flow of positively charged ions, such as $Na^+$, $K^+$ and occasionally $Ca^{2+}$, upon activation of glutamate. This amino acid is the major excitatory neurotransmitter in the human central nervous system (CNS). The positively charged ions raise the potential across the membrane in the postsynaptic cells upon activation of the receptor, initiating electric response in the postsynaptic neuron.[1] Apart from regulating synaptic transmission, iGluRs also play an important role in synapse formation, synaptic plasticity and in numeral neurological diseases, such as Parkinson, Alzheimer's and epilepsy.[1,2] There are several iGluR, whereas four of them are ligand-gated ion channels, N-methyl-D-aspartate (NMDA), α-amino-3-hydroxy-5-methyl-4-isoxazole-propionate (AMPA), kainate and δ receptors. What differs the NMDA receptors from the other three is that these ion channels allow $Ca^{2+}$ ions to pass through as well as the monovalent cations. Secondly, NMDA receptors need a co-agonist, glycine, together with glutamate to open the channel. Additionally, NMDA receptors exhibit voltage-dependent ion flow due to a $Mg^{2+}$ block. This means that if the channel is blocked by $Mg^{2+}$, no cations can flow through regardless of glutamate and glycine binding to the receptor.[3]

## Structure of NMDA receptors

The NMDA receptor family consists of three subunits, GluN1-3 encoded by different genes. All functional NMDA receptors contain two GluN1 subunits together with two subunits of either GluN2 and/or GluN3, see figure 1. These subunits are all similar in structure with conserved organization of domains.[4] These subunits in turn have subunits of their own. GluN1 has eight different subunits, GluN2 has four (A, B, C and D) and GluN3 has two (A and B).

As seen in figure 2, there is an extracellular amino-terminal domain (ATD). This domain plays an important part in the assembly of the different subunits, e.g. in GluN2A and GluN2B the ATD contains an additional site, specifically for allosteric modulators.[5] The ATD is then connected to an extracellular agonist binding domain (ABD) which is constructed of two folds, S1 and S2. In

a dimer where two ABDs are present, an S1 domain forms a rigid interface with the other S1 domain while the S2 domains stay apart and are mobile in comparison.[4] The ligand in the ABD differs between subunits, while GluN1 and GluN3 bind the co-agonist glycine, GluN2 binds glutamate.[5] The ABD is then, via linkers, connected to the transmembrane domain (TMD), which constructs the ion channel. The TMD contains three helices, M1, M3 and M4, together with a re-entrant loop, M2. The M2 loop and M3 are important for channel gating, in particular M3 due to it being a highly conserved region throughout glutamate-gated ion channels. Nevertheless, part of the M2 loop contains an important site that, in firsthand, determines the permeability of $Ca^{2+}$ of the channel.[4] This site is referred to as the QRN site, based on the amino acids in this region.[6] The sequence lining around the pore is highly conserved in GluN2 subunits. Thus, permeation properties together with the affinity for $Mg^{2+}$ as the pore blocker, do not differ immensely among GluN1/GluN2 receptor types.[5] The TMD domain then interacts with the intracellular carboxy terminal domain (CTD).[4] This domain varies in size depending on the subunit, which leads to multiple different sites of interactions with multiple intracellular proteins.[5]

The mode of gating is not fully understood, despite progress in transmembrane protein crystallography.[4] However, due to the presence of the M2 loop in the TMD domain, together with the tetrameric quaternary structure, hypotheses have been made that NMDA receptor pores are homologous to an inverted potassium channel.[5]

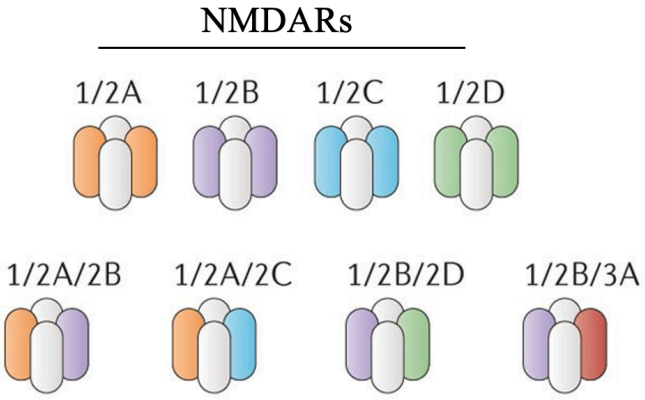


*Figure 1. Examples of di-heteromeric and tri-heteromeric NMDA receptors believed to be present in the CNS.*

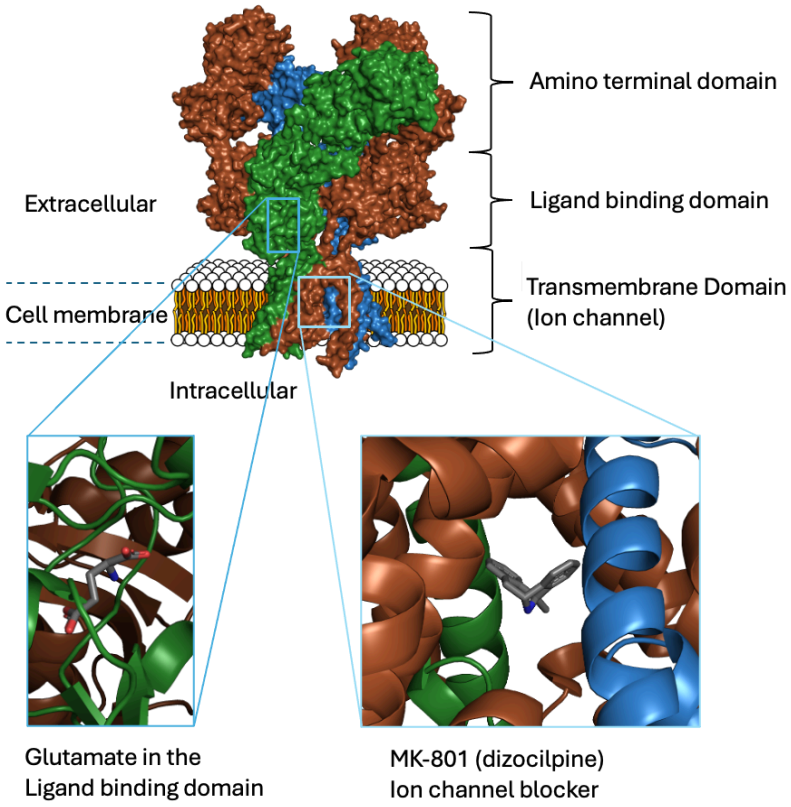


*Figure 2. Representation of the NMDA receptor crystal structure highlighting the different elements of the receptor.*

## Function of NMDA receptors

As described above, GluN1 and GluN3 subunits bind glycine while GluN2 binds glutamate. Therefore, GluN1/GluN2 tetrameric receptors need to bind two glycine molecules and two glutamate molecules for activation, while GluN1/GluN3 receptors only need to bind glycine molecules. Different GluN2 subunits have different potency for glutamate, single-channel conductance, $Ca^{2+}$ permeability, sensitivity for $Mg^{2+}$ etc. The GluN2 subunits thus have an influence on cell-surface expression, subcellular localization and recycling/degradation of NMDA receptor subtypes.[6] The NMDA receptors composed of GluN1/GluN2 subunits are therefore described to be more important from a physiological perspective, thus GluN1/GluN3 receptors will not be mentioned further.[4]

The quite constant concentration of extracellular glycine, together with the EC50 value of glycine as co-agonist for GluN1/GluN2 receptors, which is approximately 1µM, suggests that the

many of the binding sites are naturally occupied. Hence, the NMDA receptors are controlled by the synaptic release of glutamate.[4,6] When glutamate is released from the presynaptic synapse, it activates the NMDA receptors by binding to the binding site in the ABD of the GluN2 subunit.[4] The binding of glutamate, with already bound glycine, triggers conformational changes in the structure of the receptor. These effects are dependent on which GluN2 subunit that is present. The four GluN2 subunits, A-D, therefore establish diversity between the NMDA receptors and can give rise to different synaptic response times and variation of parameters that control synaptic strength and plasticity.[6] Out of the four subunits, GluN2A is the most abundant.[8] The conformational changes trigger the mobile S2 domain of the ABD to move, which in turn impacts the linker regions that are connected to the TMD.[4] All three transmembrane helices, M1, M3 and M4, including the reentrant loop, M2, take part in the process of opening the channel pore. The M3 helices block the pore by forming a cluster across the pore, seen in figure 3. The movement of the linker region changes the position of the M3 helices and opens the pore. Even though the channels opened, the extracellular $Mg^{2+}$ can still block the influx of cations. The $Mg^{2+}$ binds strongly to the NMDA receptor and is released when the membrane is depolarized. NMDA receptors activate at a slow rate compared to, e.g. AMPA receptors. Hence, the activation of AMPA receptors leads to a depolarization of the membrane and in turn a release of the $Mg^{2+}$ block, activating the NMDA receptors. Therefore, NMDA receptors are dependent on both membrane potential, voltage-gated, and the frequency of glutamate release, ligand-gated, to be activated.[6] The NMDA receptor is now activated, and the channel is open and can influx cations, such as $N^{+}$, $K^{+}$ and $Ca^{2+}$ shown in figure 4. The NMDA receptors show a 10-fold permeability of $Ca^{2+}$ compared to $Na^{+}$ which leads to a significant increase in the intracellular $Ca^{2+}$ concentration.[4] This increase in $Ca^{2+}$ concentration, signals the need for multiple changes in the postsynaptic neuron. These changes depend on how often and for how long the NMDA receptor is activated. These events can also be described as excitatory postsynaptic currents (EPSCs).[6]

As mentioned before, the mechanism of channel opening is not fully understood but the mechanism described is proposed due to the structural similarity to the potassium channel.[4]

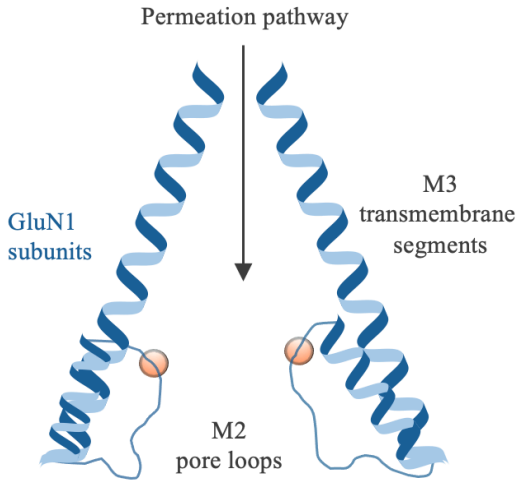


*Figure 3. Representation of the pore-lining of the NMDA receptors.*

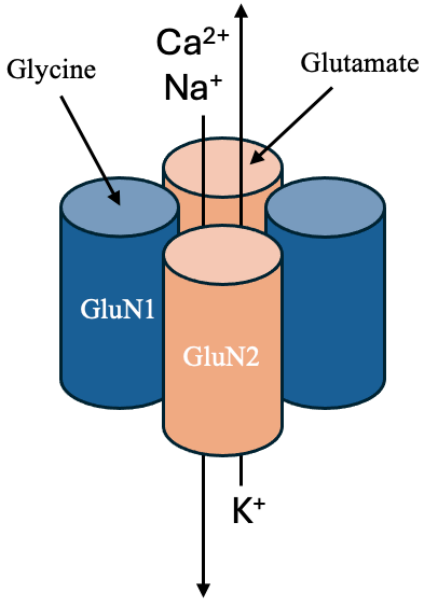


*Figure 4. Representation of the GluN1/2 receptor with shown function.*

## Research into NMDA receptors

IGluRs play an important role in regulating synaptic transmission, synapse formation, synaptic plasticity and in neurological diseases.[1,2] IGluRs are spread widely in the brain, both on pre- and postsynaptic sites to contribute to communication and signal processing of the neurons. These functions are vital in e.g. learning and memory formation. NMDA receptors, specifically, are the classic learning and memory receptors.[9] However, NMDA receptors are most known for their

role in excitotoxicity, which is a process where overactivation of NMDA receptors is caused by excessive glutamate release. This leads to a buildup of intracellular $Ca^{2+}$ which eventually leads to neuronal death. Cerebral ischemia and neurodegenerative disorders, such as Parkinson's and Huntington's disease, leads to excitotoxicity which is also observed in e.g. epilepsy. There has also been evidence that suggests that insufficient function of NMDA receptors is an essential aspect in major human cognitive disorders, especially schizophrenia. Dysfunctional NMDA receptors are involved in the pathogenesis of human psychoses, which indicates that cognitive disorders should be benefitted by increased activity of NMDA receptors.[5]

There is an abundance of neurological diseases, both acute and chronic, that are associated with dysfunctional glutamate release/uptake, specifically. The extracellular glutamate concentration reaches a peak when it is synaptically released and is then rapidly lowered by diffusion and uptake of glutamate. This brief high concentration of glutamate results in a phasic activation of NMDA receptors, due to the fluctuation of glutamate. Phasic activation contributes to normal synaptic transmission. The efficiency of the glutamate uptake leads to low extracellular glutamate concentration at rest which prevents overactivation of NMDA receptors, which is called tonic activation and can lead to excitotoxicity, neuron death.[4] With this in mind, it has been shown that glutamate and NMDA binding is decreased in patients with Alzheimer's. Moreover, the level of NMDA receptors decline, in parts of the brain, over the years which compromises synaptic plasticity, which could be one cause of memory impairment. Dysfunctional release and uptake of glutamate therefore is a major cause for some neurological diseases.[9]

Since NMDA receptors have an impact on many different diseases and are spread across the brain, efforts are being made to develop drugs that target specific subunits to be able to control NMDA receptor properties at specific parts of the brain.[6] The majority of the early NMDA receptor antagonists developed showed many side effects, which is partly explained by the lack of subunit-selectivity in these antagonists.[5] One common side effect of NMDA receptor antagonists is the disruption of normal synaptic transmission. However, blocking excessive NMDA receptor activation without blocking normal NMDA receptor transmission have been proven difficult.[4]

To this day, there have been several agonists and antagonists developed for targeting NMDA receptors, yet not many are clinically approved. One exception is the antagonist Memantine, seen in figure 6. The agonists and antagonists either target the agonist binding site, the co-agonist site, the pore-binding site or the allosteric modulatory sites.[9] Both positive allosteric modulators (PAMs), figure 5, which increase the response or the affinity for the agonist, and negative allosteric modulators (NAMs), figure 6, which does the opposite, have been developed.[4]

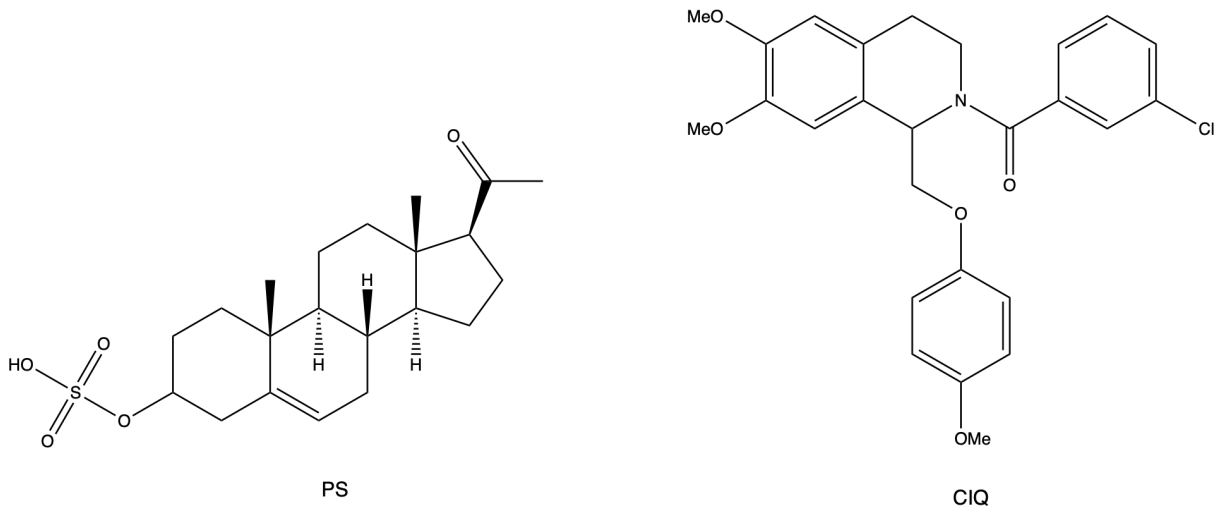


*Figure 5. Chemical structures of exemplified PAMs.*

As mentioned before, PAMs increase the response of the receptor. Figure 5 shows two examples of developed PAMs, where both increase the open probability of the NMDA receptor, thus increasing the response. PS is selective for GluN1/2A and GluN1/2B while CIQ is selective for GluN1/2C and GluN1/2D.[10]

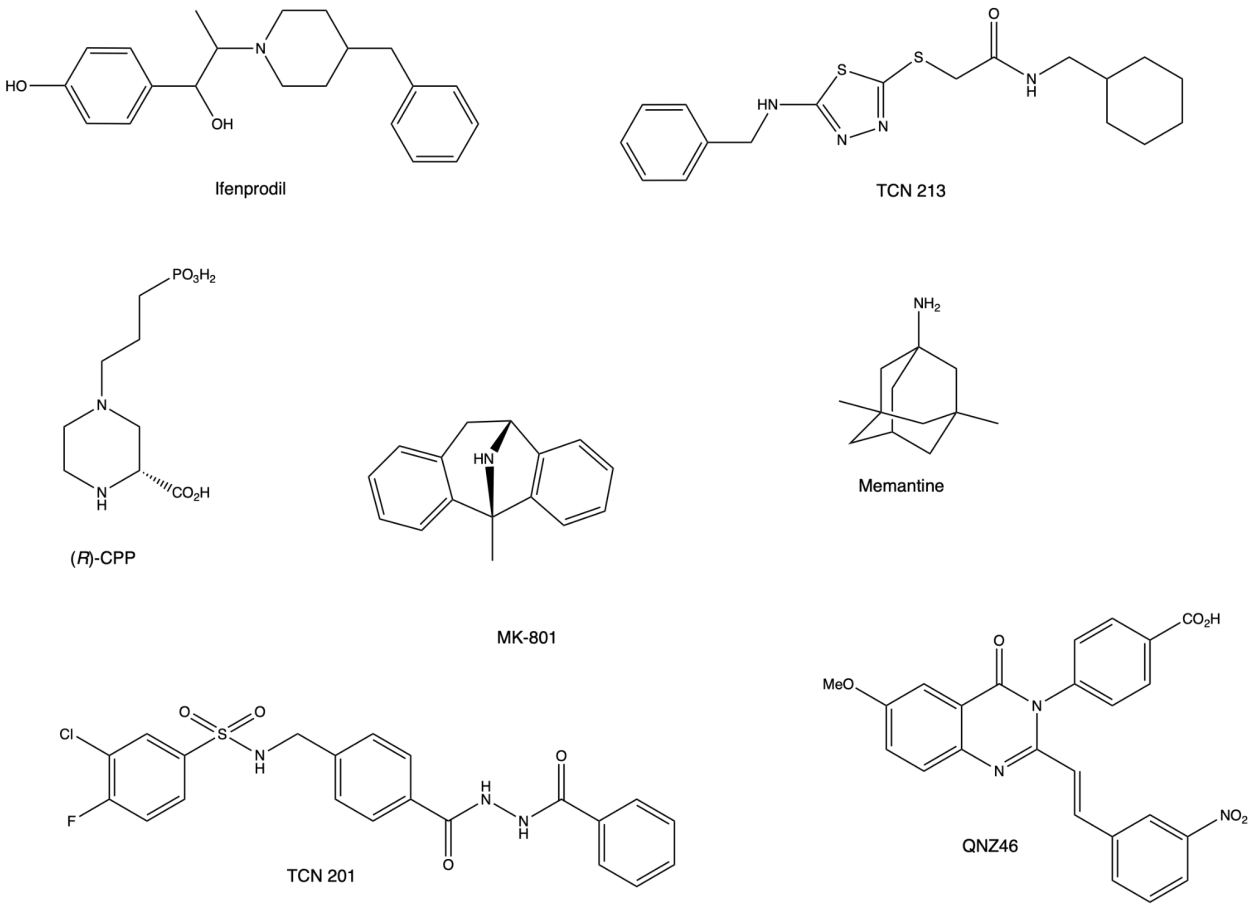


*Figure 6. Chemical structures of exemplified antagonists including competitive antagonist (CPP), channel blockers (MK-801 & Memantine) and NAMs (Ifenprodil, QNZ46, TCN201 & TCN213).*

In contrast, NAMs decrease the response of the receptor. NAMs have been developed due to the lack of subtype specific antagonists that interact with the NMDA receptor as competitive antagonists or channel blockers. CPP, figure 6, is an example of a competitive antagonist that binds at the glutamate binding site. These antagonists show slight selectivity for GluN1/2A > GluN1/2B > GluN1/2C > GluN1/2D and CPP is one exception of these competitive antagonists that is 50 times more selective for GluN1/2A over GluN1/2D. Additionally, competitive antagonists that bind at the glycine binding site have also been developed but since the glycine binding site is found in the GluN1 subunit, these are not GluN2 subtype specific. Furthermore, MK-801 and Memantine, figure 6, are examples of two antagonists acting as channel blockers. A problem with channel blockers is that research has shown that psychosis is a side effect for potent NMDA channel blockers.[10] Phencyclidine and ketamine are two known potent NMDA channel blockers that are used as dissociative anesthetics but have also been used as

hallucinogenic drugs for this reason. This showcases the problem with potent NMDA channel blockers.[4] MK-801 is another potent channel blocker with high bioavailability but with a small therapeutic window.[9] In contrast, as described above, Memantine is a channel blocker that is clinically tolerated. This due to its fast dissociation from the channel upon inactivation, which leads to minimal interference with normal synaptic transmission. Despite this, channel blockers have a slow onset due to the dependence of the probability of channel opening.[4]

Ifenprodil, figure 6, is one of the first selective NAM for NMDA receptors and is selective for GluN1/2B. It is voltage- and use-independent and binds to the interface between ATDs of the GluN1/2B heterodimers.[4] Following the development of ifenprodil, more selective NAMs were developed. For example, QNZ46, figure 6, is 50-fold selective for GluN1/2D, compared to GluN1/2A and GluN1/2B. It is voltage independent, but it needs glutamate to bind to the receptor to be active.[10] Sulfonamide derivatives have been another success in subtype specific NAMs, TCN201 and TCN213, seen in figure 6. Both are highly selective for GluN1/2A and are dependent on the concentration of glycine in a non-competitive manner.[11] The NAMs have shown to bind to the S2 region of GluN2 subunit LBD, which is essential for the antagonistic activity.[4]

There are still only a few subtype selective NMDA receptor antagonists that have been developed. The difficulty in developing selective targets without disrupting normal transmission have been prominent, and further development is essential to aid the development of clinically tolerated NMDA receptor antagonists.[4,8]

## Subunits GluN2A & GluN2B

As mentioned earlier, NMDA receptors composed of GluN1/GluN2 subunits are stated to be more important from a physiological perspective. In this essay, GluN1/2A and GluN1/2B, specifically the GluN2 subunits, will be described further.[4] Figure 7 show an x-ray image, unpublished, of TCN213 with an added ethyl group on the carbon next to the secondary amine, bound to GluN2A and GluN2B respectively. In the same figure, one amino acid is highlighted in both pictures, which represents a major difference between the two subunits. GluN2A consists of a valine 267 residue while GluN2B consists of a phenylalanine 262 residue instead. This change from valine 267 to phenylalanine 262 alters the size and interaction possibilities within the

binding pocket. Phenylalanine is approximately 4 Ångströms larger than valine and can interact via hydrophobic interactions together with pi-stacking.[12] Thus, this difference in GluN2 subunits gives insight into the structure-activity relationship (SAR) between possible analogues and the receptor.

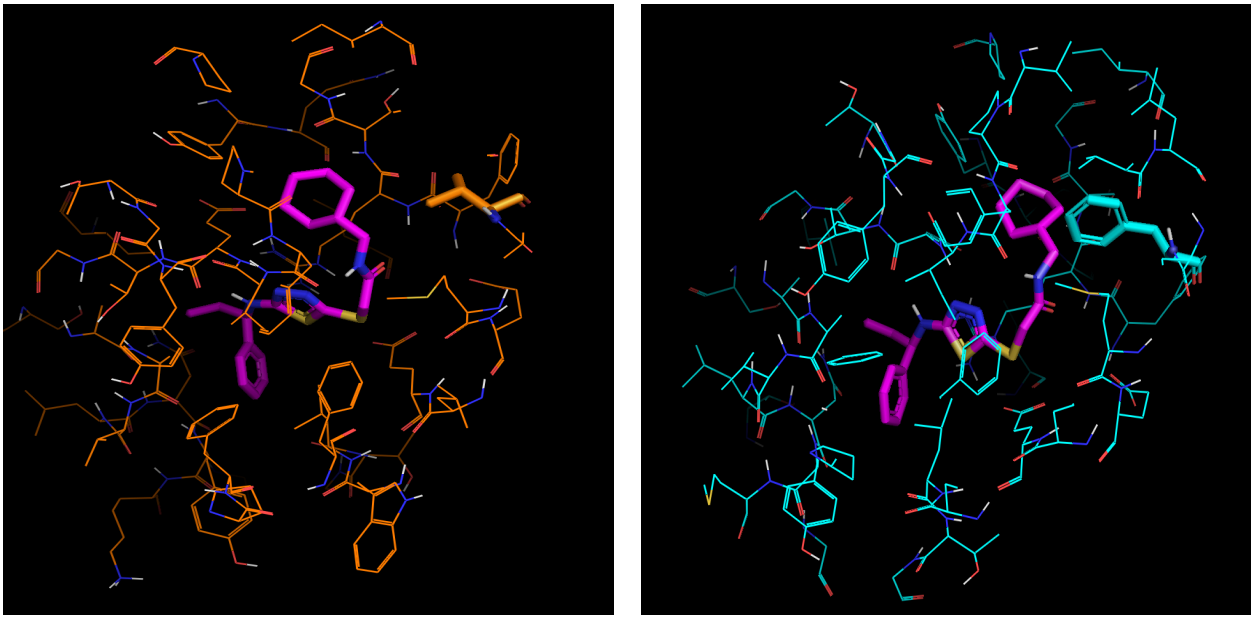

*Figure 7. Binding pose of TCN213 with an added ethyl group on the carbon next to the secondary amine (magenta) in GluN1/2A (orange) and GluN1/2B (cyan), with highlighted non-conserved amino acid, visualized using PyMOL.*

# Aim

The overall aim of this project is to synthesize analogues that aid the research into selective antagonists for NMDA receptor subtypes GluN1/2A or GluN1/2B. These analogues should be negative allosteric modulators that are able to pass the blood brain barrier (BBB) and that metabolize at a reasonable rate. Specifically, the core of the TCN213 analogue with an added methyl group with R stereochemistry, is used to synthesize these new analogues by either changing the amide by synthesizing amide bioisosteres or by changing the length and the identity of the right-side chain, see figure 8. The R stereochemistry was used since functional assay has shown that the S stereochemistry shows no activity. These changes are aimed to improve the knowledge of what parts of the TCN213 analogue are important for its relatively high potency and selectivity for GluN1/2A, and to synthesize selective analogues for GluN1/2A and GluN1/2B respectively.

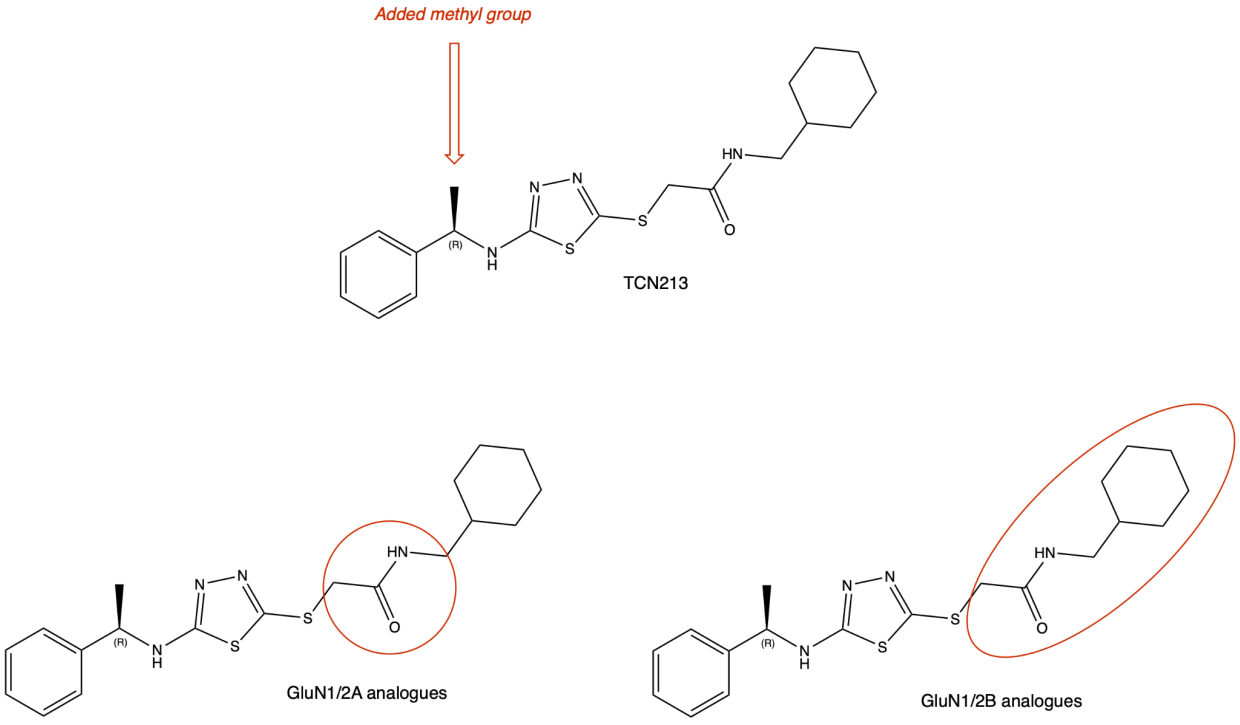


*Figure 8. Figure of the structure TCN213 with added methyl group (top), core structure of analogues that aim to be GluN1/2A selective with the amide circled to point out what is changed during synthesis (left), core structure of analogues that aim to be GluN1/2B selective with the right side circled to point out what is changed during synthesis (right).*

# Results & Discussion

## Starting synthesis

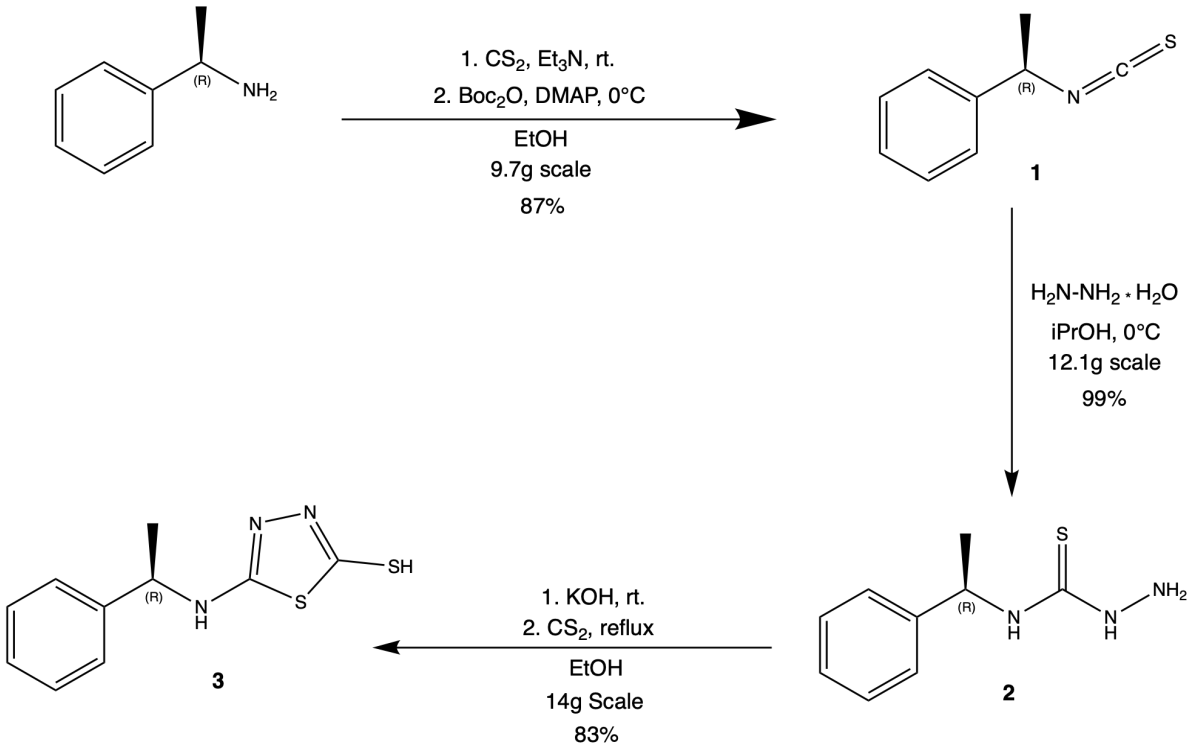


*Scheme 1. Reaction scheme of the synthesis of products **1-3** with scale and yield.*

Starting off, scheme 1 shows a robust synthetic route on how to form the first part of the TCN213 analogue, which is synthesizing the 1,3,4-thiadiazole, **3**. This synthetic route had already been established in the research group.

In the first step, methylbenzylamine was used together with $CS_2$ to form product **1** through a dithiocarbamate intermediate, in good yield. No further purification was performed after work up. A nucleophilic attack from hydrazine on the newly formed electrophilic carbon led to product **2**. Small impurities could be detected after purification, but the NMR looked clean enough to continue without further purification.

Next, addition of KOH and $CS_2$ under reflux yielded the 1,3,4-thiadiazole product **3**. Proposed mechanism is seen in scheme 2. The pKa values of the three nitrogens in the structure was

suggested to be 13.9, 15.3, 26.1 from left to right.[13] This indicates that the nitrogen on the left-hand side of the sulfur is to be deprotonated first. Due to the resonance formed between the nitrogen and sulfur, the negative charge is delocalized between the nitrogen and sulfur. However, nitrogen is more electronegative compared to sulfur and would theoretically be the more stable form between the two.[14] Though, as can be seen in scheme 2, both pathways lead to the wanted product, **3**. The driving force of the reaction is the formation of the aromatic thiadiazole ring and due to the evolution of $H_2S$ gas, the reaction is irreversible.

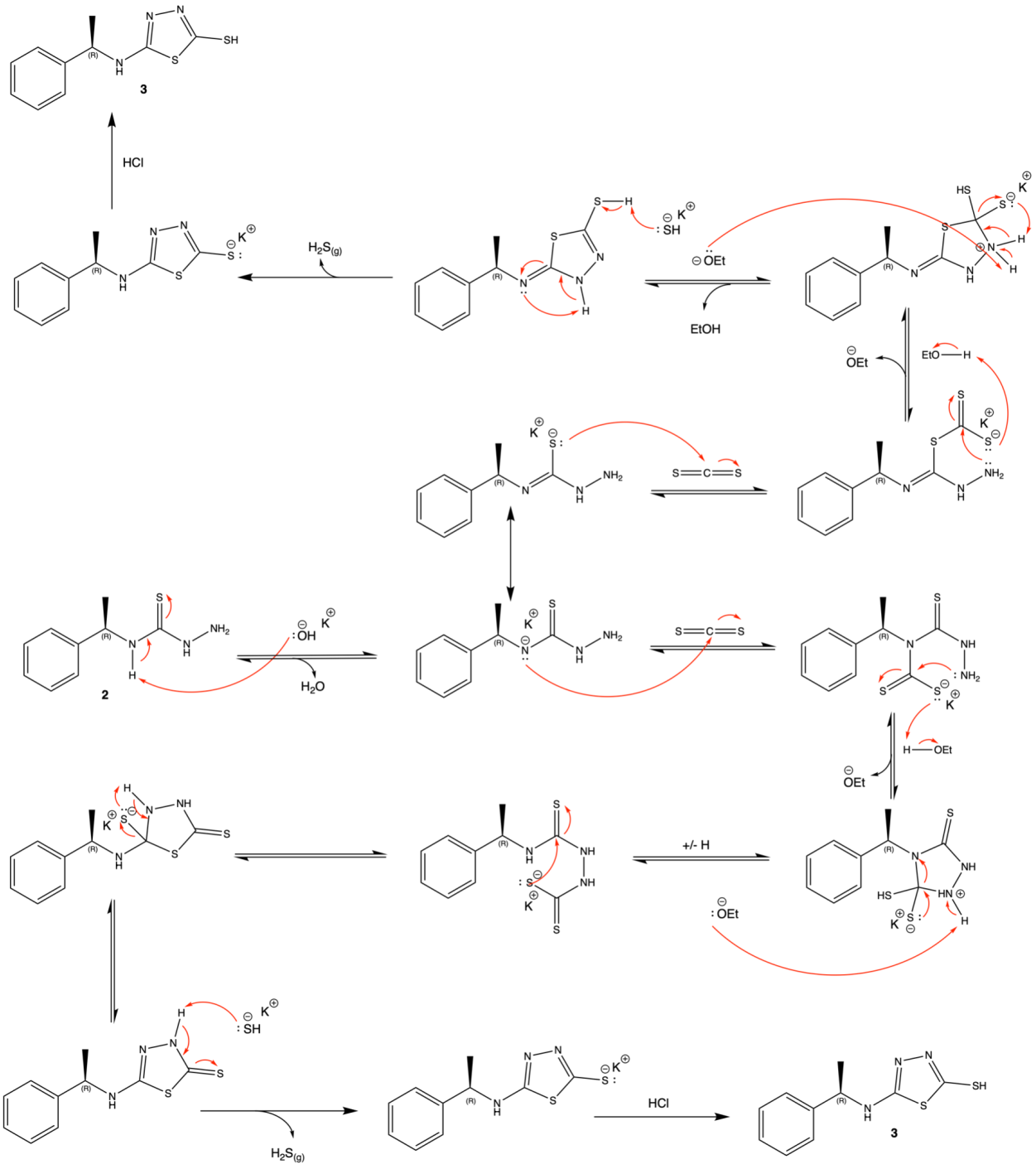


*Scheme 2. Reaction mechanism of the formation of product **3**.*

Spectrum 1 indicates that product **3** has been formed, mainly due to protons 9 and 15 that are particularly deshielded. They are remarkably deshielded due to binding to heteroatoms, but also

being part of a conjugated system. Interestingly, there is a large difference in ppm between proton 9 and 15 although both bind to a heteroatom and are part of the conjugated system. This can be explained by the electronegativity difference between nitrogen and sulfur. Nitrogen has 3.04 on the pauling scale, which describes electronegativity ranging from 0-4, while sulfur has 2.58.[14] Scheme 3, shows the different possibilities of deprotonation of product **3**. Following the yellow route, the sulfur is deprotonated, and the negative charge ends up between two nitrogen atoms and one sulfur atom. Following the purple route, the nitrogen is deprotonated, and the negative charge ends up between one nitrogen atom and two sulfur atoms. Due to the electronegativity difference between the atoms, the negative charge is more stabilized in the yellow route. Hence, this is the preferred deprotonation route. Therefore, proton 15 is more deshielded from electrons compared to proton 9 since it is presumably more acidic.

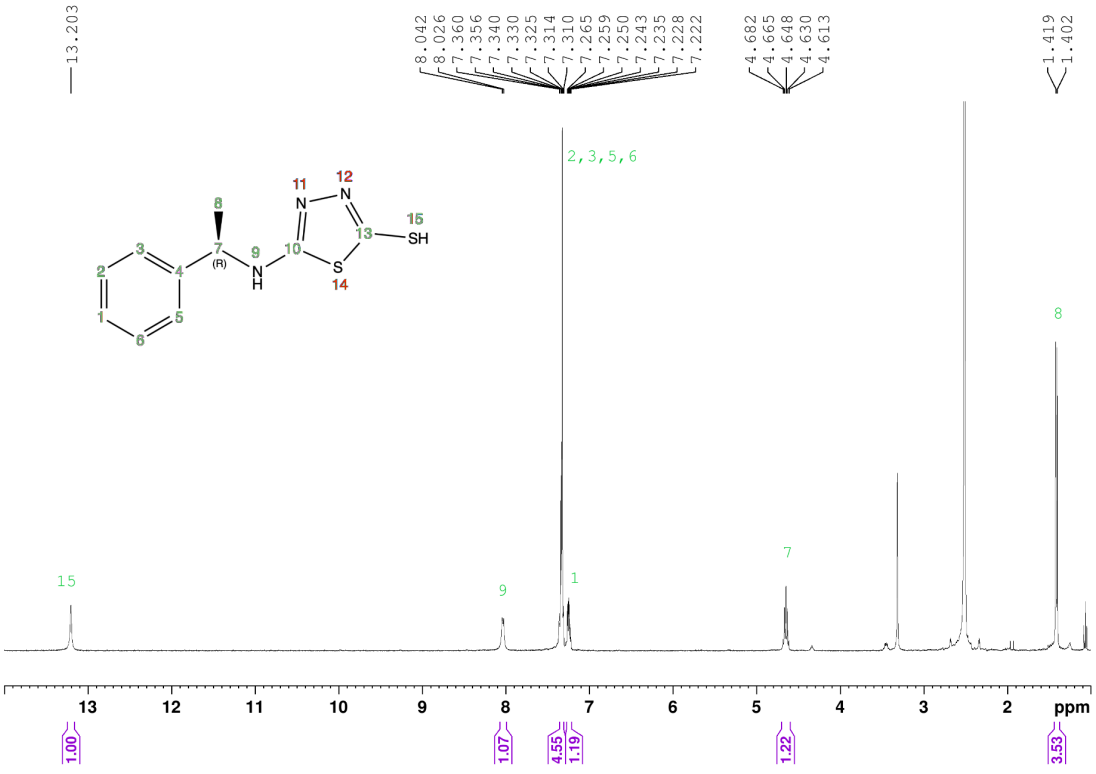


*Spectrum 1. $^{1}H$ NMR of (R)-5-((1-phenylethyl)amino)-1,3,4-thiadiazole-2-thiol (**3**) in DMSO-$d_6$; with all the peaks assigned to protons in the molecule.*

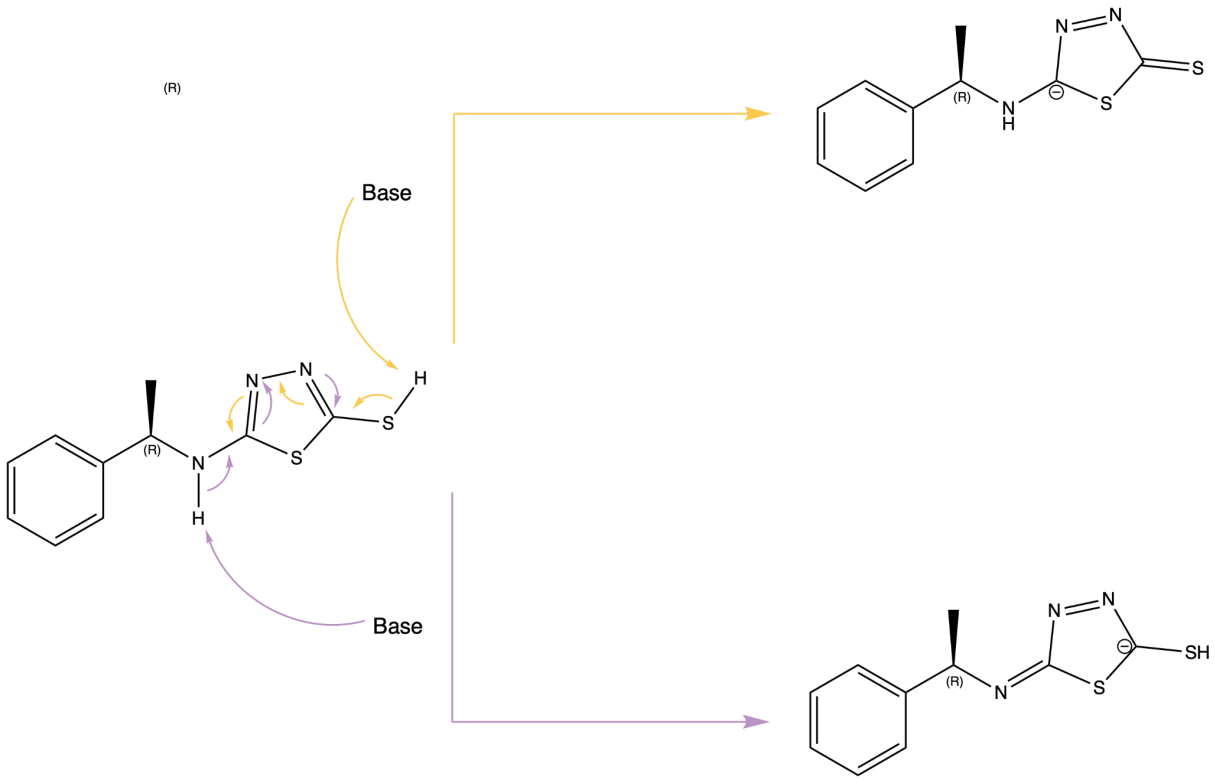


*Scheme 3. Illustration of two different mechanisms for deprotonation of product **3**.*

# Synthesis of GluN1/2A analogues

## Triazoles

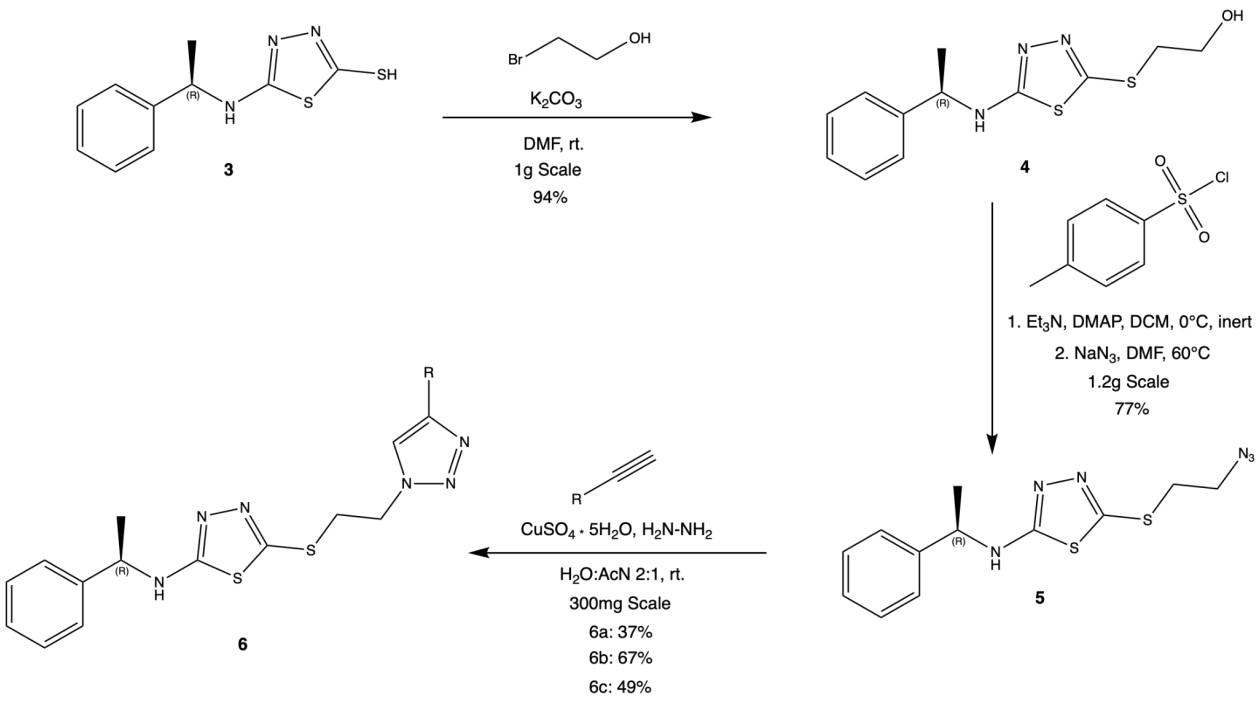


*Scheme 4. Reaction scheme of the synthesis of products **3-6a-c** with scale and yield.*

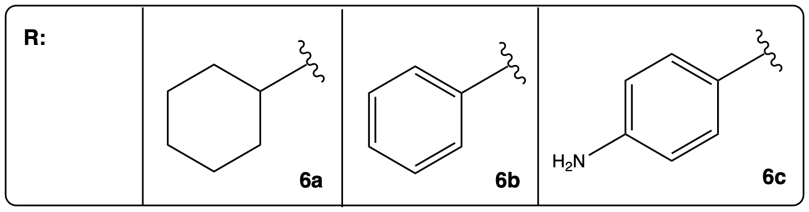


*Figure 9. R-groups synthesized for products **6a-c**.*

Scheme 4 shows the synthetic route to the formation of triazole moieties and figure 9 shows the R-groups for the three different products. Firstly, 2-bromoethanol was added to the 1,3,4-thiadiazole, **3**, to form the alcohol moiety, **4**, via an SN2 reaction. Due to the difference in ppm for proton 9 and 15 discussed above, theoretically the sulfur would be more prone to take part in the SN2 reaction, which experimentally this reaction adheres to. NMR, spectrum A18, indicated sufficient purity, therefore no further purification was performed after work up.

Secondly, 4-toluenesulfonyl chloride was added to convert the alcohol into a good leaving group to aid the substitution into the azide moiety, **5**. Scheme 5 shows failed attempts to form the azide moiety, **5**. First attempt was to turn the hydroxyl group into an azide in one step which did not work. Due to the similarity between starting material and product, together with impurities in the crude, NMR was inconclusive in the indication of the wanted product. Due to no information found on how an azide moiety behaves in MS, this was also inconclusive. To figure out what was formed, cyclohexylacetylene was added together with $CuSO_4$ and hydrazine to see if the product **6a** would form. This reaction did not work which indicated that the azide moiety was indeed not formed. Another route was carried out to try and form the alcohol into a tosylate to, in a second step, form the azide. This reaction did indeed work, however the secondary amine in the molecule was able to attack the tosylate, leading to a side product. Most likely, the dimer is formed since an attack from another molecule is not as sterically hindered. However, there is a chance that the side product in brackets could also be formed. Since the difference between the dimer and the other side product can't be seen in the NMR or in MS due to the same mass to charge ratio and the same amounts of protons in similar positions, which side product is formed is inconclusive. However, since the chance of another product encountering another molecule is higher compared to the nitrogen being in proximity to its own tosylate, the dimer is theoretically the formed side product. There was no interest in testing this compound's activity and no further investigation was therefore made. This dimerization happened over one to two days. This suggests that the amine is indeed nucleophilic enough to take part in reactions such as e.q. the SN2 reaction, discussed above, to form the alcohol moiety, **4**. The reason for why this was not seen in that reaction could be sterical hindrance from the hydroxyl group.

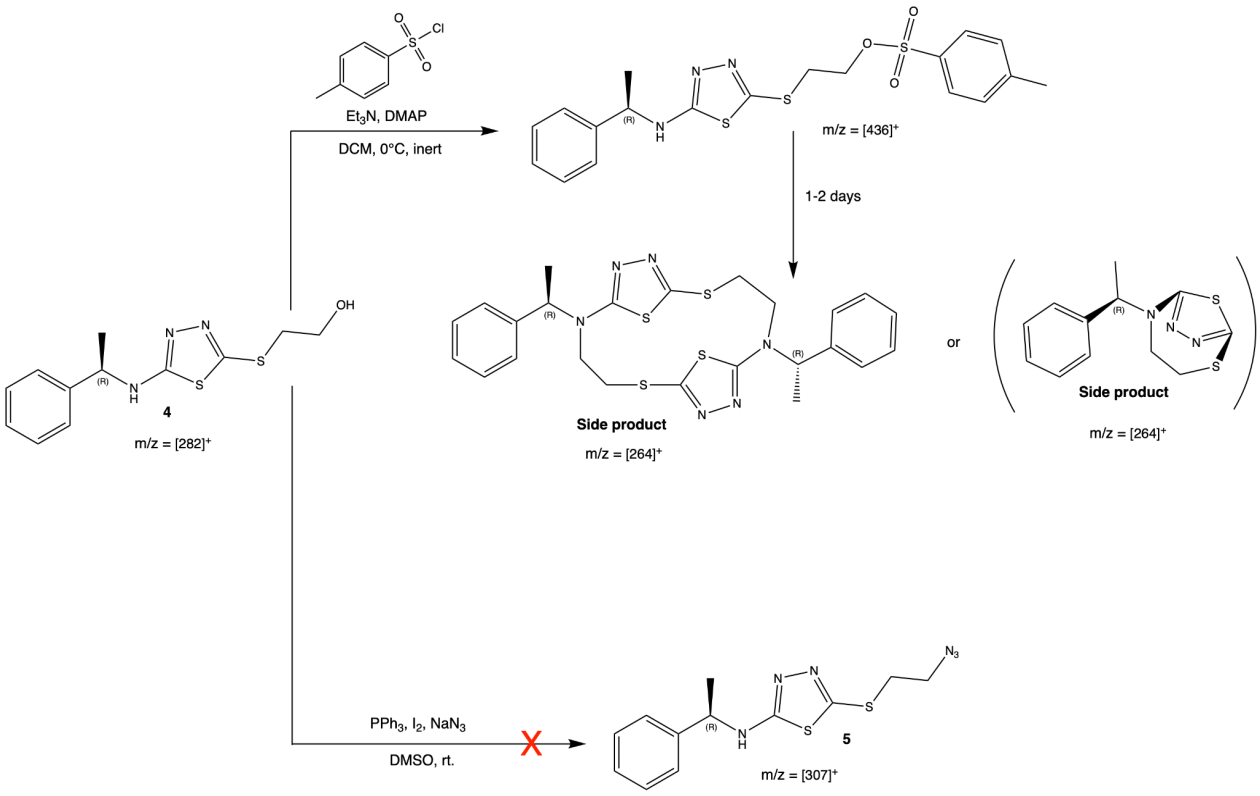


*Scheme 5. Reaction scheme of failed attempts to synthesize product **5**.*

Furthermore, a combined route was proposed, seen in scheme 4, which eventually led to the wanted azide moiety, **5**. Here, the hydroxyl group was converted into the tosylate which was known to work, but was immediately, after work up, treated with $NaN_3$ to form the azide moiety **5**. This azide molecule was stable in LCMS and was able to ionize. NMR, spectrum A20, showed enough purity to continue without purification.

One difficulty in determining the formation of product **5**, is the similarity between the starting material and the product. Figure 10 displays the part of the NMR that differs between product **4** and **5**. Since the reaction is a conversion from a hydroxyl group into an azide, the only difference seen in the NMR is the carbon next to the functional group and the OH proton. However, the proton on the hydroxyl group does not always show up in NMR spectra, specifically when $H_2O$ is present.[15] Also due to impurities in the crude, this proton was hard to distinguish in product **5**. Regardless, as can be seen in figure 10, there is a split difference for the more deshielded protons. This difference is due to the presence of the additional proton in the hydroxyl group.

This indicates that there has been a conversion from a hydroxyl group to an azide. Scheme 5, shows the mass to charge ratios of product **4** and **5**. The change in mass from m/z = $[282]^+$ to m/z = $[307]^+$ observed in the MS complies with the NMR analysis.

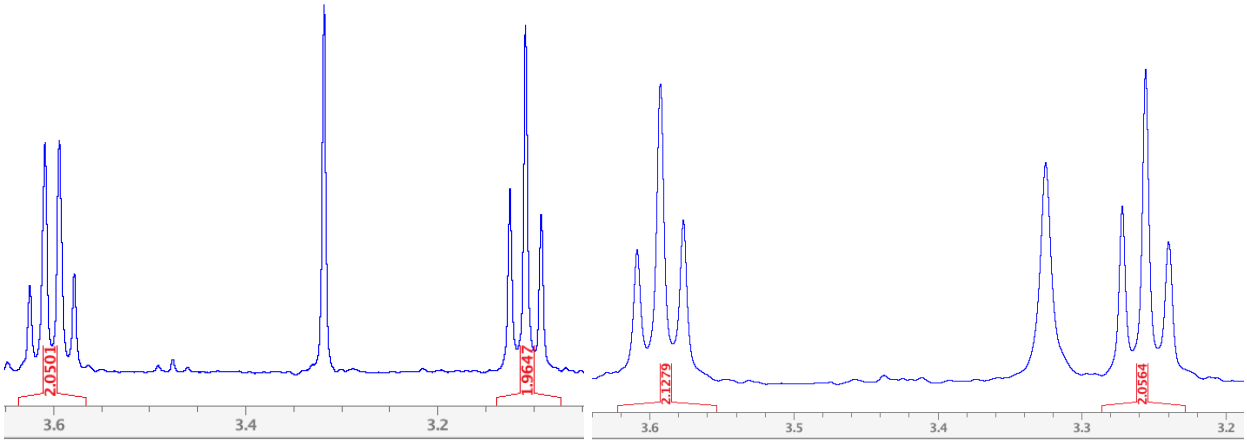


*Figure 10. Part of the $^1$H NMR for product **4** (left) and $^1$H NMR for product **5** (right) taken from appendix.*

Moreover, the azide moiety was treated with three different alkynes to form three triazole moieties, seen in figure 9, using click chemistry. Determination of purity was accomplished with ana. HPLC. The slightly low yields were due to product lost in work up. This could be fixed by using an internal standard in the NMR analysis of the crude.

Product **6a** was synthesized to mimic the TCN213 analogue to be able to compare the difference between the amide and the triazole moieties from the pharmacological data. Secondly, product **6b** was then formed to add a functional group with vastly different properties compared to the group added for product **6a**. Lastly, product **6c** was formed since computational modeling had suggested that a polar moiety, at the right side of the molecule, generated an antagonistic effect. Therefore, an amine was added to add a more polar functional group at this position. Although polar moieties show greater difficulty in penetrating the BBB, if physiological data show good activity, potential prodrugs could be synthesized.

The triazoles were formed by Copper catalyzed azide-alkyne cycloaddition (CuAAC), seen in scheme 6 First, Cu(II)$SO_4$ was treated with hydrazine to form Cu(I), which is required for the activation of the catalyst. Copper coordinates the alkyne in a π-coordination which acidifies the terminal hydrogen enough to be deprotonated by water, forming the σ-bound copper acetylide

with another copper molecule. The copper that is π-bound to the acetylide coordinates the azide forming a six-membered metallacycle which is stabilized by the second copper. This step is endothermic, but the barrier is significantly lowered due to the presence of copper. Ring contraction then leads to a triazole-copper derivative that is protonated by surrounding media to form the triazole moiety.[16]

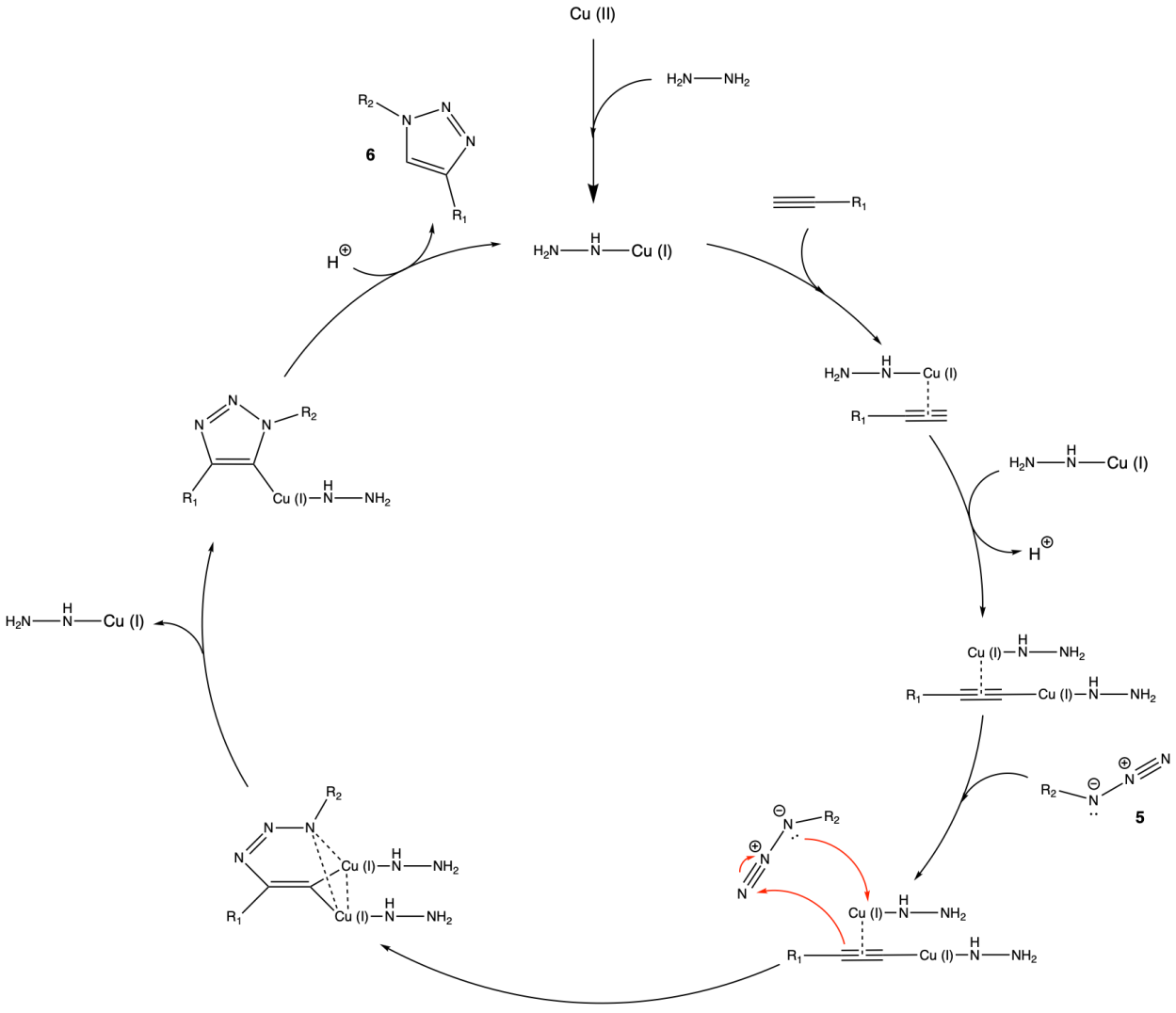


*Scheme 6. Reaction mechanism of the formation of products **6a-c**.*

## Reversed amides

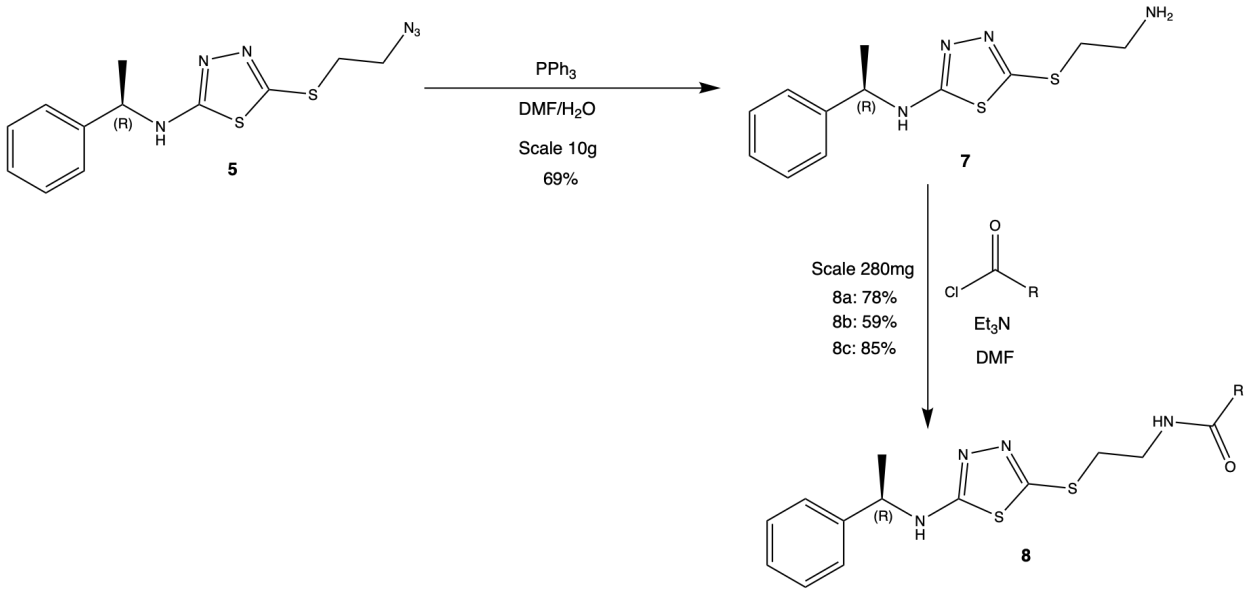


*Scheme 7. Reaction scheme of the synthesis of products **5-8a-c** with scale and yield.*

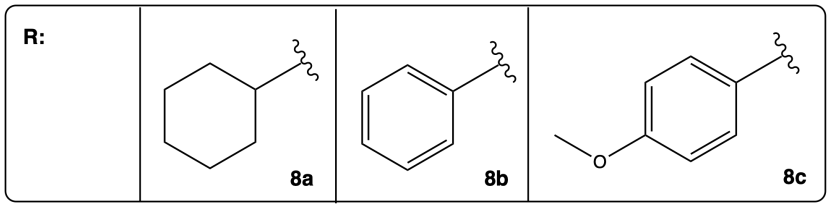


*Figure 11. R-groups synthesized for products **8a-c**.*

Scheme 7 shows the synthetic route to the formation of reversed amide moieties. 'Reversed amide', in this context, is meant by the switch in position of the carbonyl group in the amide compared to TCN213. Figure 11 shows the R-groups for the three different products. Firstly, the azide moiety formed above was treated with triphenylphosphine to convert the azide to an amine, product **7**, via the Staudinger reaction. The amine moiety, **7**, showed high solubility in water which made it difficult to remove DMF. On a small scale, it worked to make the aqueous phase basic to extract the amine to remove DMF via washing with $CaCl_2$. However, on a big scale this was not a viable option since it was not possible to extract all the product from the aqueous phase. Instead, water and DMF was removed by freeze drying. The formed triphenylphosphine oxide was not soluble in water and precipitated when water was added to the solution after DMF removal. Although, all DMF could not be removed and therefore some triphenylphosphine oxide

was still present in the sample. Prep. HPLC was performed to remove the last of DMF and triphenylphosphine oxide. The formed product, **7**, was then used to form reversed amide moieties but also as a final compound to test for the GluN2B receptor, which will be discussed later.

Secondly, product **7** was treated with three different acyl chlorides to form the desired products **8a-c**, via the Schotten-Baumann reaction. Prep. HPLC of product **7**, left the amine protonated, as a TFA salt due to TFA being present in the mobile phase. Because of this, the amine moiety **7**, was treated with $Et_3N$ before adding the acyl chloride to neutralize the amine for it to be able to react with the acyl chloride to form the wanted products **8a-c**. It should be noted that product **8a**, was formed before the amine moiety, **7**, was purified with prep. HPLC. This reaction was performed to determine if the reaction could be performed despite some triphenylphosphine oxide still being present and if the residue could be removed in the next step. This turned out to be difficult due to triphenylphosphine coeluting with product **8a** in silica gel chromatography. Prep. HPLC was therefore performed to try and remove it. Here, most of the triphenylphosphine oxide was removed but there was still some present. Ana. HPLC indicated a purity of 91.3% but calculations from the NMR indicated it to be approximately 4% of triphenylphosphine oxide left. This difference could be due to the high intensity of triphenylphosphine oxide in the chromatogram compared to the product. Both molecules had maximal absorbance around 200nm, due to the aromatic rings in the molecules. Since triphenylphosphine oxide has three aromatic rings that absorb at this wavelength and product **8a** has less, triphenylphosphine oxide could show a higher intensity leading to the difference in purity result between ana. HPLC and NMR. Therefore, the result of the NMR determined the product to be pure enough for functional assay. Product **8b** and **8c** was performed after prep. HPLC of the amine moiety **7** due to the difficulty in removing triphenylphosphine oxide in the formation of reversed amides. Another difference between the formation of **8a** compared to **8b** and **8c**, is that **8a** was not performed under inert and dry conditions. Due to the literature not stating it was performed under inert conditions and since the chemical did not have a septum, inert and dry conditions were not done. However, during the reaction additional reagent had to be added since the acyl chloride is very electrophilic and can easily react with nucleophiles, such as water to form the carboxylic acid. Due to this, the next reaction was performed under inter and dry conditions.

All products, **8a-c**, show good yield except for the slightly lowered yield for **8b**. This could be that the reaction was not fully converted and was mistaken for full conversion due to the reagent baselining like the starting material, and since the amide moiety **7**, dissolves in water, it was not seen in UPLCMS after work up. UPLCMS of the crude before work up would fix this problem.

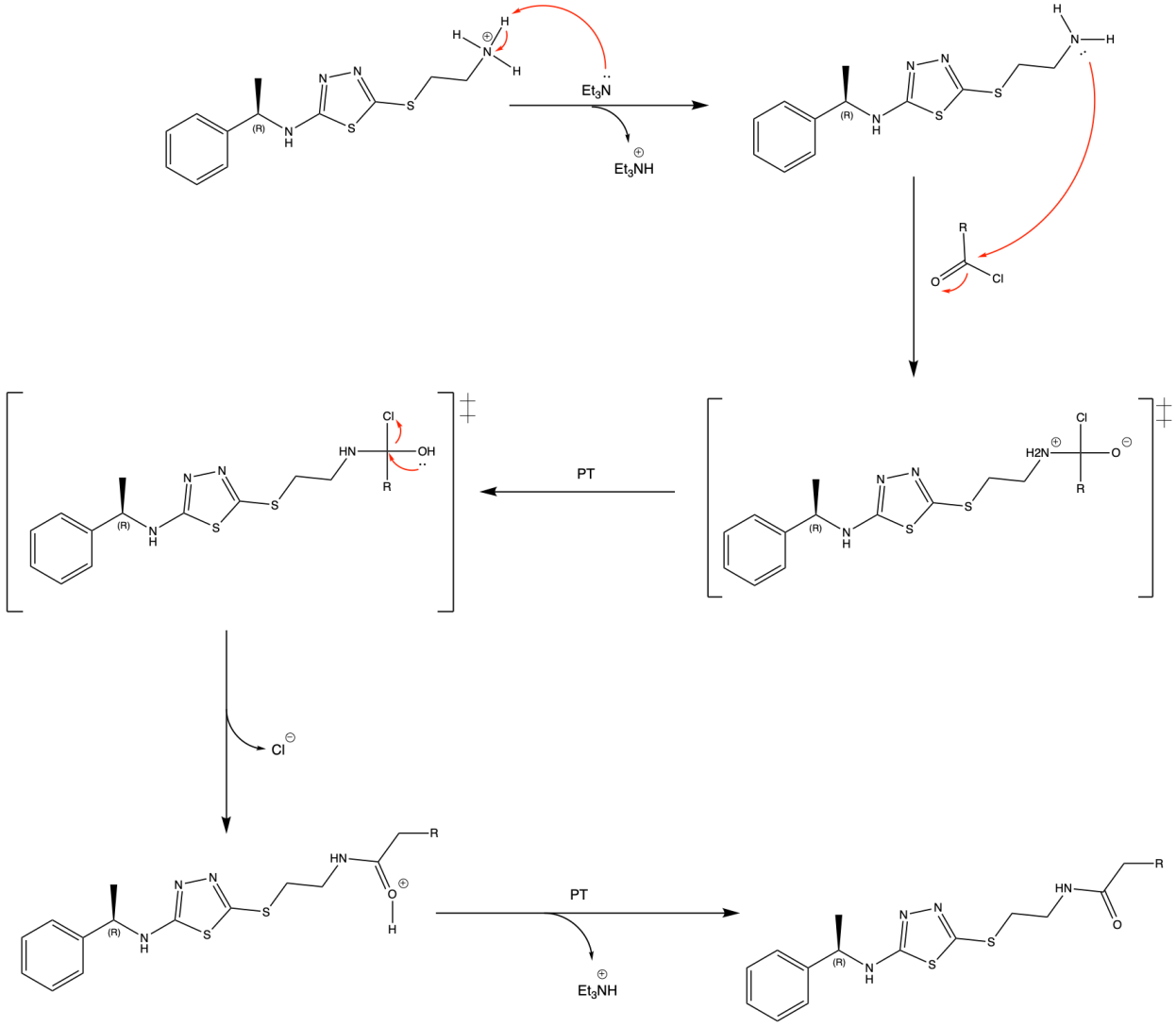


*Scheme 8. Reaction mechanism of the formation of products **8a-c**.*

Scheme 8 shows the mechanism for the formation of reversed amide moieties. $Et_3N$ deprotonates the amine which then, in turn, does a nucleophilic attack on the carbonyl carbon to form a tertiary transition state, which, after a proton transfer, kicks out the chloride ion to form back the carbonyl moiety. After another proton transfer the amide moiety is formed.

Product **8a** was synthesized to mimic the TCN213 analogue in order to determine the importance of the carbonyl position in the amide. Again, product **8b** was synthesized to add a functional group with vastly different properties compared to the group added for product **8a**. Lastly, product **8c** was performed to add a polar and EDG on the aromatic ring since, from the information given, had not been tested before. This reaction was also performed with an EWG on the aromatic ring instead. However, this reaction did not work due to the degradation of reagent. Since an EWG on the aromatic ring increases the electrophilicity of the acyl chloride, this reagent was more susceptible to oxidation in contact with air, and NMR taken from two different reagents, one with a cyanide group and one with a nitro group as EWG, both show the formation of the carboxylic acid formed. LCMS indicated the product could be formed, but with insufficient yield for analysis even after additional reagent and base added. Since there was no time to order a new chemical, this reaction was not performed again.

Spectrum 2 shows the aliphatic part of the $^{1}$H NMR of product **8a**. The protons from the cyclohexane ring are split into two multiplets. The reason for this is that one proton on each carbon is more influenced by the carbonyl group and is therefore more deshielded due to the electronegativity of the oxygen. Figure 12 illustrates the cyclohexane ring in 3D, and gives an indication to which protons are influenced.

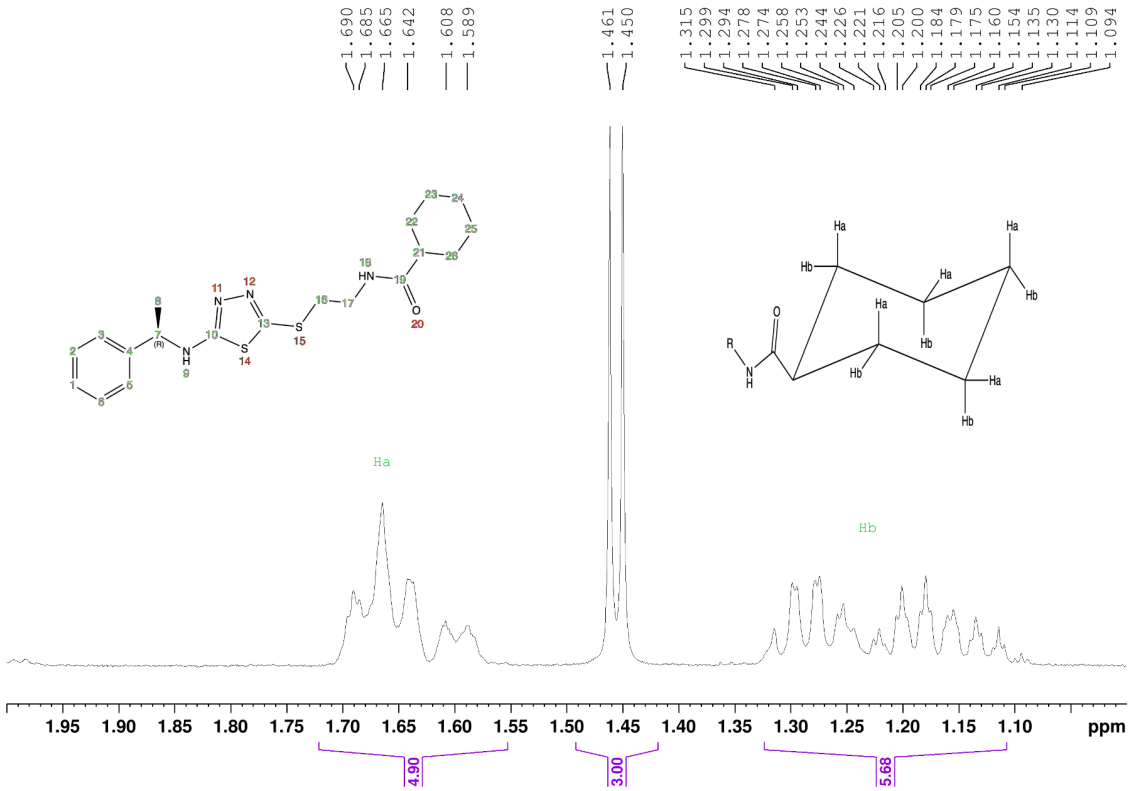


*Spectrum 2. $^{1}$H NMR of (R)-N-(2-((5-((1-phenylethyl)amino)-1,3,4-thiadiazol-2-yl)thio)ethyl)cyclohexanecarboxamide* ***(8a)*** *in DMSO-$d_6$,; zoomed in on aliphatic section.*

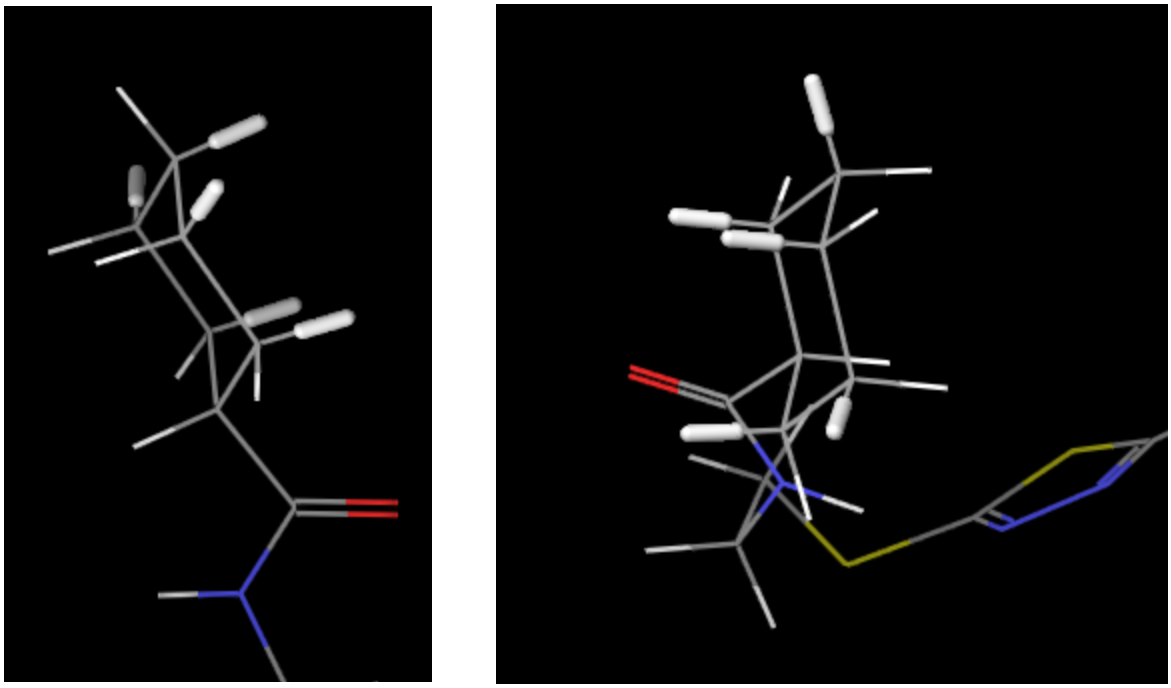

*Figure 12. 3D schematic of product **8a** in maestro, built using the 3D builder, with the carbonyl in red and the influenced protons in thick white.*

Spectrum 3 and 4, shows the aromatic part of the $^{1}$H NMRs of product **8b** and **8c** respectively. There is a significant difference in the shift of protons 23 and 25 between the products.This can be explained by the methoxy group in para position in product **8c**. The lone pair of the oxygen in the methoxy group can donate electrons into the aromatic system by mesomeric effects, and delocalize the electrons as seen in the resonance structures in spectrum 4. This makes protons 23 and 25 more shielded in product **8c** due to being more electron dense. Protons 22 and 26 have similar shifts between the structures and are the most deshielded due to the amide functionality that draws electrons to it due to its electron withdrawing properties.

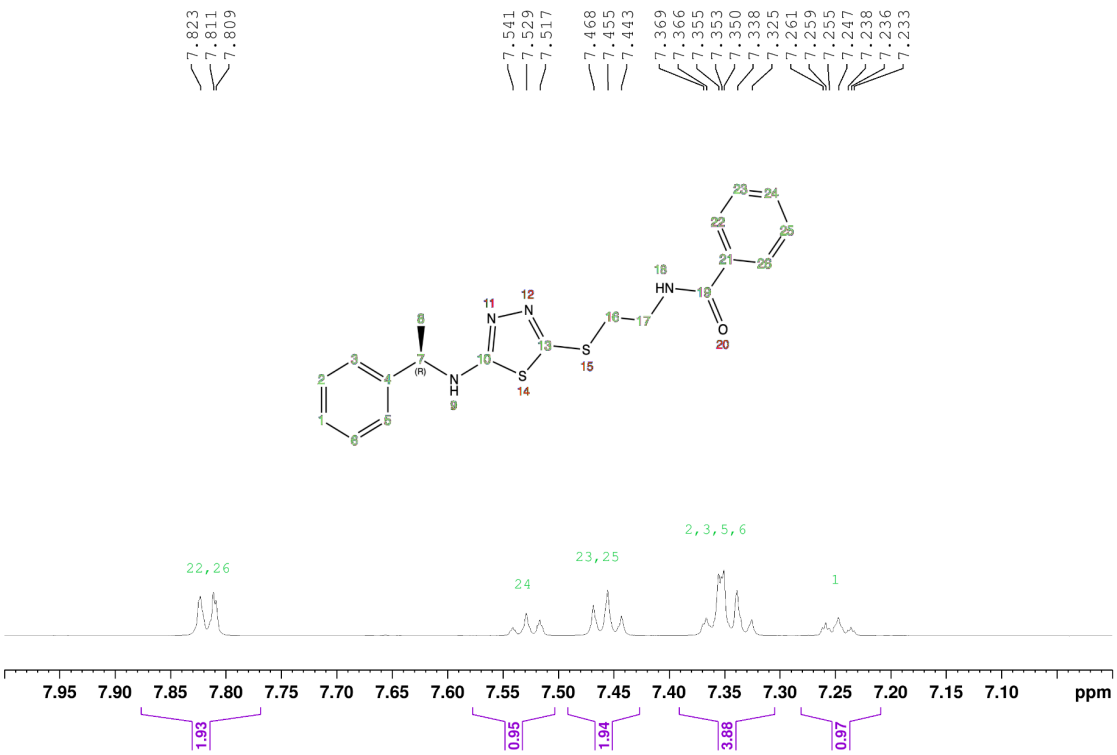


*Spectrum 3. $^{1}H$ NMR of (R)-N-(2-((5-((1-phenylethyl)amino)-1,3,4-thiadiazol-2-yl)thio)ethyl)benzamide **(8b)** in DMSO-$d_6$,; zoomed in on aromatic section.*

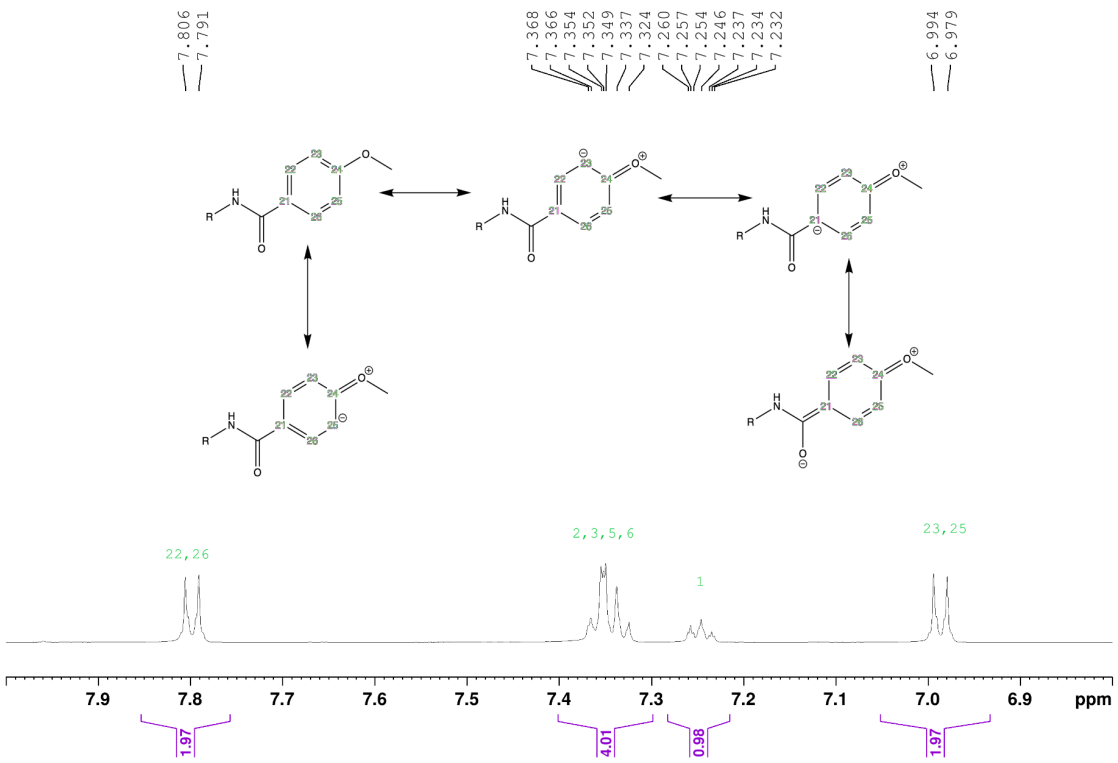


*Spectrum 4. $^{1}H$ NMR of (R)-4-methoxy-N-(2-((5-((1-phenylethyl)amino)-1,3,4-thiadiazol-2-yl)thio)ethyl)benzamide (**8c**) in DMSO-$d_6$,; zoomed in on aromatic section, with the resonance stabilisation illustrated.*

Another interesting thing between products **8a-c** is the shift of the amide proton. Spectra 5, 6 and 7 show the shift of the amine and the amide protons of product **8a-c** respectively. In product **8a** the amide proton has a shift around 7.9ppm, which is significantly lower compared to the amide proton in product **8b**, 8.6ppm, and in product **8c**, 8.5 ppm. The big difference between these is the shift from an aliphatic ring to an aromatic ring. Since the aromatic ring is planar, the ring is perpendicular to the magnetic field in the NMR machine and creates its own magnetic field. This leads to more deshielded protons, and since the amide can be part of the conjugated system it is directly influenced by this magnetic field.[17] Due to this, the amide proton is more deshielded in product **8b** and **8c** since the aromatic system is drawing electrons away from the amide. There is a slight difference in shift between product **8b** and **8c** as well, where the amide proton is more deshielded in product **8b**. This is explained by the methoxy group in **8c** that, as described before,

donates electrons into the system which makes the amide functionality less electron deficient compared to product **8b**.

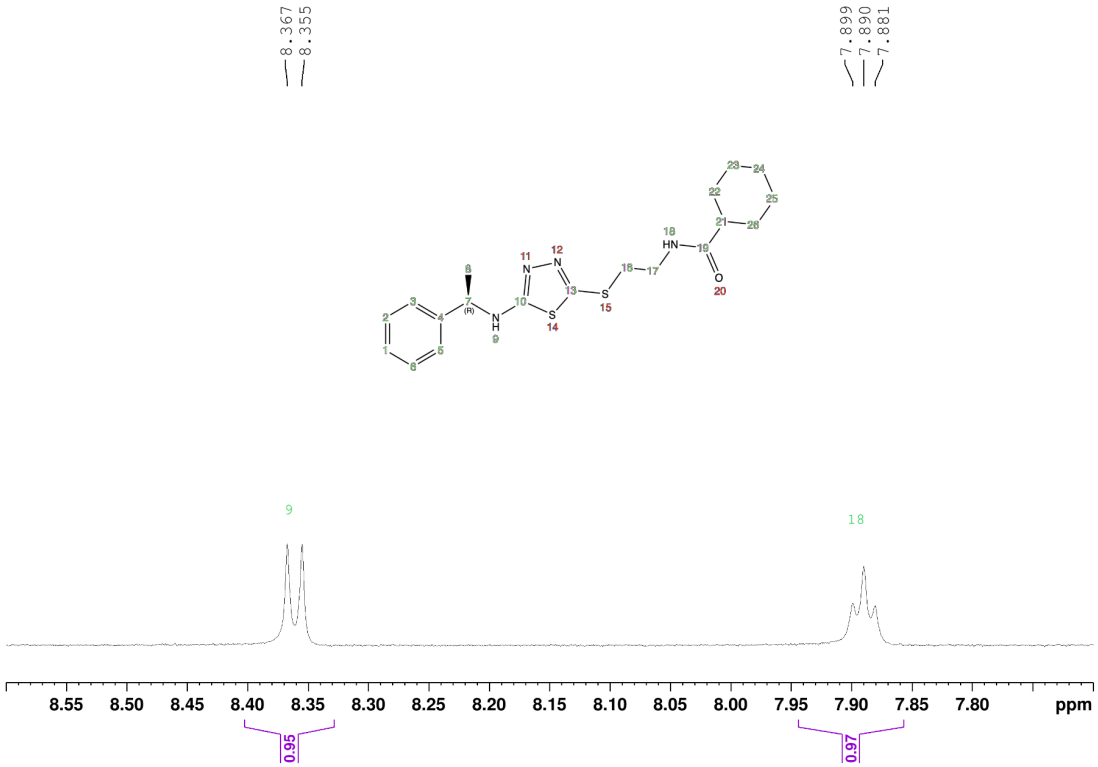


*Spectrum 5. $^{1}H$ NMR of (R)-N-(2-((5-((1-phenylethyl)amino)-1,3,4-thiadiazol-2-yl)thio)ethyl)cyclohexanecarboxamide (**8a**) in DMSO-$d_6$,; zoomed in on amine and amide protons.*

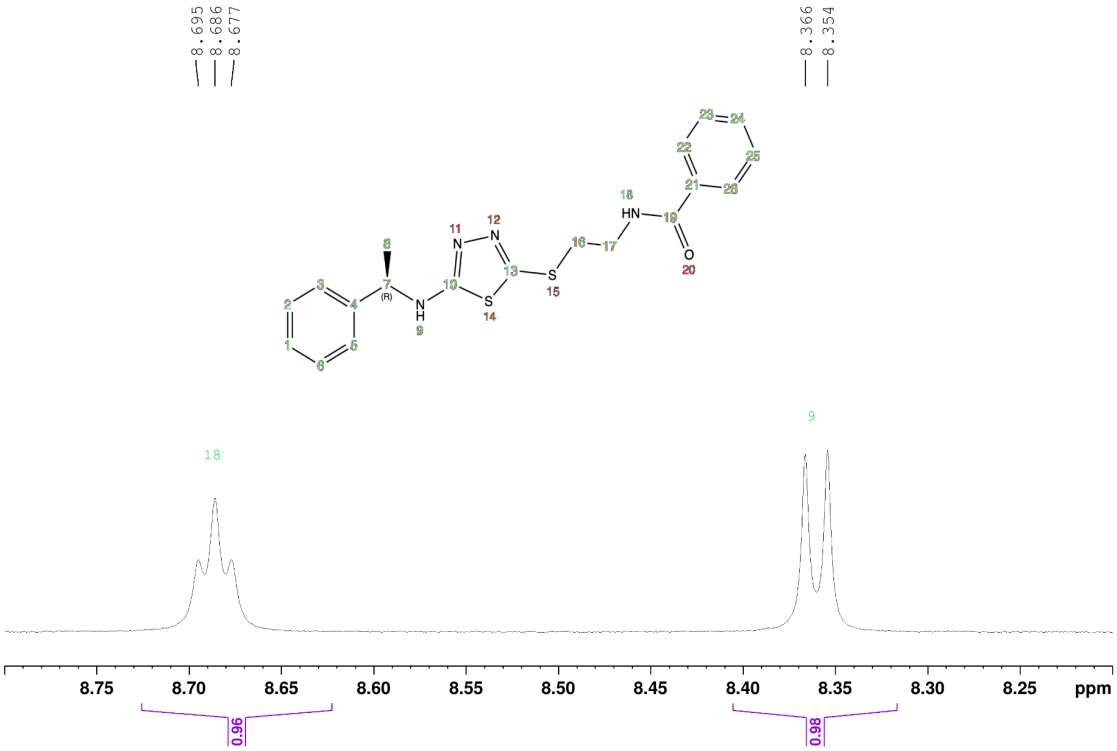


*Spectrum 6. $^{1}H$ NMR of (R)-N-(2-((5-((1-phenylethyl)amino)-1,3,4-thiadiazol-2-yl)thio)ethyl)benzamide **(8b)** in DMSO-$d_6$,; zoomed in on amide and amine protons.*

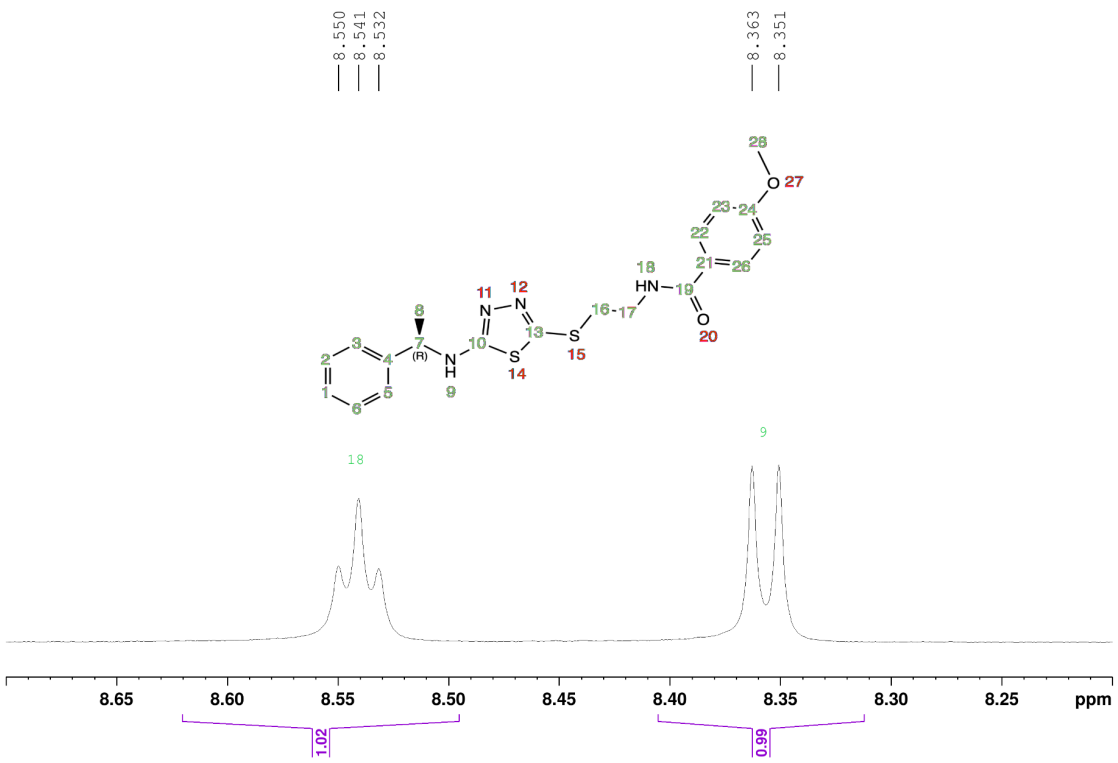


*Spectrum 7. $^{1}H$ NMR of (R)-4-methoxy-N-(2-((5-((1-phenylethyl)amino)-1,3,4-thiadiazol-2-yl)thio)ethyl)benzamide* ***(8c)*** *in DMSO-$d_6$,; zoomed in on amine and amide protons.*

As explained above, product **7** was also used as a final product for the GluN2B receptor. The thought behind this was that since the change from valine 267 to phenylalanine 262 in the GluN2B receptor provides the possibility of a cation-π interaction between the amine functionality and the phenyl group. Scheme 9 shows the mechanism for the Staudinger reaction. Triphenylphosphine attacks the electrophilic nitrogen in the azide moiety. The lone pair on the first nitrogen attacks the phosphor to the transition state ring formation. The ring decomposes to form nitrogen gas that evaporates. Without addition of water the reaction stops here. But since phosphor has a higher affinity for oxygen compared to nitrogen due to the double bond formation,[18] triphenylphosphine attacks water and after two proton transfers, nitrogen takes the proton on the oxygen to form the double bond between the oxygen and the phosphor to form the stable triphenylphosphine oxide and the amine moiety is formed.

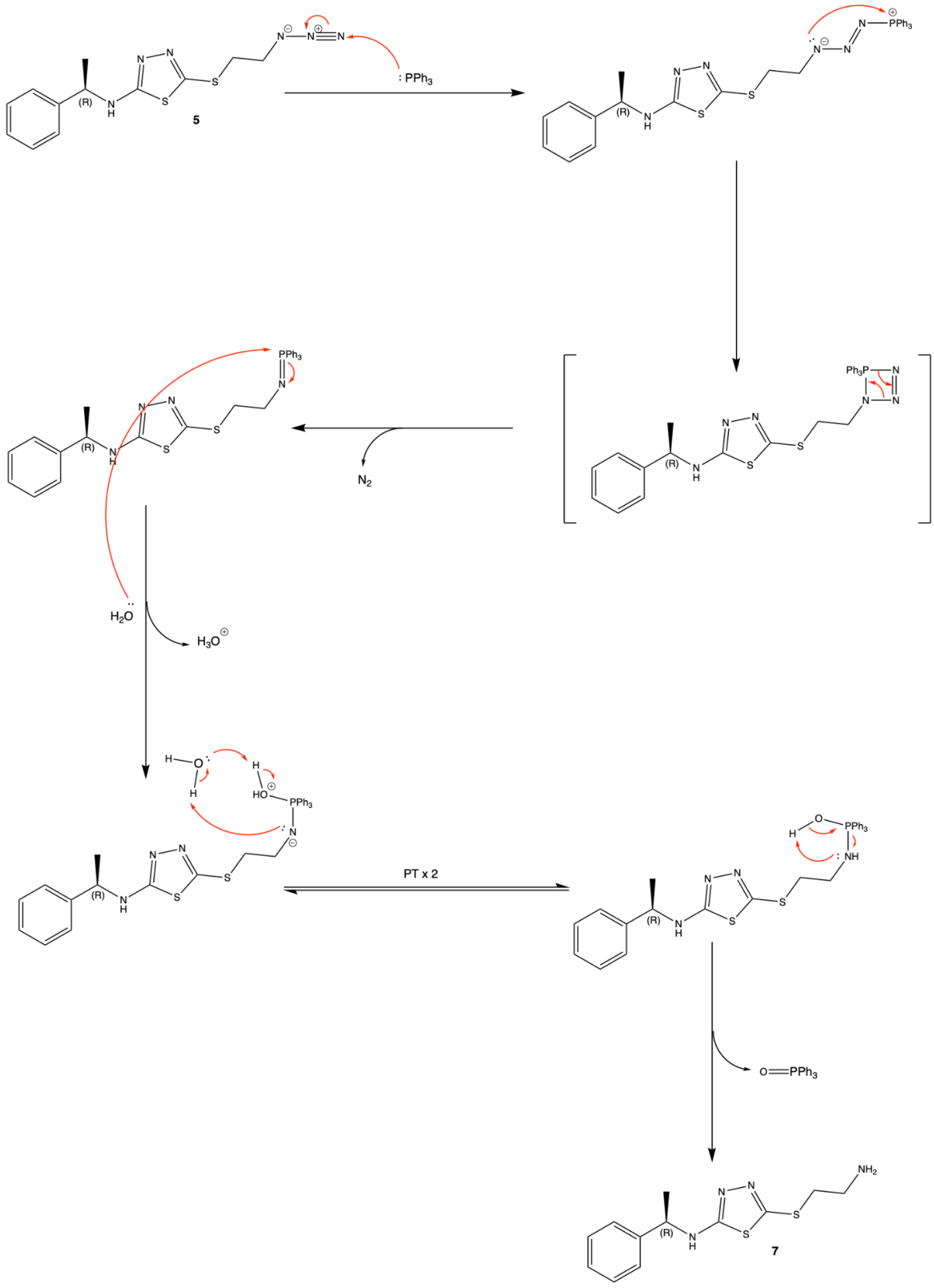


*Scheme 9. Reaction mechanism of the formation of product 7.*

The conversion from azide to amine moiety was performed in sufficient yield and with good purity after prep. HPLC purification. However, ana. HPLC indicated two distinctive peaks in the chromatogram and the purity was calculated to be 93.6% despite the NMR, spectrum A28, displaying different results. An explanation for this could be that a portion of the nitrogens in the molecule are protonated and a portion is not within the mobile phase system. This could explain why two peaks are seen in the chromatogram. The ratio between the two states is determined by pKa and will differ depending on pH. The pKa values of the nitrogens in product **7**, seen in scheme 9, was estimated using empirical pKa in Maestro Scrödinger (-0.5, 1.0, 1.6 and 8.9 from left to right). Based on these estimated pKa values, the primary amine is basic while the other three are acidic. The pH of the mobile phase A of the ana. HPLC is around 2.[19] This would indicate that in this media the primary amine is fully protonated, the secondary and one of the nitrogens in the ring is most likely fully deprotonated. However, the third nitrogen, from the left, has a pKa close to the pH value. This suggests that this nitrogen could be protonated, because when pKa equals pH, 50% of the molecules are protonated/deprotonated.[20] Since the pKa (1.6) is close to 2, this could be the explanation for the 2 peaks seen in the chromatogram. Therefore, the product was determined to have sufficient purity and was sent for functional assay.

## Imines

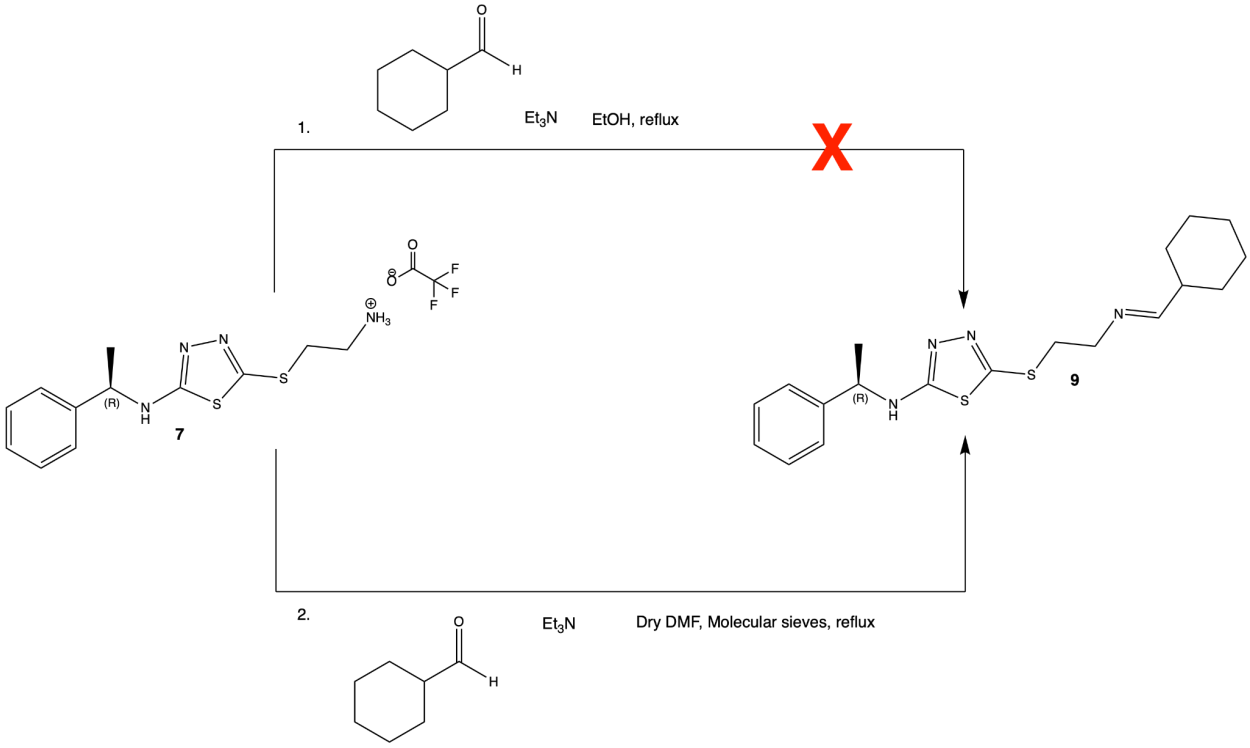


*Scheme 10 Reaction scheme of the different synthetic routes performed to form product **9**.*

Scheme 10 shows the attempts on forming the imine moiety, **9**. The imine moiety was intended to be synthesized to analyze the importance of the hydrogen donating properties of the nitrogen in that position. Route 1 was performed by adding $Et_3N$ to product **7** to neutralize it before adding cyclohexanecarbaldehyde and heating it to around 80°C to form the wanted imine moiety, **9**. This route did not work, both TLC, LCMS and NMR indicated only starting material and reagent present in the sample. More research was needed to optimize the method since the reaction is an equilibrium reaction, optimal conditions and something to drive the reaction forward was needed. This reaction is the first step in a reductive amination. However, in reductive amination, a reducing agent is used to reduce the imine to an amine. This is the driving force for the reaction. Since the imine was supposed to be isolated here, new reaction conditions were needed. It was found that the optimal pH for the reaction is around 3-4 [21] and since this reaction produces water, something to remove the water would help the reaction forward. Therefore, the reaction was optimized to route 2, where only one equivalent of $Et_3N$ was used to neutralize the amine instead of two to not make the solution more basic than needed. Also, the

solvent was switched to DMF instead of EtOH in order to have dry conditions, and DMF was chosen in order to have a solvent with a high boiling point to still be able to heat it above 80°C and since DMF was one of the few organic solvents that could solubilize the amine moiety. Molecular sieves were also added to absorb the formed water to drive the reaction forward. TLC and LCMS indicated only starting material present in the sample. However, NMR indicated the product was indeed formed. Spectrum 8 shows the crude NMR from the route 2 reaction. Here two protons are particularly distinctive, proton I that indicates the reagent is still present and proton 19 that shows the vinyl proton that is not present in the starting material. The reason for the imine moiety **9** not being seen in TLC or LCMS could be explained by the imine moiety not being stable in acidic conditions. Since silica is slightly acidic and the mobile phase in the LCMS is also slightly acidic this could reverse the imine moiety formed back to the starting material. Although the NMR indicated the product was indeed formed, the yield was still very low. Since the NMR was taken after work up since it was believed the reaction did not work from TLC and LCMS results, the starting material was present in the aqueous phase. The crude yield was 10.7% which is the reagent and the product together. The imine moiety **9**, needed to be purified for analysis. Nevertheless, this could not be performed with silica gel chromatography or the normal HPLC system used. This could be purified by switching the column on the HPLC and running a basic mobile phase instead of an acidic but since this was at the end of the time in the lab, there was no time to do this purification. From this, the reaction performed in route 2, was successful and the imine moiety **9** was formed, but more optimization of the reaction conditions is needed for a higher yield. Neutralizing the amine in a separate step could rule out the interference of TFA on the pH value, which would lead to more pH control.

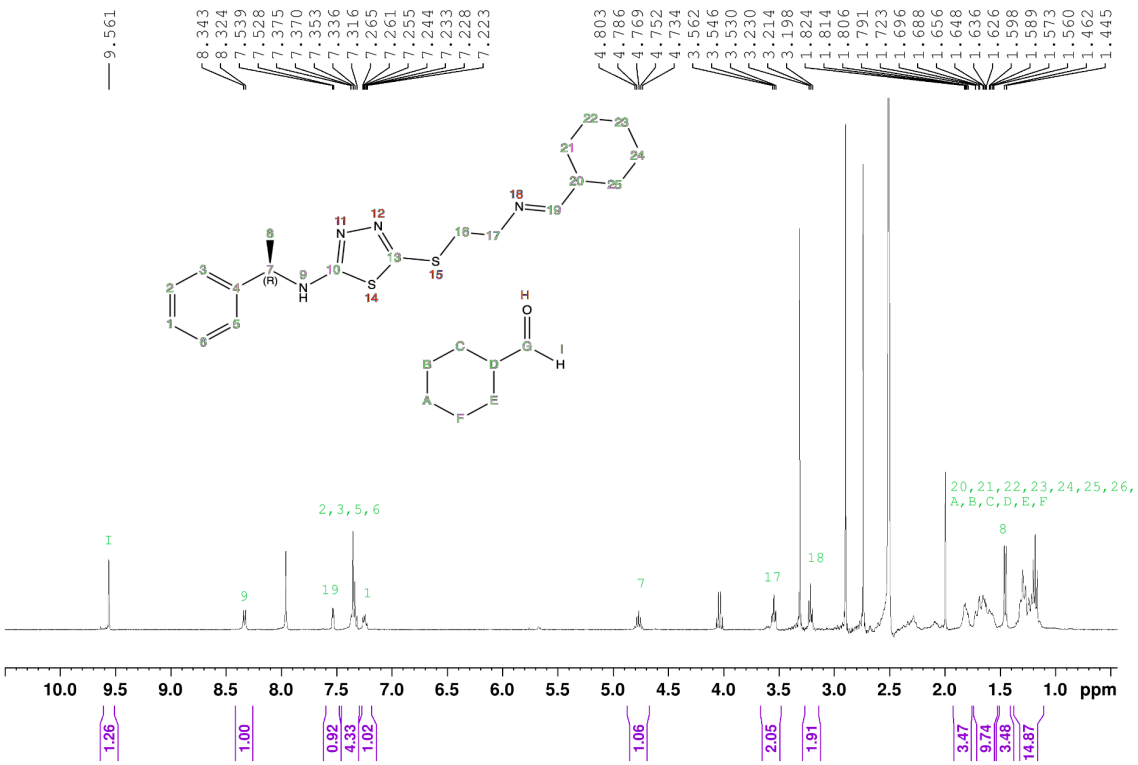


*Spectrum 8. $^{1}H$ NMR of the (R,E)-5-((2-((cyclohexylmethylene)amino)ethyl)thio)-N-(1-phenylethyl)-1,3,4-thiadiazol-2-amine crude (**9**) in DMSO-$d_6$; with all the peaks assigned to protons in the molecule.*

## Synthesis of GluN1/2B analogues

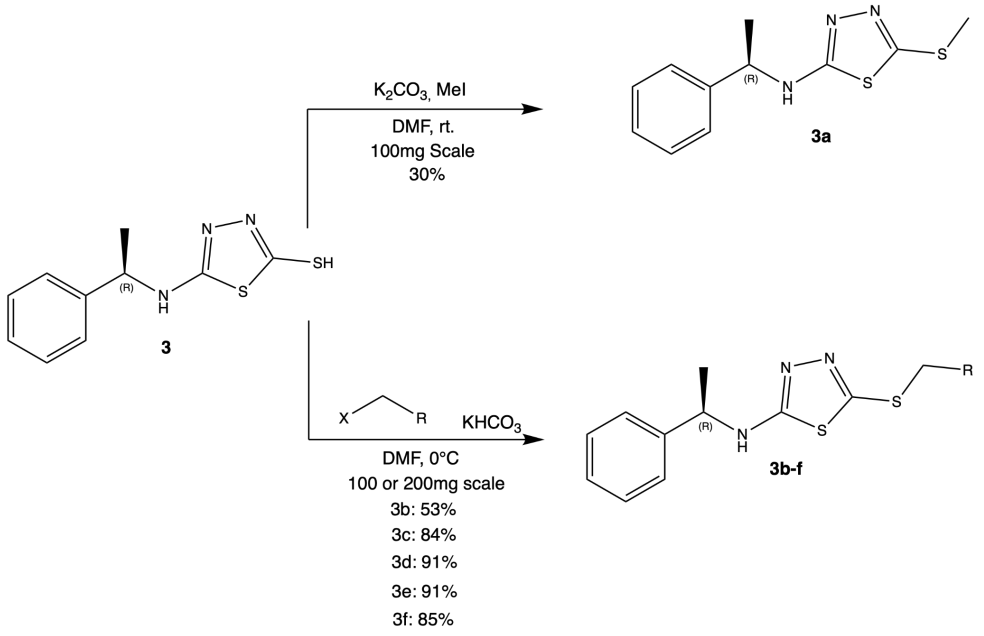


*Scheme 11. Reaction scheme of the synthesis of products **3-3a-f** with scale and yield, x indicating different halogens.*

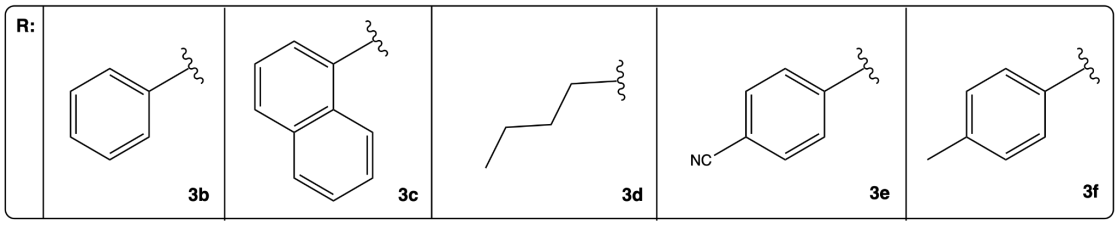


*Figure 13. R-groups synthesized for products **3b-f**.*

The formation of GluN2B analoges was synthesized according to scheme 11 and figure 13 shows the R-groups for six different products. Product **3a** was formed using the same reaction conditions as used for the formation of product **4**, with the exchange of 2-bromoethanol to methyl iodide. The low yield is explained by a double methylation occurring as a side product. The formation of product **3a** yielded a side product. Again, the amine within the product shows nucleophilicity and competes with sulfur in the SN2 reaction. Methyl iodide does not contain the electron density as the hydroxyl group in 2-bromoethanol, leading to no sterical hindrance. The reaction was tracked using TLC and both the product, **3a**, and the side product formed simultaneously. Therefore, for the formation of product **3b**, the reaction conditions were changed

to aid the formation of the wanted product without formation of the side product. The temperature was lowered, and a weaker base was used. This indeed led to a higher yield of the wanted product, although the side product was still formed. Same reasoning as to why applies here as for product **3a**. The conditions were not changed for the formation of product **3c**, in the hope that the change in reagent would not yield a side product. Due to the results of this, the same reaction conditions were used for the formation of products **3d-f**. Determination of purity was accomplished with ana. HPLC and all products showed good yield, apart from product **3a** and **3b** which showed side product formation.

Scheme 12 shows the mechanism of the formation of product **3a**. Potassium carbonate deprotonates the sulfur which leads to a nucleophilic attack on the methyl iodide, yielding product **3a**. After the formation of **3a**, potassium carbonate deprotonates the nitrogen which leads to an additional attack on methyl iodide, yielding the side product. The mechanism is the same for product **3b** except for a different base used, potassium bicarbonate, and for products **3c-f** the mechanism is the same as for product **3b** without the second addition of the reagent. The reasoning behind why there is no double addition for product **3c-f**, could be the same as for product **4**, sterical hindrance. The interesting part is the addition of a methyl group, product **3f** is enough to not get double addition compared to product **3b**. This could perhaps also be a reason for the higher yield in product **3b** compared to **3a**, that the size of the phenyl group is just small enough for the nitrogen to attack, but the sulfur is more available and thus is major.

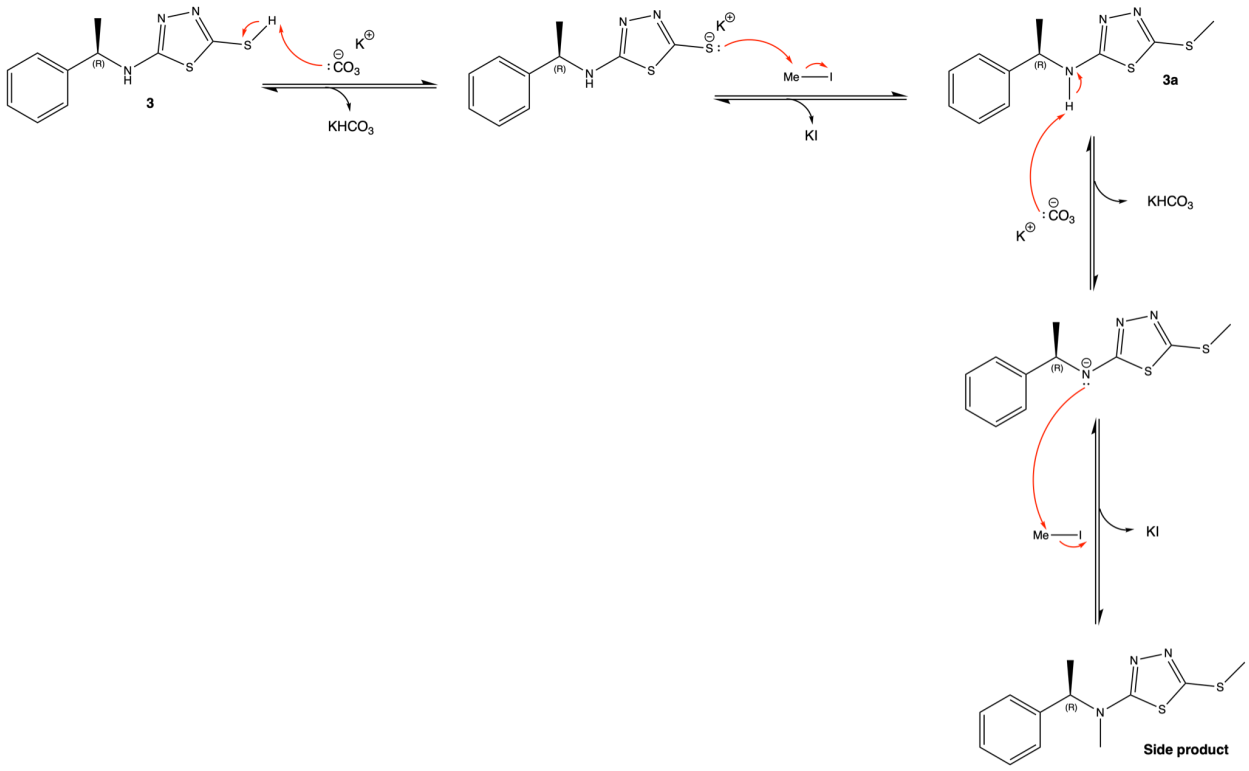


*Scheme 12. Reaction mechanism of the formation of product **3a**.*

There is not as much information on what structural elements yield good activity for the GluN2B receptor. Hence, the reasoning behind the products synthesized was the exchange from valine 267 to phenylalanine 262 and the change in binding properties that entails, together with the difference in size between the pockets due to this amino acid difference between GluN2A and GluN2B. Thus, product **3a** was synthesized to make a small molecule to determine if a smaller molecule would have higher affinity for the GluN2B receptor. Product **3b** was synthesized due to the possibility of a π-π interaction between the phenyl group and phenyl alanine 262. Both products **3c** and **3d** were synthesized to enlarge products **3a** and **3b** to see if a change in size would affect the activity. Lastly, products **3e** and **3f** were both synthesized to add an EWG and an EDG to the phenyl ring to change the electron density within the aromatic system to see what effects this could have on a π-π interaction. Also if a polar group, such as the cyanide group, could interact within the pocket via example hydrogen bonding.

Spectrum 9 shows the aromatic section of the $^{1}$H NMR of product **3c**. The aromatic region was particularly difficult to assign due to the multiple aromatic protons with different shifts. With the

help of the COSY NMR, spectrum 10, and the predicted $^{1}$H NMR from chemdraw, figure 14, the protons were assigned as follows. Seen in the COSY NMR, the doublet assigned as proton 19 and the doublet assigned as proton 22 couple to the multiplet integrated for two protons, assigned as proton 20 and 21. The doublet assigned as proton 24 and the doublet assigned as proton 26 couples to the triplet assigned as proton 25. These protons were assigned accordingly since the protons 19-22 should couple to each other and proton 24-26 should couple to each other according to the structure. Additionally, since there are three protons, 20, 21 and 25 that couple to more than one proton, these were assigned as the multiplet and triplet. Furthermore, the four doublets should be the protons only sitting next to one other proton, 19, 22, 24 and 26. To distinguish between which doublet is 19 and 22, and which doublet is 24 and 26, the predicted $^{1}$H NMR from chemdraw was useful. Figure 14 shows the predicted shifts for all the protons in the molecule. This indicates that proton 22 should have a higher shift than proton 19, and that proton 24 should have a significantly higher shift than proton 26, which correlates with the $^{1}$H NMR. Another indication to distinguish proton 19 and 22, is that proton 19 has a small split in the doublet, this could be due to influence from the protons in position 16. This agrees with the suggestion that proton 22 should have a higher shift than proton 19. Protons one to six were assigned based on the integration in the $^{1}$H NMR, proton 9 was assigned based on no coupling with any other aromatic protons.

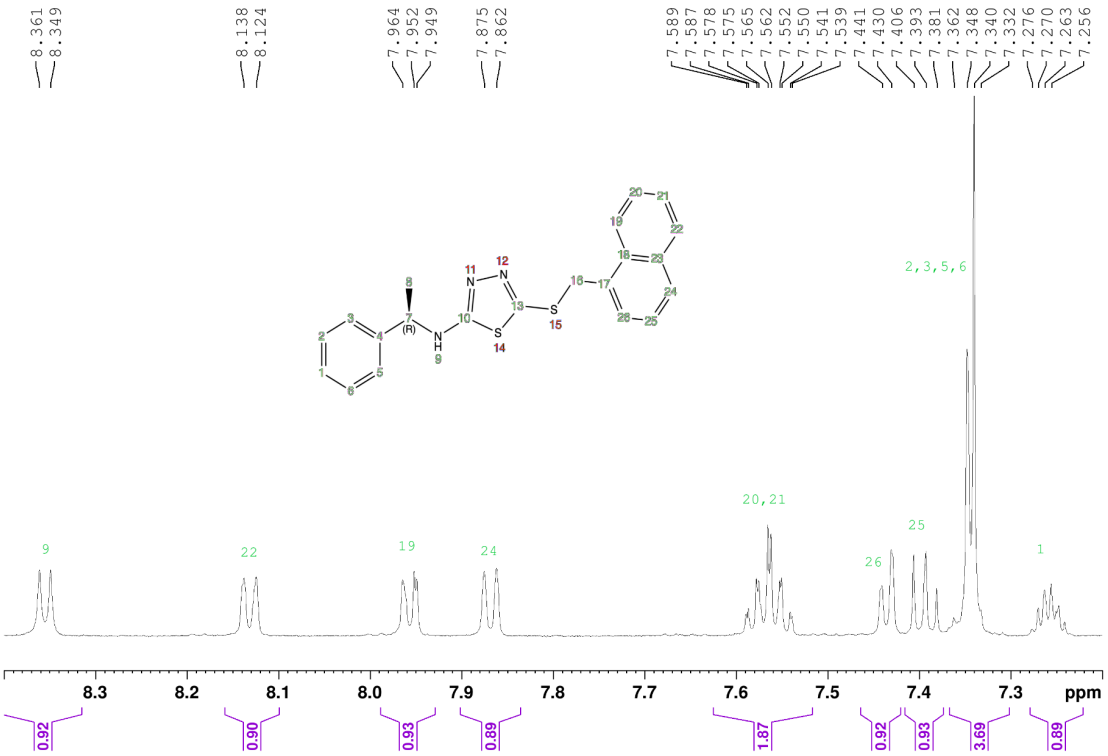


*Spectrum 9. $^{1}H$ NMR of (R)-5-((naphthalen-1-ylmethyl)thio)-N-(1-phenylethyl)-1,3,4-thiadiazol-2-amine (**3c**) in DMSO-$d_6$,; zoomed in on aromatic section.*

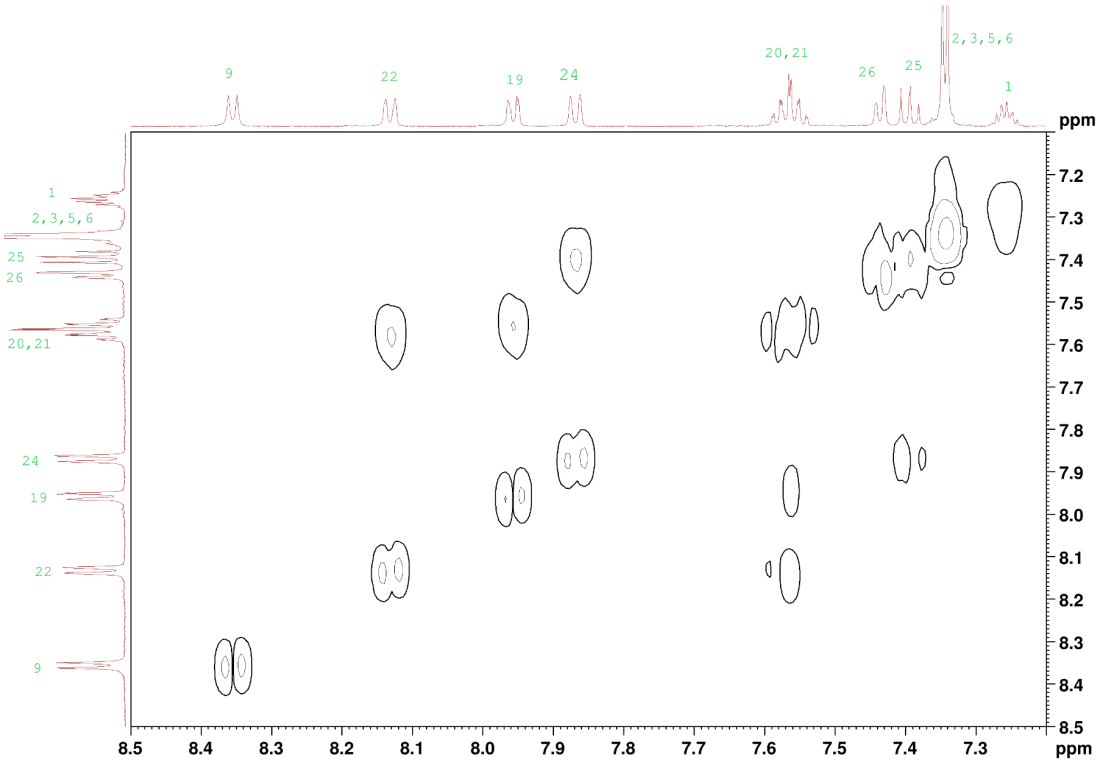


*Spectrum 10. COSY NMR of (R)-5-((naphthalen-1-ylmethyl)thio)-N-(1-phenylethyl)-1,3,4-thiadiazol-2-amine (**3c**) in DMSO-$d_6$,; zoomed in on aromatic section.*

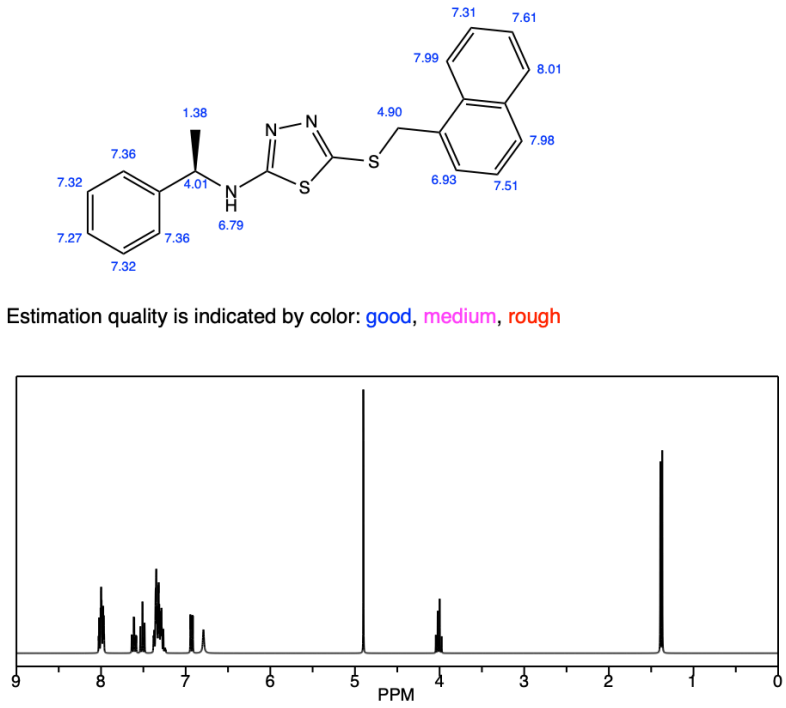


*Figure 14. Predicted $^{1}H$ NMR from chemdraw v. 19.1.*[22]

## Computational modeling

A homology model of the receptor GluN1/2B was made based on an existing crystal structure of the agonist binding domains from one GluN1-subunit together with one GluN2A-subunit with an agonist in the binding site. This homology model was made using Schrödinger functions, such as Prime Energy. Known ligands were processed using Schrödinger's Ligprep. This was used to construct 3D- structures for each ligand. These poses were used for Induced-Fit docking for both the GluN1/2A model and the GluN1/2B model, using the Schrödinger's IFD software, and poses with good IFD-scores and binding like the ligand in the crystal structure were selected for Root Mean Square Deviation (RMSD)-metadynamics simulations. These simulations give an indication into the binding properties of each ligand but also the stability of the pose within the binding domain. Molecular dynamics were used to predict binding poses and metadynamics were used for stability predictions. Both molecular dynamics and metadynamics were run with gromacs.[23]

Product **3a**, **3b**, **6a**, **6b**, **6c** was used in the simulations. From these simulations, products **3b**, **6b** and **6c** did not show any stable poses and therefore will not be discussed further. Firstly, product **3a** showed a stable pose when bound to the GluN1/2A complex even though showing a higher scoring in the Induced Fit Docking. It should be noted that a small ligand could yield a low RMSD despite the Induced Fit Docking results. Secondly, product **6a** showed low scores in the Induced Fit Docking and relatively stable poses for both complexes GluN1/2A and GluN1/2B. It should be noted that for the pose in the GluN1/2A complex one amino acid is largely shifted towards the triazole moiety. Another interesting result is the binding interaction with the closest amino acids in the GluN1/2B complex, seen in figure 15. The triazole interacts via π-π interaction with the non-conserved phenylalanine.[23]

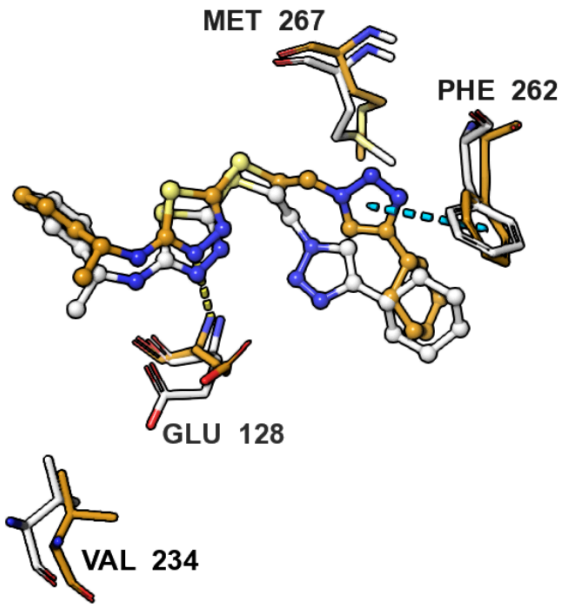


*Figure 15. 3D schematic of product **6a** bound in the GluN1/2B complex.[23]*

These results would indicate that product **3a** could be a potential antagonist for GluN1/2A but not for GluN1/2B. This contradicts the theory behind the synthesis of product **3a**. However, as stated above, better metadynamics results could be produced due to the size of the structure. The results for product **6a** indicate that it binds well within the GluN1/2A complex which correlates with the theory behind its synthesis. However, it also shows promising results for the GluN1/2B complex. This pose indicates that the π-π interaction between the phenylalanine and the triazole

ring within the product produces a strong interaction that yields a stable pose within the GluN1/2B complex. Although theoretically the size of this product should favor the binding for the GluN1/2A complex. This interaction does indicate that an interaction with the phenylalanine is possible at the triazole position. Since product **6b** and **3b** does not show stable poses, it could indicate that an aromatic ring at the further distance, such as in product **6b**, and at a shorter distance, such as in product **3b**, can't make this interaction. This would strengthen the theory behind the synthesis of product **3c** and **7** since product **3c** is an extension of product **3b** and product **7** could theoretically make a cation-π interaction at the same distance as for the triazole interaction. Nevertheless, it should be stated that molecular modeling results only give an indication of the ligands binding poses and the binding properties but can be used to strengthen the theory behind what properties yield wanted activity results.

# Conclusion & Future aspects

As presented earlier, it is difficult to make potent antagonists for the NMDA receptors without major side effects. Despite antagonists such as ketamine and memantine that are both clinically tolerated, no NAMs are yet clinically tolerated. Although efforts are being made to make potent selective antagonists that bind allosterically, it has been proven difficult due to e.g. the similarity between NMDA subtypes. Therefore, more research is needed to fill the gap of clinically tolerated NAMs for NMDA receptors.

In this thesis, the focus has been on synthesizing potential NAMs for the GluN1/2A and GluN1/2B subtypes. For the GluN1/2A receptor, there has been a lot of research already done. Therefore, the focus has been on finding bioisosteres for the amide moiety from the TCN213 scaffold. Here synthesis of triazole moieties have been made in the purpose of rigidifying the amide moiety and adding new interaction possibilities. It was also desired to identify the importance of the amide within the TCN213 analogue and what binding properties there are. Therefore, a reversed amide moiety was synthesized to switch the position of the carbonyl to see if the specific position of the carbonyl is of importance. Efforts were also made to make an imine moiety to identify the importance of the nitrogen as a hydrogen bond donor. Due to time restraints the imine moiety was not isolated due to difficulty in synthesizing the imine in enough yield together with stability issues. The importance of the hydrogen bond donor property of the nitrogen in the amide can be tested by synthesizing other analogues such as a tertiary amine or an ester to keep the rigidity. Other amide bioisosteres that would be interesting to synthesize is e.g. a fluoroalkane, since this removes the hydrogen bond interactions completely and would give insight into the importance of this interaction.

For the GluN1/2B there has not been as much research done already. Therefore, potential GluN1/2B NAMs were made based on the knowledge of a non-conserved amino acid between the receptors GluN1/2A and GluN1/2B. Here different analogues were synthesized based on the knowledge that the binding pocket in GluN1/2B is smaller compared to in GluN1/2A and the different binding properties that the change in valine to phenylalanine present. For this reason, analogues with different aromatic rings were synthesized in hope of a $\pi$-$\pi$ interaction occurring.

Other analogues without aromatic properties were also synthesized since in theory a smaller and more flexible molecule could be selective for the GluN1/2B receptor due to the size decrease of the binding pocket. Additionally, one molecule was synthesized due to the possibility of a cation-π interaction. For this thesis, the main focus has been on making changes on the right-hand side of the TCN213 scaffold due to the known change in amino acid in this location.

What the activity of these synthesized analogues do have and what results that give can't be determined without functional assay results. Since the department sends these samples to the USA to be performed, the results have not yet been presented and are therefore not included in this thesis. However, computational modeling results have been given on some of the products synthesized. These results indicate that a π-π interaction is possible in the GluN1/2B receptor, which adheres to theory. But it also indicates at what distance this interaction is possible. Therefore, synthesizing analogues with an aromatic property at a 3-atom distance from the 1,3,4-thiadiazole would be suggested. Specifically, a heterocyclic aromatic ring since this would add other interactions possibilities, such as hydrogen bond interactions, together with changing the electron density of the ring compared to the phenyl rings synthesized.

# Experimental

## General

### Thin layer chromatography - TLC

TLC was performed using silica gel 60 $F_{254}$ (supelco) and visualized with UV-light or staining agents. The different staining agents used were $KMnO_4$ as a common staining agent and Ninhydrin for amines.

### Flash Chromatography

Flash chromatography was performed using silica gel 60A, particle size 35-70 micron, Davisil.

### Nuclear magnetic resonance - NMR

NMR spectra were obtained with a 400 or 600 MHz Bruker instrument and processed using Topspin 4.3.0 software. The signals were expressed in ppm (δ) and the coupling constants in Hertz (Hz). Signal assignments were assessed from chemical shifts and comparison from previous experiments. The multiplet pattern is given by these abbreviations: m - multiplet, s - singlet, d - doublet, t - triplet, q - quartet, quin - quintet, sext - sextet.

### Liquid Chromatography Mass Spectrometry - LCMS

LC-MS spectra were obtained with an Agilent 6130 mass spectrometer instrument, using electron spray ionization (ESI), coupled to an Agilent 1200 HPLC system (ESI-LC-MS) with a C18 reverse phase column (Zorbax Eclipse XBD-C18, 4.6mm x 50mm), together with an autosampler and diode array detector, using a linear gradient of the binary solvent system of buffer A (milliQ $H_2O$:AcN:formic acid, 95:5:0.1 v/v%) to buffer B (AcN:formic acid, 100:0.1 v/v%) with a flow rate of 1 ml/min.

The samples were prepared in 1:1 AcN:$H_2O$ with a concentration between 0.2-0.5mg/ml with an injection volume of 5 µl.

## Ultra Performance Liquid Chromatography Mass Spectrometry - UPLCMS

UPLC-MS spectra were obtained with a Waters Acquity H-class UPLC using a sample manager FTN and a TUV dual wavelength detector, coupled to a QDa single quadrupole analyser, using ESI. Separation was achieved with a C18 reverse phase column (Acquity UPLC BEH C18, 2.1mm x 50 mm, 1.7µm), operated at 40°C using a linear gradient of the binary system of buffer A (milliQ $H_2O$:AcN:formic acid, 95:5:0.1 v/v%) to buffer B (AcN:formic acid, 100:0.1 v/v%) with a flow rate of 0.8 ml/min.

The samples were prepared in 1:1 AcN:$H_2O$ with a concentration <0.1mg/ml, filtered through 0.22µm, with an injection volume of 1µl.

## High Resolutions Mass Spectrometry - HRMS

The samples were prepared by dissolving the sample in the matrix solution below, with a concentration of 1mg/ml, added onto a Matrix-assisted laser desorption/ionization plate and sent for analysis.

Matrix solution: 20mg/ml 2.5-Dihydroxybenzoic acid in Methanol.

## Analytical High performance liquid chromatography - Ana. HPLC

Ana. HPLC was used to identify the purity of final compounds and to optimize methods for Prep. HPLC.

Instrument 1: Ultimate 3000 HPLC system with an LGP-3400A pump (1ml/min), WPS-3000SL analytical autosampler (100µl loop) and a DAD-3000D diode array detector (200, 210, 225, 254 nm). Using a Gemini-NX C18 column (4.6 x 250mm, 3µm, 110Å) and mobile phase A: $H_2O$:TFA - 100:0.1 v/v%, mobile phase B: AcN:$H_2O$:TFA - 90:10:0.1 v/v/v%. The data was processed using Chromeleon software v. 6.8.

Instrument 2: Thermo Scientific UltiMate 3000 HPLC system with an HPG-3400SD pump (1ml/min), WPS-3000SL Analytical Autosampler (100µl loop) and a DAD-3000D diode array

detector (210, 214, 254, 280 nm). Using a Gemini-NX C18 column (4.6 x 250mm, 3µm, 110Å) and mobile phase A: $H_2O$:TFA - 100:0.1 v/v%, mobile phase B: AcN:$H_2O$:TFA - 90:10:0.1 v/v/v%. The data was processed using Chromeleon software v. 7.3.

The mobile phase compositions in the methods are based on mobile phase A and B.

Method A: Gradient 0-15 min going from 0-100% mobile phase B.
Method B: Gradient 0-20 min going from 0-100% mobile phase B.
Method C: Isocratic 0-15 min with 50% mobile phase B.
Method D: Isocratic 0-10min with 60% mobile phase B.
Method E: Gradient 0-15 min going from 20-80% mobile phase B.
Method F: Gradient 0-8min going from 20-55% mobile phase B and then isocratic 8-12min with 100% mobile phase B.

The samples were prepared in AcN or $H_2O$ with a concentration between 0.4-1.0mg/ml.

Retention times ($t_R$) are expressed in minutes (min).

The purity calculation is based on the relative area of the peaks in the chromatogram. Each peak in a chromatogram is integrated, generating a measure of the area under the peak which corresponds to the relative area. The relative area describes how much of the combined peak areas that a specific peak occupies. This is expressed in percent, generating the purity of the sample. The software automatically calculates the relative area based on the integration.

## Preparative High performance liquid chromatography - Prep. HPLC

Compounds were purified using Prep. HPLC.

Instrument 1: Ultimate 3000 HPLC system with an HGP-3200BX pump (20ml/min), a Rheodyne 9725i injector, a 10ml loop, a MWD-3000SD detector (210, 225, 254, 280 nm), and an AFC-3000SD automated fraction collector. Using a Gemini-NX C18 column (21.2 x 250 mm,

5µm, 110Å) (Phenomenex) and mobile phase A: $H_2O$:TFA - 100:0.1 v/v%, mobile phase B: AcN:$H_2O$:TFA - 90:10:0.1 v/v/v%. The data was processed using Chromeleon software v. 6.8.

Instrument 2: Dionex HPLC system with an HGP-3200BX pump (20ml/min), a Rheodyne 7725i injector, a 10ml loop, MWD-3000SD detector (200, 210, 254, 280 nm), and an AFC-3000SD automated fraction collector. Using a Gemini-NX C18 column (21.2 x 250 mm, 5µm, 110Å) (Phenomenex) and mobile phase A: $H_2O$:TFA - 100:0.1 v/v%, mobile phase B: AcN:$H_2O$:TFA - 90:10:0.1 v/v/v%. The data was processed using Chromeleon software v. 7.3.

Same methods as for Ana. HPLC was used for prep. HPLC.

The samples were prepared in the initial mobile phase system as the method that was used.

## Functional Assay

The samples are sent to the USA for functional assay.

The functional assay is performed using the two-electrode voltage clamp assay. The GluN1/2 receptors are expressed in frog eggs, also called Xenopus oocytes. When the receptors are expressed, the oocytes are injected with a solution to prevent activity dependent increases in the measured response. The potential NAMs are then dissolved in DMSO before addition to the oocytes.[24] As seen in figure 16, electrodes are inserted to be able to add a current over the system to measure a membrane potential.[25] When glutamate is added to the oocytes, the potential across the membrane is decreased due to ion channel opening. The potential NAMs are then added in different concentrations to calculate the $EC_{50}$ value by measuring the difference in membrane potential when a NAM is added, with the presence of glutamate at a set concentration. If the potential does not decrease, the potential NAM is blocking the channel from opening.[24]

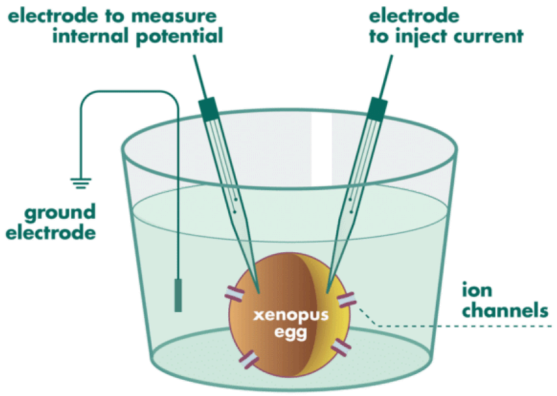


*Figure 16. Representation of the two-electrode voltage clamp assay.*[25]

# Synthesis

All synthesized products were analyzed using TLC, LCMS or UPLCMS, and NMR. The final products have additionally been analyzed using HRMS and ana. HPLC. The purity of the intermediates was determined with NMR while the purity for the final products were determined with ana. HPLC. Product 3a-f, 6a-c, 7 and 8a-c were sent for functional assay.

## Starting synthesis

**Formation of (*R*)-(1-isothiocyanoethyl)benzene (1)**

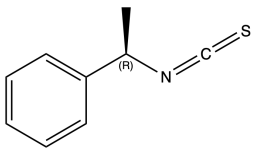


$CS_2$ (48.0ml, 794.3mmol, 9.93 eq.) and $Et_3N$ (11.5ml, 82.5mmol, 1.0 eq.) was added successively in small portions to a solution of α-methylbenzylamine (10.0ml, 80.0mmol, 1.0 eq.) in absolute EtOH (47ml) and left to stir for 40 min at rt. Afterwards, the reaction mixture was cooled to 0°C and a solution of $Boc_2O$ (17.3g, 79.3mmol, 0.99 eq.) in EtOH (19ml) was added followed by the immediate addition of DMAP (197.3mg, 1.6mmol, 0.02 eq.) in EtOH (19ml). Gas evolution was noted. The reaction mixture was left in the ice bath and allowed to reach r.t overnight. The reaction mixture was extracted with 2 x 80 ml EtOAc (some brine was added to separate the phases) and the combined organic layers were washed with 150 ml brine. The

solvent was evaporated under reduced pressure. HCl (aq.) (15ml, 0.2M) was added to acidify the SM to be able to extract the product. EtOAc (50ml) was added, and the phases were separated. The organic layer was washed with brine (25ml) and the solvent was evaporated under reduced pressure to afford (*R*)-(1-isothiocyanoethyl)benzene (11.3g, 69.6mmol, 87%) as a yellow liquid. **TLC**: 1:2 EtOAc:Heptane, Rf: 0.85, **$^{1}$H NMR** (600MHz, $CDCl_3$): δ 7.16-7.31 (m, 5H), 4.83 (q, *J* = 6.8Hz, 1H), 1.58 (d, *J* = 6.8Hz, 3H) ppm. **$^{13}$C NMR** (600MHz, $CDCl_3$): δ 140.2, 128.9, 128.2, 125.5, 57.1, 25.0 ppm.

**Formation of (*R*)-*N*-(1-phenylethyl)hydrazinecarbothioamide (2)**

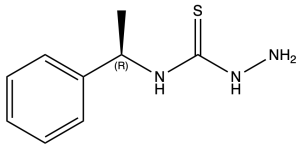


(1-isothiocyanoethyl)benzene (12.1g, 74.4mmol, 1.0 eq.) was added to a stirred solution of hydrazine hydrate (4.5ml of a 50-60% aq. solution, 89.9mmol, 1.2 eq.) in iPrOH (340ml) at r.t. After 30 min, the reaction was cooled down to 0°C and left to reach r.t O/N. The crude product was purified by flash chromatography (Gradient from 1:3 EtOAc:Heptane to 1:10 DCM:MeOH) to afford (*R*)-*N*-(1-phenylethyl)hydrazinecarbothioamide (14.4g, 73.6mmol, 99%) as a white solid. **TLC**: 1:1 EtOAc:Heptane, Rf: 0.32, **LCMS**: 3.8min, $[196.2]^{+}$, **$^{1}$H NMR** (400MHz, DMSO-$d_6$): δ 8.70 (s, 1H), 7.99 (d, *J* = 8.7Hz, 1H), 7.37-7.30 (m, 4H), 7.23 (tt, *J* = 6.93, 1.67Hz, 1H), 5.54 (quin, *J* = 7.3Hz, 1H), 4.52 (s, 1H), 1.46 (d, *J* = 7.0, 3H) ppm. **$^{13}$C NMR** (400MHz, DMSO-$d_6$): δ 181.0, 144.7, 128.7, 127.1, 126.7, 52.2, 22.5 ppm.

**Formation of (*R*)-5-((1-phenylethyl)amino)-1,3,4-thiadiazole-2-thiol (3)**

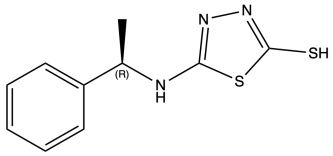


KOH (72.0ml, 72.0mmol, 1.0eq. 1N aq.) was added to a stirred solution of (*R*)-*N*-(1-phenylethyl)hydrazinecarbothioamide (14.0g, 71.7mmol, 1.0 eq) in absolute EtOH (355ml). $CS_2$ (21.1ml, 349.2mmol, 4.9eq.) in absolute EtOH (36ml) was added in small portions (slightly yellow to yellow) and the reaction mixture was refluxed O/N. Excess EtOH was removed under reduced pressure and the mixture was diluted with ice water (260ml). The

reaction mixture was acidified with HCl (28.5ml, 1M aq.) and the formed precipitate was filtered, washed with ice water (150ml) and dried under reduced pressure to afford (*R*)-5-((1-phenylethyl)amino)-1,3,4-thiadiazole-2-thiol (14.6g, 61.7mmol, 83%) as a white solid. **TLC**: 1:1 EtOAc:Heptane, Rf: 0.58, **LCMS**: 4.1min, $[238.1]^+$ , **$^1$H NMR** (400MHz, DMSO-$d_6$): δ 13.20 (s, 1H), 8.03 (d, *J* = 6.6, 1H), 7.31-7.36 (m, 4H), 7.22-7.26 (m, 1H), 4.65 (quin, *J* = 6.9, 1H), 1.41 (d, *J* = 6.9, 3H) ppm. **$^{13}$C NMR** (600MHz, DMSO-$d_6$): δ 181.0, 160.5, 144.3, 128.9, 127.5, 126.3, 53.8, 23.6 ppm.

## Triazole synthesis

**Formation of (*R*)-2-((5-((1-phenylethyl)amino)-1,3,4-thiadiazole-2-yl)thio)ethan-1-ol (4)**

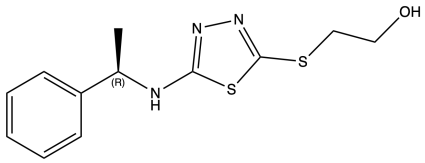


$K_2CO_3$ (1.2g, 8.4mmol, 2.0eq.) and 2-bromoethanol (0.37ml, 5.2mmol, 1.2eq.) was added to a solution of (*R*)-5-((1-phenylethyl)amino)-1,3,4-thiadiazole-2-thiol (1.0g, 4.2mmol, 1.0 eq.) dissolved in DMF (10ml). The reaction mixture was left to stir at r.t O/N. The reaction mixture was diluted with $H_2O$ (20ml) and extracted with EtOAc (3x40ml). The combined organic layers were washed with $CaCl_2$ (3 x 10ml), dried over $MgSO_4$ and then the solvent was removed under reduced pressure to afford (*R*)-2-((5-((1-phenylethyl)amino)-1,3,4-thiadiazole-2-yl)thio)ethan-1-ol (1.1g, 3.98mmol, 94%) as a slightly yellow oil (DMF contamination). **TLC**: 3:1 EtOAc:Heptane, Rf: 0.46, **LCMS**: 3.8min $[282.1]^+$, **$^1$H NMR** (600MHz, DMSO-$d_6$): δ 8.34 (d, *J* = 7.3Hz, 1H), 7.32-7.37 (m, 4H), 7.23-7.26 (m, 1H), 5.00 (t, *J* = 5.5Hz, 1H), 4.77 (quin, *J* = 7.0Hz, 1H), 3.61 (q, *J* = 6.2Hz, 2H), 3.11 (t, *J* = 6.5, 2H), 1.46 (d, *J* = 6.9Hz, 3H) ppm. **$^{13}$C NMR** (600MHz, $CDCl_3$): δ 173.6, 155.6, 149.3, 133.6, 132.2, 131.3, 70.2, 65.1, 59.6, 28.4 ppm.

**Formation of (*R*)-5-((2-azidoethyl)thio)-*N*-(1-phenylethyl)-1,3,4-thiadiazol-2-amine (5)**

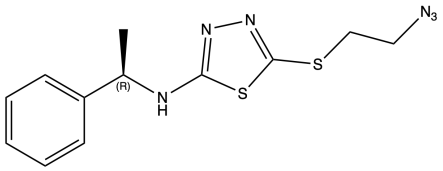

(*R*)-2-((5-((1-phenylethyl)amino)-1,3,4-thiadiazole-2-yl)thio)ethan-1-ol (242mg, 0.84mmol, 1.0 eq.) in dry DCM (5ml) was added to a solution of p-toluenesulfonyl chloride (210.8mg, 1.1mmol, 1.3 eq.), DMAP (12.3mg, 0.10mmol, 0.12 eq.) and $Et_3N$ (0.3ml, 2.2mmol, 2.6 eq.) in dry DCM (5ml) at 0°C. The reaction mixture was then stirred in the ice bath for 1.5 h and then diluted with $H_2O$ (20ml). The clear yellow mixture was then extracted with DCM (3 x 10ml) and the combined organic layers were dried over $MgSO_4$ and then evaporated under reduced pressure. After drying under vacuum for an additional 15 min the crude was dissolved in DMF (5ml). $NaN_3$ (264mg, 4.1mmol, 4.8 eq.) in DMF (10ml) was added to the reaction mixture and left to stir at 60°C for 2 h. The reaction mixture was quenched with $H_2O$ (20ml) and then extracted with EtOAc (3 x 15ml). The combined organic layers were washed with $CaCl_2$ (3 x 20ml), dried over $MgSO_4$ and then the solvent was evaporated under reduced pressure to afford (*R*)-5-((2-azidoethyl)thio)-*N*-(1-phenylethyl)-1,3,4-thiadiazol-2-amine (198mg, 0.65mmol, 77%) as a as a slightly yellow oil (DMF contamination). **TLC**: 2:1 EtOAc:Heptane, Rf: 0.6, **LCMS**: 4.4min $[307.1]^+$, **$^1$H NMR** (400MHz, DMSO-$d_6$): δ 8.39 (d, *J* = 7.2Hz, 1H), 7.32-7.37 (m, 4H), 7.23-7.26 (m, 1H) 4.78 (quin, *J* = 6.8Hz, 1H), 3.59 (t, *J* = 6.4Hz, 2H), 3.25 (t, *J* = 6.5Hz, 2H), 1.46 (d, *J* = 6.8, 3H) ppm. **$^{13}$C NMR** (400MHz, DMSO-$d_6$): δ 169.1, 149.5, 144.4, 128.9, 127.8, 126.5, 60.3, 54.8, 50.3, 23.6 ppm.

**(*R*)-5-((2-(4-(cyclohexylmethyl)-1*H*-1,2,3-triazol-1-yl)ethyl)thio)-*N*-(1-phenylethyl)-1,3,4-thiadiazol-2-amine (6a)**

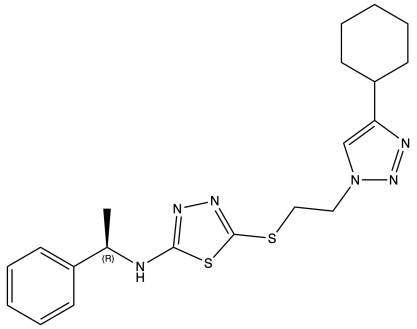

(*R*)-5-((2-azidoethyl)thio)-N-(1-phenylethyl)-1,3,4-thiadiazol-2-amine (221mg, 0.72mmol, 1 eq.), $CuSO_4 \cdot 5H_2O$ (19.4mg, 0.08mmol, 0.11 eq.) and cyclohexylacetylene (0.14ml, 1.08mmol, 1.5 eq.) was dissolved in 2:1 $H_2O$:AcN (12ml). The reaction mixture got murky, with dark solids swirling around. Hydrazine monohydrate (0.02ml, 0.72mmol, 1.0 eq.) was added dropwise under vigorous stirring at rt. After 20 min the reaction was stopped. The precipitate was filtered and washed with $H_2O$. The solids were then dissolved in DCM, dried with $MgSO_4$ and then filtered through a pad of celite. The solvent was then evaporated under reduced pressure. The crude was purified with flash chromatography (Gradient from 100% Heptane to 100% EtOAc with 10% DCM, all with 0.5% $Et_3N$) to afford (*R*)-5-((2-(4-(cyclohexylmethyl)-1*H*-1,2,3-triazol-1-yl)ethyl)thio)-*N*-(1-phenylethyl)-1,3,4-thiadiazol-2-amine (110mg, 0.27mmol, 37%) as a white solid. **TLC**: 1:1 EtOAc:Heptane, Rf: 0.17. **UPLCMS**: 2.6min $[415.2]^+$, **HRMS**; Theoretical mass (M+H): $[415.1733]^+$, measured mass (M+H): $[415.1734]^+$, **$^1$H NMR** (400MHz, DMSO-$d_6$): δ 8.39 (d, *J* = 7.2Hz, 1H), 7.81 (s, 1H), 7.32-7.37 (m, 4H), 7.23-7.26 (m, 1H), 4.78 (quin, *J* = 7.0Hz, 1H) 4.59 (t, *J* = 6.5Hz, 2H), 3.53 (t, *J* = 6.6Hz, 2H), 1.91-1.94 (m, 2H), 1.72-1.75 (m, 2H), 1.65-1.68 (m, 1H), 1.46 (d, *J* = 6.9Hz, 3H), 1.31-1.37 (m, 4H), 1.16-1.24 (m, 2H) ppm. **$^{13}$C NMR** (400MHz, DMSO-$d_6$): δ 169.0, 152.6, 149.3, 144.4, 128.9, 127.5, 126.5, 121.3, 54.8, 49.1, 35.0, 34.2, 33.0, 26.1, 26.0, 23.6 ppm. **Ana. HPLC**: $t_R$= 13.02 min, Method A, Instrument 1. **Purity**: 96.0%.

**Formation of**

**(*R*)-5-((2-(4-phenyl-1H-1,2,3-triazol-1-yl)ethyl)thio)-N-(1-phenylethyl)-1,3,4-thiadiazol-2-amine (6b)**

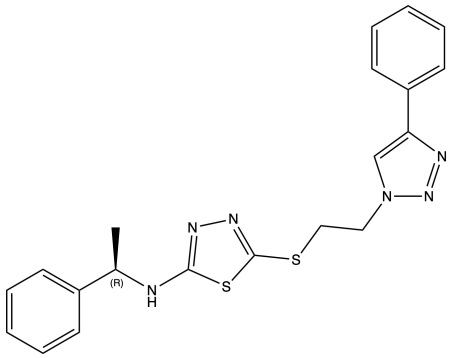


(*R*)-5-((2-azidoethyl)thio)-N-(1-phenylethyl)-1,3,4-thiadiazol-2-amine (300mg, 0.98mmol, 1 eq.), $CuSO_4 \cdot 5H_2O$ (24.5mg, 0.10mmol, 0.10 eq.) and phenylacetylene (0.16ml, 1.47mmol, 1.5

eq.) was dissolved in 2:1 $H_2O$:AcN (12ml). The reaction mixture got murky, with dark solids swirling around. Hydrazine monohydrate (0.03ml, 0.98mmol, 1.0 eq.) was added dropwise under vigorous stirring at rt. After 20 min the reaction was stopped. The precipitate was filtered and washed with $H_2O$. The solids were then dissolved in DCM, dried with $MgSO_4$ and then filtered through a pad of celite. The solvent was then evaporated under reduced pressure. The crude was re-dissolved in EtOAc:$H_2O$ 1:1, the phases were separated and the aqueous phase was extracted with EtOAc (3 x 10ml). The combined organic layers were dried over $MgSO_4$, and the solvent was evaporated under pressure. The crude was dissolved in AcN and $H_2O$ was added until the product precipitated. The mixture was filtered to afford (*R*)-5-((2-(4-phenyl-1H-1,2,3-triazol-1-yl)ethyl)thio)-N-(1-phenylethyl)-1,3,4-thiadiazol-2-amine (268mg, 0.66mmol, 67%) as a beige solid. **TLC**: 2:1 EtOAc:Heptane, Rf: 0.22, **UPLCMS**: 2.5min $[409]^+$, **HRMS**; Theoretical mass (M+H): $[409.1263]^+$, measured mass (M+H): $[409.1265]^+$, **$^1$H NMR** (400MHz, DMSO-$d_6$): δ 8.57 (s, 1H), 8.39 (d, *J* = 7.2Hz, 1H), 7.83 (dd, *J* = 7.3, 1.6Hz, 2H), 7.46 (dt, *J* = 7.3, 1.6Hz, 2H), 7.32-7.37 (m, 5H), 7.22-7.28 (m, 1H), 4.76 (quin, *J* = 7.0Hz, 1H), 4.71 (t, *J* = 6.5Hz, 2H), 3.62 (t, *J* = 6.6Hz, 2H), 1.44 (d, *J* = 6.9Hz, 3H) ppm. **$^{13}$C NMR** (600MHz, DMSO-$d_6$): δ 169.3, 149.3, 146.8, 144.4, 131.1, 129.4, 128.9, 128.4, 127.5, 126.5, 125.6, 122.2, 54.9, 49.3, 34.3, 23.6 ppm. **Ana. HPLC**: $t_R$= 12.51 min, Method A, Instrument 1. **Purity**: 96.5%.

**Formation of**

**(*R*)-5-((2-(4-(4-aminophenyl)-1*H*-1,2,3-triazol-1-yl)ethyl)thio)-*N*-(1-phenylethyl)-1,3,4-thiadiazol-2-amine (6c)**

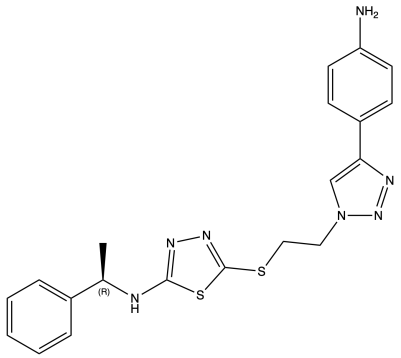


(*R*)-5-((2-azidoethyl)thio)-N-(1-phenylethyl)-1,3,4-thiadiazol-2-amine (301mg, 0.98mmol, 1 eq.), $CuSO_4 \cdot 5H_2O$ (26.5mg, 0.11mmol, 0.11 eq.) and 4-ethynylaniline (172mg, 1.47mmol, 1.5

eq.) was dissolved in 2:1 $H_2O$:AcN (12ml). The reaction mixture got murky, with dark solids swirling around. Hydrazine monohydrate (0.03ml, 0.98mmol, 1.0 eq.) was added dropwise under vigorous stirring at rt. After 1h, the reaction was stopped and then extracted with DCM (4 x 10ml), dried over $MgSO_4$ and then the solvent was evaporated under reduced pressure. The crude was purified with flash chromatography (Gradient from 100% Heptane to 100% EtOAc with 10% MeOH, all with 0.5% $Et_3N$) to afford (*R*)-5-((2-(4-(4-aminophenyl)-1*H*-1,2,3-triazol-1-yl)ethyl)thio)-*N*-(1-phenylethyl)-1,3,4-thiadiazol-2-amine (205mg, 0.48mmol, 49%) as a pale yellow solid. **TLC**: 2:1 EtOAc:Heptane, Rf: 0.09, **LCMS**: 3.6min, $[424.2]^+$, **HRMS**; Theoretical mass (M+H): $[424.1372]^+$, measured mass (M+H): $[424.1373]^+$, **HRMS**: $[424.1]^+$, **$^1$H NMR** (400MHz, DMSO-$d_6$): δ 8.39 (d, *J* = 7.2Hz, 1H), 8.26 (s, 1H), 7.47 (d, *J* = 8.5Hz, 2H), 7.32-7.36 (m, 4H), 7.23-7.27 (m, 1H), 6.61 (d, *J* = 8.5Hz, 2H), 5.22 (s, 2H), 4.77 (quin, *J* = 7.0Hz, 1H), 4.65 (t, *J* = 6.5Hz, 2H), 3.58 (t, *J* = 6.6Hz, 2H), 1.45 (d, *J* = 6.9Hz, 3H) ppm. **$^{13}$C NMR** (400MHz, DMSO-$d_6$): δ 169.1, 149.2, 149.1, 147.8, 144.4, 128.9, 127.5, 126.6, 126.5, 119.9, 118.8, 114.4, 54.9, 49.1, 34.2, 23.6 ppm. **Ana. HPLC**: $t_R$= 9.02 min, Method A, Instrument 1. **Purity**: 97.3%.

## Reversed amide synthesis

**Formation of (R)-5-((2-aminoethyl)thio)-N-(1-phenylethyl)-1,3,4-thiadiazol-2-amine (7)**

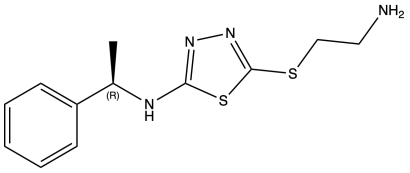


$PPh_3$ (17.1g, 65.3mmol, 2.0 eq.) and $H_2O$ (6.0ml, 333.0mmol, 10.2 eq.) was added to a solution of (R)-5-((2-azidoethyl)thio)-N-(1-phenylethyl)-1,3,4-thiadiazol-2-amine (10.0g, 32.6mmol, 1.0 eq.) in DMF (150ml) at rt. The reaction was heated to 65°C. After 2.5h, the reaction mixture was cooled to rt, and then diluted with $H_2O$ (300ml). HCl was added to lower the pH to approx. pH 5 to protonate the product. The solution was filtered and then freeze dried. Acidic $H_2O$ was added again, the crude was filtered and then freeze dried until the solution ran clear. Prep. HPLC was performed due to insufficient purity using method D to afford (R)-5-((2-aminoethyl)thio)-N-(1-phenylethyl)-1,3,4-thiadiazol-2-amine (TFA salt) (6.3g,

22.5mmol, 69%) as a clear oil. **TLC:** 3:1 EtOAc:Heptane, Rf: 0.0, **UPLCMS**: 1.68min $[281]^+$, **HRMS**; Theoretical mass (M+H): $[281.0889]^+$, measured mass (M+H): $[281.0889]^+$, **$^1$H NMR** (600MHz, DMSO-$d_6$): δ 8.51 (d, *J* = 7.2Hz, 1H), 8.02 (s, 3H), 7.33-7.37 (m, 4H), 7.23 - 7.26 (m, 1H), 4.79 (quin, *J* = 6.9Hz, 1H), 3.26 (t, *J* = 7.1Hz, 2H), 3.09 (sext, *J* = 6.5Hz, 2H), 1.46 (d, *J* = 6.9Hz, 3H) ppm. **$^{13}$C NMR** (600MHz, DMSO-$d_6$): δ 169.2, 149.0, 144.4, 128.9, 127.5, 126.5, 54.9, 39.0, 31.5, 23.6 ppm. **Prep. HPLC**: $t_R$=5.99 min Method F. **Ana. HPLC**: $t_R$= 9.7min, Method A, Instrument 1. **Purity**: > 95.0%.

**Formation of**

**(R)-N-(2-((5-((1-phenylethyl)amino)-1,3,4-thiadiazol-2-yl)thio)ethyl)cyclohexanecarboxamide (8a)**

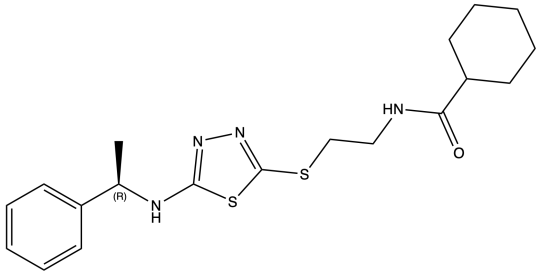


$Et_3N$ (0.18ml, 1.29mmol, 1.29 eq.) was added to a solution of (R)-5-((2-aminoethyl)thio)-N-(1-phenylethyl)-1,3,4-thiadiazol-2-amine (281mg, 1.0mmol, 1.0 eq.) in DMF (15ml). The reaction mixture was cooled down to 0°C and cyclohexanecarbonyl chloride (0.13ml, 1.0 mmol, 1.0 eq.) was added dropwise. Reaction mixture was slightly murky/white. The reaction mixture was stirred for 6h. TLC indicated no cyclohexanecarbonyl chloride. Therefore, additional $Et_3N$ (0.1ml, 0.72mmol, 1.0 eq.) and cyclohexanecarbonyl chloride (0.13ml, 0.97mmol, 1.4eq.) was added and left to stir O/N. The reaction mixture was quenched with $H_2O$ (10ml), extracted with EtOAc (3 x 12ml), washed with $CaCl_2$ (3 x 15ml) and dried over $MgSO_4$. The solvent was removed under reduced pressure and the crude was purified using silica gel chromatography (Gradient from 100% Heptane to 6:1 EtOAC:Heptane with 10% MeOH, all with 0.5% $Et_3N$). Due to insufficient purity, prep. HPLC was performed using method C to afford (R)-N-(2-((5-((1-phenylethyl)amino)-1,3,4-thiadiazol-2-yl)thio)ethyl)cyclohexanecarboxamide (126.7mg, 0.32mmol, 33%) as a white solid. **TLC**: 2:1 EtOAc:Heptane, Rf: 0.37, **UPLCMS**:

2.37min $[391]^+$, **HRMS**; Theoretical mass (M+H): $[391.1621]^+$, measured mass (M+H): $[291.1620]^+$, **$^1$H NMR** (600MHz, DMSO-$d_6$): δ 8.36 (d, *J* = 7.3Hz, 1H), 7.89 (t, *J* = 5.5Hz, 1H), 7.32-7.37 (m, 4H), 7.23-7.26 (m, 1H), 4.78 (quin, *J* = 7.0Hz, 1H), 3.28 (q, *J* = 6.4Hz, 2H), 3.08 (t, *J* = 6.8Hz, 2H), 2.01-2.06 (m, 1H), 1.59-1.69 (m, 5H), 1.46 (d, *J* = 6.9Hz, 3H), 1.11-1.31 (m, 5H) ppm. **$^{13}$C NMR** (600MHz, DMSO-$d_6$): δ 175.8, 168.9, 150.4, 144.5, 128.9, 127.5, 126.5, 54.8, 44.4, 38.8, 34.3, 29.6, 25.9, 25.7, 23.6 ppm. **Prep. HPLC**: $t_R$=6.01 min Method D. **Ana. HPLC**: $t_R$=4.41min, Method D, Instrument 2. **Purity**: 96.1%.

**Formation of**

**(*R*)-*N*-(2-((5-((1-phenylethyl)amino)-1,3,4-thiadiazol-2-yl)thio)ethyl)benzamide**

**(8b)**

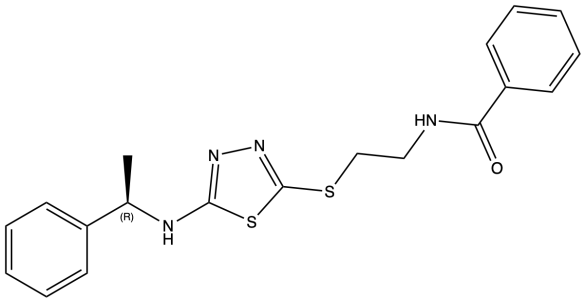


$Et_3N$ (0.4ml, 2.2mmol, 3.0 eq.) was added to a solution of (R)-5-((2-aminoethyl)thio)-N-(1-phenylethyl)-1,3,4-thiadiazol-2-amine (265mg, 0.67mmol, 1.0 eq.) in dry DMF (10ml). The reaction mixture was cooled down to 0°C and Benzoyl chloride (0.12ml, 1.06 mmol, 1.50 eq.) was added dropwise. The reaction mixture was allowed to slowly reach rt. The reaction mixture was stirred O/N. The reaction mixture was quenched with $H_2O$ (15ml) and extracted with EtOAc (3 x 15ml). The combined organic layers were washed with $CaCl_2$ (3 x 15ml) and dried over $MgSO_4$. The solvent was removed under reduced pressure. Recrystallization using EtOAc and Heptane was performed to yield (*R*)-*N*-(2-((5-((1-phenylethyl)amino)-1,3,4-thiadiazol-2-yl)thio)ethyl)benzamide (105mg, 0.27mmol, 40%) as a white solid. **TLC**: 2:1 EtOAc:Heptane, Rf: 0.26, **UPLCMS**: 2.23min $[385]^+$, **HRMS**; Theoretical mass (M+H): $[385.1151]^+$, measured mass (M+H): $[385.1153]^+$, **$^1$H NMR** (600MHz, DMSO-$d_6$): δ 8.69 (t, *J* = 5.4Hz, 1H), 8.36 (d, *J* = 7.2Hz, 1H), 7.82 (dd, *J* = 7.2, 1.2Hz, 2H), 7.53 (t, *J* = 7.4Hz, 1H), 7.46 (t, *J* = 7.6Hz, 2H), 7.35 (m, 4H), 7.25 (m, 1H), 4.77

(quin, *J* = 7.0Hz, 1H), 3.54 (q, *J* = 6.4Hz, 2H), 3.24 (t, *J* =6.8Hz, 2H), 1.45 (d, *J* = 6.9Hz, 3H) ppm. **$^{13}$C NMR** (600MHz, DMSO-$d_6$): δ 169.0, 166.8, 150.3, 144.5, 134.6, 131.7, 128.9, 128.8, 127.6, 127.5, 126.5, 54.8, 40.6, 34.0, 23.6 ppm. **Ana. HPLC**: $t_R$=14.6min, Method B, Instrument 2. **Purity**: 96.3%.

**Formation of**

**(R)-4-methoxy-N-(2-((5-((1-phenylethyl)amino)-1,3,4-thiadiazol-2-yl)thio)ethyl)benzamide (8c)**

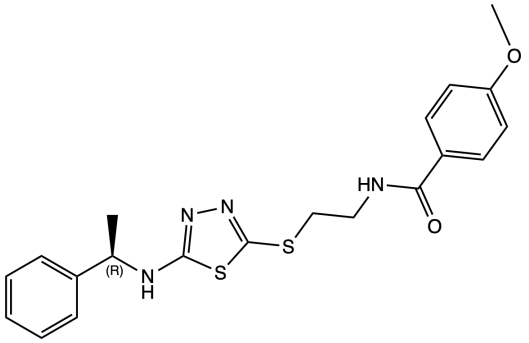


$Et_3N$ (0.3ml, 2.1mmol, 3.0 eq.) was added to a solution of (R)-4-methoxy-N-(2-((5-((1-phenylethyl)amino)-1,3,4-thiadiazol-2-yl)thio)ethyl)benzamide (286mg, 0.73mmol, 1.0 eq.) in dry DMF (5ml). The reaction mixture was cooled down to 0°C and 4-cyanobenzyl chloride (180mg, 1.06 mmol, 1.5 eq.) in dry DMF (5ml) was added dropwise. The reaction mixture was allowed to slowly reach rt. The reaction mixture was stirred O/N. The reaction mixture was quenched with $H_2O$ (15ml) and extracted with EtOAc (3 x 15ml). The combined organic layers were washed with $CaCl_2$ (3 x 15ml) and dried over $MgSO_4$. The solvent was removed under reduced pressure to afford (R)-4-methoxy-N-(2-((5-((1-phenylethyl)amino)-1,3,4-thiadiazol-2-yl)thio)ethyl)benzamide (249.9mg, 0.6mmol, 85.0%) as a beige solid. **TLC**: 2:1 EtOAc:Heptane, Rf: 0.20, **LCMS**: 4.2min $[415.2]^+$, **HRMS**; Theoretical mass (M+H): $[415.1257]^+$, measured mass (M+H): $[415.1261]^+$, **$^1$H NMR** (600MHz, DMSO-$d_6$): δ 8.54 (t, *J* = 5.5Hz, 1H), 8.36 (d, *J* = 7.2Hz, 1H), 7.80 (d, *J* = 8.9Hz, 2H), 7.35 (m, 4H), 7.25 (m, 1H), 6.99 (d, *J* = 8.9Hz, 2H), 4.77 (quin, *J* = 7.0Hz, 1H), 3.81 (s, 3H), 3.51 (q, *J* = 6.4Hz, 2H), 3.22 (t, *J* = 6.8Hz, 2H), 1.45 (d, *J* = 6.9Hz, 3H) ppm. **$^{13}$C NMR** (600MHz, DMSO-$d_6$): δ 169.0, 166.2, 162.1, 150.4, 144.5, 129.5, 128.9, 127.5,

126.9, 126.5, 113.9, 55.8, 54.8, 40.6, 34.1, 23.6 ppm. **Ana. HPLC**: $t_R$=12.3min, Method A, Instrument 2. **Purity**: 96.6%.

## GluN1/2B analogue synthesis

**Formation of (*R*)-5-(methylthio)-N-(1-phenylethyl)-1,3,4-thiodiazol-2-amine (3a)**

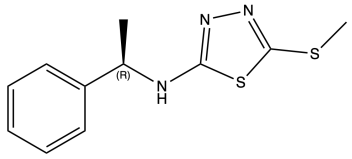

$K_2CO_3$ (117.0mg, 0.85mmol, 2.0 eq.) was added to a solution of (*R*)-5-(methylthio)-N-(1-phenylethyl)-1,3,4-thiodiazol-2-amine (100.0mg, 0.42mmol, 1.0 eq.) dissolved in DMF (1.5ml). Iodomethane (0.03ml, 0.51mmol, 1.2 eq.) was added after 30 min to the reaction mixture and left to stir O/N at rt. The reaction mixture was diluted with $H_2O$ (2ml) and extracted with EtOAc (3 x 4ml). The combined organic layers were washed with $CaCl_2$ (3x2ml), and dried over $MgSO_4$. The solvent was removed under reduced pressure. The crude product was purified with flash chromatography (Gradient from 1:5 EtOAc:Heptane to 1:2 EtOAc:Heptane) to afford (*R*)-5-(methylthio)-N-(1-phenylethyl)-1,3,4-thiodiazol-2-amine (32mg, 0.13mmol, 30%) as a white solid. **TLC**: 1:1 EtOAc:Heptane, Rf: 0.37, **LCMS**: 4.3min, $[252.1]^+$, **HRMS**; Theoretical mass (M+H): $[252.0624]^+$, measured mass (M+H): $[252.0622]^+$, **$^1$H NMR** (400MHz, DMSO-$d_6$): δ 8.28 (d, *J* = 7.2Hz, 1H), 7.31-7.37 (m, 4H), 7.22-7.26 (m, 1H), 4.77 (quin, *J* = 7.0Hz, 1H), 2.56 (s, 3H), 1.45 (d, *J* = 6.9Hz, 3H) ppm. **$^{13}$C NMR** (600MHz, $CDCl_3$): δ 169.4, 154.2, 142.2, 128.9, 127.9, 126.3, 56.9, 23.8, 16.9 ppm. **Ana. HPLC**: $t_R$=10.97 min, Method A, Instrument 1. **Purity**: 98.6%.

**Formation of (*R*)-5-(benzylthio)-N-(1-phenylethyl)-1,3,4-thiodiazol-2-amine (3b)**

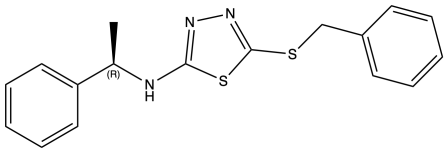

$KHCO_3$ (85.0mg, 0.85mmol, 2.0 eq.) was added to a solution of (*R*)-2-((5-((1-phenylethyl)amino)-1,3,4-thiadiazole-2-yl)thio)ethan-1-ol (102.0mg, 0.43mmol,

1.0 eq.) dissolved in DMF (1.1ml) at 0°C. After 15 min benzyl bromide (0.05ml, 0.42mmol, 1.0 eq.) was added and the reaction was stirred at 0°C for 30min. Reaction was left to stir at rt. The crude was dissolved in EtOAc (8ml) and then purified with flash chromatography (Gradient from 1:10 EtOAc:Heptane to 2:1 EtOAc:Heptane, all with 0.5% $Et_3N$) Due to insufficient purity, prep. HPLC was performed using method B, to afford (*R*)-5-(benzylthio)-N-(1-phenylethyl)-1,3,4-thiodiazol-2-amine (44mg, 0.13mmol, 52.9 %) as a clear oil. **TLC**: 1:3 EtOAc:Heptane, Rf: 0.34, **LCMS**: 4.7min $[328.1]^+$, **HRMS**; Theoretical mass (M+H): $[328.0937]^+$, measured mass (M+H): $[328.0934]^+$, **$^1$H NMR** (400MHz, DMSO-$d_6$): δ 8.33 (d, *J* = 7.3Hz, 1H), 7.22-7.34 (m, 10H), 4.75 (quin, *J* = 7.0Hz, 1H), 4.28 (s, 2H), 1.44 (d, *J* = 6.9Hz, 3H) ppm. **$^{13}$C NMR** (400MHz, DMSO-$d_6$): δ 169.2, 144.4, 137.5, 129.4, 128.9, 128.8, 127.9, 127.5, 126.5, 54.8, 38.8, 23.6 ppm. **Prep. HPLC**: $t_R$=10.5 min Method C. **Ana. HPLC**: $t_R$=7.95 min, Method C, Instrument 1. **Purity**: 96.6%.

**Formation of**

**(R)-5-((naphthalen-1-ylmethyl)thio)-N-(1-phenylethyl)-1,3,4-thiadiazol-2-amine (3c)**

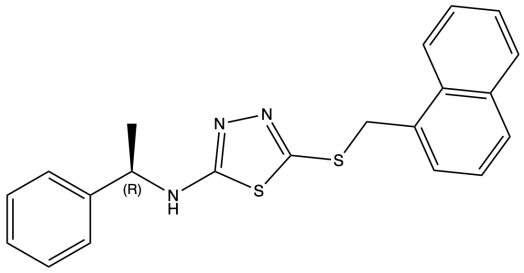


$KHCO_3$ (181mg, 1.81mmol, 2.2 eq.) was added to a solution of (*R*)-2-((5-((1-phenylethyl)amino)-1,3,4-thiadiazole-2-yl)thio)ethan-1-ol (201mg, 0.84mmol, 1.0 eq.) dissolved in DMF (3 ml) at 0°C. After 15 min 2-(Chloromethyl)naphthalene (0.15ml, 1.01mmol, 1.2 eq.) was added and the reaction was stirred at 0°C for 30min. Reaction was left to stir at rt O/N. The reaction mixture was diluted with $H_2O$ (5ml), extracted with EtOAc (3 x 3ml) and then washed with ice cold $H_2O$ (3 x 3ml). The combined organic layers were dried with $MgSO_4$, and the solvent was evaporated under reduced pressure. Recrystallization of the crude was performed to afford (R)-5-((naphthalen-1-ylmethyl)thio)-N-(1-phenylethyl)-1,3,4-thiadiazol-2-amine (266mg, 0.7mmol, 83.6%) as a yellowish solid. **TLC**: 1:1 EtOAc:Heptane, Rf: 0.61, **LCMS**: 5.1min $[378]^+$, **HRMS**; Theoretical mass (M+H): $[378.1093]^+$, measured mass (M+H): $[378.1095]^+$, **$^1$H**

**NMR** (600MHz, DMSO-$d_6$): δ 8.36 (d, *J* = 7.3Hz, 1H), 8.13 (d, *J* = 8.0Hz, 1H), 7.96 (dd, *J* = 7.5, 1.7Hz, 1H), 7.87 (d, *J* = 8.1Hz, 1H), 7.56 (m, 2H), 7.44 (d, *J* = 6.1Hz, 1H), 7.39 (d, *J* = 7.5Hz, 1H), 7.34 (m, 4H), 7.26 (m, 1H), 4.76 (m, 3H), 1.45 (d, *J* = 6.9Hz, 3H) ppm. **$^{13}$C NMR** (600MHz, DMSO-$d_6$): δ 169.5, 149.7, 144.4, 134.0, 132.8, 131.3, 129.1, 128.9, 128.8, 128.3, 127.5, 126.8, 126.5, 126.4, 125.8, 124.4, 54.8, 37.1, 23.6 ppm. **Ana. HPLC**: $t_R$= 14.0, Method A, Instrument 2. **Purity**: 95.5%.

**Formation of (R)-5-(butylthio)-N-(1-phenylethyl)-1,3,4-thiadiazol-2-amine (3d)**

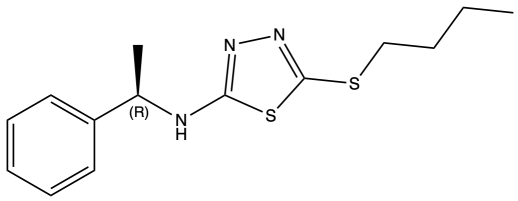


$KHCO_3$ (173mg, 1.73mmol, 2.1 eq.) was added to a solution of (*R*)-2-((5-((1-phenylethyl)amino)-1,3,4-thiadiazole-2-yl)thio)ethan-1-ol (200mg, 0.84mmol 1.0 eq.) dissolved in DMF (3 ml) at 0°C. After 15 min Iodobutane (0.11ml, 1.01mmol, 1.2 eq.) was added and the reaction was stirred at 0°C for 30min. Reaction was left to stir at rt O/N. The reaction mixture was diluted with $H_2O$ (5ml), extracted with EtOAc (3 x 3ml) and then washed with ice cold $H_2O$ (3 x 3ml). The combined organic layers were dried with $MgSO_4$, and the solvent was evaporated under reduced pressure to afford (R)-5-(butylthio)-N-(1-phenylethyl)-1,3,4-thiadiazol-2-amine (226mg, 0.77mmol, 91.4%) as a yellowish solid.

**TLC**: 1:1 EtOAc:Heptane, Rf: 0.57, **LCMS**: 4.9min $[294.2]^+$, **HRMS**; Theoretical mass (M+H): $[294.1093]^+$, measured mass (M+H): $[294.1093]^+$, **$^1$H NMR** (600MHz, DMSO-$d_6$): δ 8.34 (d, *J* = 7.2Hz, 1H), 7.32-7.37 (m, 4H), 7.23-7.26 (m, 1H), 4.77 (quin, *J* = 7.0Hz, 1H), 3.02 (t, *J* = 7.3Hz, 2H), 1.58 (m, 2H), 1.45 (d, *J* = 6.9Hz, 3H), 1.36 (m, 2H), 0.86 (t, *J* = 7.4Hz, 3H) ppm. **$^{13}$C NMR** (600MHz, DMSO-$d_6$): δ 168.9, 150.7, 144.5, 128.9, 127.5, 126.5, 54.8, 34.4, 31.6, 23.7, 21.5, 12.8 ppm. **Ana. HPLC**: $t_R$=13.1, Method A, Instrument 2. **Purity**: 95.6%.

**Formation of**

**(R)-4-(((5-((1-phenylethyl)amino)-1,3,4-thiadiazol-2-yl)thio)methyl)benzonitrile (3e)**

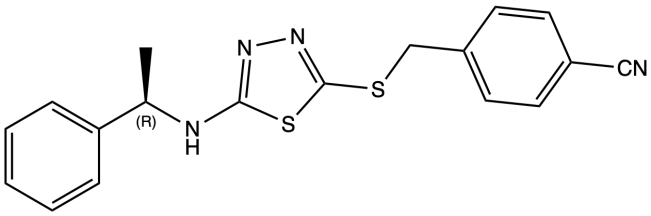

$KHCO_3$ (174mg, 1.74mmol, 2.1 eq.) was added to a solution of (*R*)-2-((5-((1-phenylethyl)amino)-1,3,4-thiadiazole-2-yl)thio)ethan-1-ol (200mg, 0.84mmol, 1.0 eq.) dissolved in DMF (3 ml) at 0°C. After 15 min 4-(bromomethyl)benzonitrile (204mg, 1.04mmol, 1.2 eq.) was added and the reaction was stirred at 0°C for 30min. Reaction was left to stir at rt O/N. The reaction mixture was diluted with $H_2O$ (5ml), extracted with EtOAc (3 x 3ml) and then washed with ice cold $H_2O$ (3 x 3ml). The combined organic layers were dried with $MgSO_4$, and the solvent was evaporated under reduced pressure. The crude was purified using silica gel chromatography (Gradient from 100% heptane to 2:1 EtOAc:Heptane, all with 0.5% $Et_3N$) to afford (R)-4-(((5-((1-phenylethyl)amino)-1,3,4-thiadiazol-2-yl)thio)methyl)benzonitrile (270mg, 0.77mmol, 90.9%) as a yellowish solid. **TLC**: 1:1 EtOAc:Heptane, Rf: 0.25, **LCMS**: 4.5min $[353.2]^+$, **HRMS**; Theoretical mass (M+H): $[353.0889]^+$, measured mass (M+H): $[353.0892]^+$, **$^1$H NMR** (600MHz, DMSO-$d_6$): δ 8.37 (d, *J* = 7.2Hz, 1H), 7.76 (d, *J* = 8.4Hz, 2H), 7.51 (d, *J* = 8.3Hz, 2H), 7.33 (m, 4H), 7.25 (m, 1H), 4.74 (quin, *J* = 7.0Hz, 1H), 4.35 (s, 2H), 1.44 (d, *J* = 6.9Hz, 3H) ppm. **$^{13}$C NMR** (600MHz, DMSO-$d_6$): δ 169.5, 149.1, 144.4, 143.8, 132.8, 130.4, 128.9, 127.5, 126.5, 119.2, 110.5, 54.8, 38.2, 23.6 ppm. **Ana. HPLC**: $t_R$= 13.2min, Method A, Instrument 2. **Purity**: 98.4%.

**Formation of 5-((4-methylbenzyl)thio)-N-(1-phenylethyl)-1,3,4-thiadiazol-2-amine (3f)**

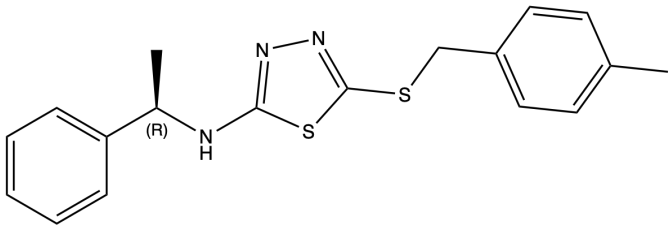

$KHCO_3$ (167mg, 1.67mmol, 2.0 eq.) was added to a solution of (*R*)-2-((5-((1-phenylethyl)amino)-1,3,4-thiadiazole-2-yl)thio)ethan-1-ol (200mg, 0.84mmol, 1.0 eq.) dissolved in DMF (3 ml) at 0°C. After 15 min 4-Methylbenzyl bromide (190mg, 1.03mmol, 1.2 eq.) was added and the reaction was stirred at 0°C for 30min. Reaction was left to stir at rt

O/N. The reaction mixture was diluted with $H_2O$ (5ml), extracted with EtOAc (3 x 3ml) and then washed with ice cold $H_2O$ (3 x 3ml). The combined organic layers were dried with $MgSO_4$, and the solvent was evaporated under reduced pressure. Recrystallization of the crude was performed to afford 5-((4-methylbenzyl)thio)-N-(1-phenylethyl)-1,3,4-thiadiazol-2-amine (243mg, 0.71mmol, 84.5%) as a yellowish solid.

**TLC**: 1:1 EtOAc:Heptane, Rf: 0.50, **LCMS**: 4.9min $[342.2]^+$, **HRMS**; Theoretical mass (M+H): $[342.1093]^+$, measured mass (M+H): $[342.1096]^+$, **$^1$H NMR** (600MHz, DMSO-$d_6$): δ 8.33 (d, *J* = 7.3Hz, 1H), 7.32-7.37 (m, 4H), 7.23-7.27 (m, 1H), 7.20 (d, *J* = 8.0Hz, 2H), 7.11 (d, *J* = 7.8Hz, 2H), 4.76 (quin, *J* = 7.0Hz, 1H), 4.23 (s, 2H), 2.27 (s, 3H), 1.44 (d, *J* = 6.9Hz, 3H) ppm. **$^{13}$C NMR** (600MHz, DMSO-$d_6$): δ 169.2, 150.0, 144.5, 137.1, 134.3, 129.5, 129.4, 128.8, 127.4, 126.5, 54.8, 38.6, 23.6, 21.2 ppm. **Ana. HPLC**: $t_R$= 13.5min, Method A, Instrument 2. **Purity**: 98.3%.

# References


1. Scott, D. B. and Ehlers, M. D. *Glutamate Receptors, Ionotropic.* In Encyclopedia of Biological Chemistry, edited by W. J. Lennarz and M. D. Lane. Elsevier, New York, Pages 213-19, 2004.
2. BalÁZs, R., Bridges, R. J. and Cotman, C. W. *269Glutamate and Glutamate Receptors in Neurological Diseases*. In Excitatory Amino Acid Transmission in Health and Disease, edited by R. Balazs, R. J. Bridges, C. W. Cotman and C. A. Cotman W. Cotman. Oxford University Press, 2005. https://doi.org/10.1093/acprof:oso/9780195150025.003.0012
3. Purves, D., Augustine, G. J., Fitzpatrick, D., et al. *Neuroscience.* Sunderland (MA): Sinauer associates, 2nd edition, 2001. https://www.ncbi.nlm.nih.gov/books/NBK10802/
4. Vyklicky, V., Korinek, M., Smejkalova, T., Balik, A., Krausova, B., Kaniakova, M., et al. *Structure, function, and pharmacology of NMDA receptor channels*. Physiol Res, Vol. 63, Issue Suppl 1, Pages S191-203, 2014.
5. Paoletti, P. and Neyton, J. *NMDA receptor subunits: function and pharmacology.* Current opinion in Pharmacology, Vol. 7, Issue 1, Pages 39-47, 2007. https://www.sciencedirect.com/science/article/pii/S1471489206001883
6. Hansen, K. B., Yi, F., Perszyk, R. E., Furukawa, H., Wollmuth, L. P., Gibb, A. J. and Traynelis, S. F. *Structure, function and allosteric modulation of NMDA receptors.* Journal of General Physiology, Vol. 150, Issue 8, Pages 1081-1105, 2018. https://doi.org/10.1085/jgp.201812032
7. Paoletti, P., Bellone, C. and Zhou, Q. *NMDA receptor subunit diversity: impact on receptor properties, synaptic plasticity and disease.* Nat Rev Neurosci, Vol. 14, Issue 6, Pages 383-400, 2013.
8. Volkmann, R. A., Fanger, C. M., Anderson, D. R., Sirivolu, V. R., Paschetto, K., Gordon, E., et al. *MPX-004 and MPX-007: New Pharmacological Tools to Study the Physiology of NMDA Receptors Containing the GluN2A subunit.* PLoS one, Vol. 11, Issue 2, Pages e014812, 2016.
9. Riedel, G., Platt, B. and Micheau, J. *Glutamate receptor function in learning and memory.* Behav Brain Res, Vol. 140, Issue 1-2, Pages 1-47, 2003.
10. Monaghan, D. T., Irvine, M. W., Costa, B. M., Fang, G. and Jane D. E. *Pharmacological*

*modulation of NMDA receptor activity and the advent of negative and positive allosteric modulators*. Neurochemistry International, Vol. 61, Issue 4, Pages 581-592, 2012. https://www.sciencedirect.com/science/article/pii/S019701861200006X

11. Edman, S., McKay, S., Macdonald, L. J., Samadi, M., Livesey, M. R., Hardinghamn, G. E. and Wyllie, D. J. *TCN201 selectively blocks GluN2A-containing NMDARs in a GluN1 co-agonist dependent by non-competitive manner.* Neuropharmacology, Vol. 63, Issue 3, Pages 441-9, 2012.
12. Calenoff, E. *Interplaying factors that affect multiple sclerosis causation and sustenance.* ISRN Neurol, Vol. 2012, Pages 851541. 2012.
13. Ieremias, L. (2018). *Design and Synthesis of Allosteric Modulators Selective for GluN1/GluN2A NMDA Receptors.* [Master Thesis, University of Copenhagen].
14. National Center for Biotechnology Information (2024). *Electronegativity in the Periodic Table of Elements.* PubChem. Retrieved August 29, 2024. https://pubchem.ncbi.nlm.nih.gov/ptable/electronegativity/
15. Charisiadis, P. Kontogianni, V. G., Tsiafoulis, C. G., Tzakos, A. G., Siskos, M., Gerothanassis, I. P. *$^1$H-NMR as a Structural and Analytical Tool of Intra- and Intermolecular Hydrogen Bonds of Phenol-Containing Natural Products and Model Compounds*. Molecule, Basel Switzerland, Pages 13643-13682, 2014.
16. Hein, J. E. and Fokin, V. V. *Copper-catalyzed azide-alkyne cycloaddition (CuAAC) and beyond: new reactivity of copper(I) acetylides.* Chem Soc Rev, Vol. 39, Issue 4, Pages 1302-15. 2010.
17. Wikipedia (2024) (2), *Aromatic ring current*. Retrieved January 3, 2025. https://en.wikipedia.org/wiki/Aromatic_ring_current
18. Chemistry (2025), *Explanation of strength of phosphorus-oxygen bond.* Retrieved January 3, 2025. https://chemistry.stackexchange.com/questions/107617/explanation-of-the-strength-of-phosphorus-oxygen-bond
19. Honeywell (2025). *Water with 0.1% trifluoroacetic acid.* Retrieved January 3, 2025. https://lab.honeywell.com/shop/water-with-0-1-trifluoroacetic-acid-34978
20. Wikipedia (2024) (1). *Acid dissociation constant.* Retrieved January 3, 2025. https://en.wikipedia.org/wiki/Acid_dissociation_constant

21. Akitsu, T. (Ed.) (2022). *Schiff Base in Organic, Inorganic and Physical Chemistry.* IntechOpen. https://www.intechopen.com/chapters/84305
22. Revvity Signals (September 2019), *Chemdraw* (version 19.1) [Computer software] https://revvitysignals.com/products/research/chemdraw?gad_source=1&gbraid=0AAAAABZL8QMCYB2fOD_tkxQVezuRgi03f&gclid=Cj0KCQiAst67BhCEARIsAKKdWOl2DMbkk05xfJncdd7BD0eHy7-H4aYzz_oXFD5bSd-RoYOKBezOQ_IaArVxEALw_wcB
23. Sellerberg, A. (2024). *Prediction of Allosteric Binding Modes in Homologous NMDA-receptors.* [Master Thesis, Lund University].
24. Yi, F., M, T., Dorsett, K. N., Volkmann, R. A., Menniti, F. S., Sprang, S. R., Hansen, K. B. *Structural Basis for Negative Allosteric Modulation of GluN2A-Containing NMDA Receptors.* Neuron 91, Pages 1316-1329, 2016.
25. Reaction Biology (2025). *Two-Electrode Voltage Clamp Assay Services.* Ion Channel Discovery. Retrieved January 3, 2025. https://www.reactionbiology.com/services/target-specific-assays/ion-channel-assays/two-eletrode-voltage-clamp/

# Appendix

## Mechanisms

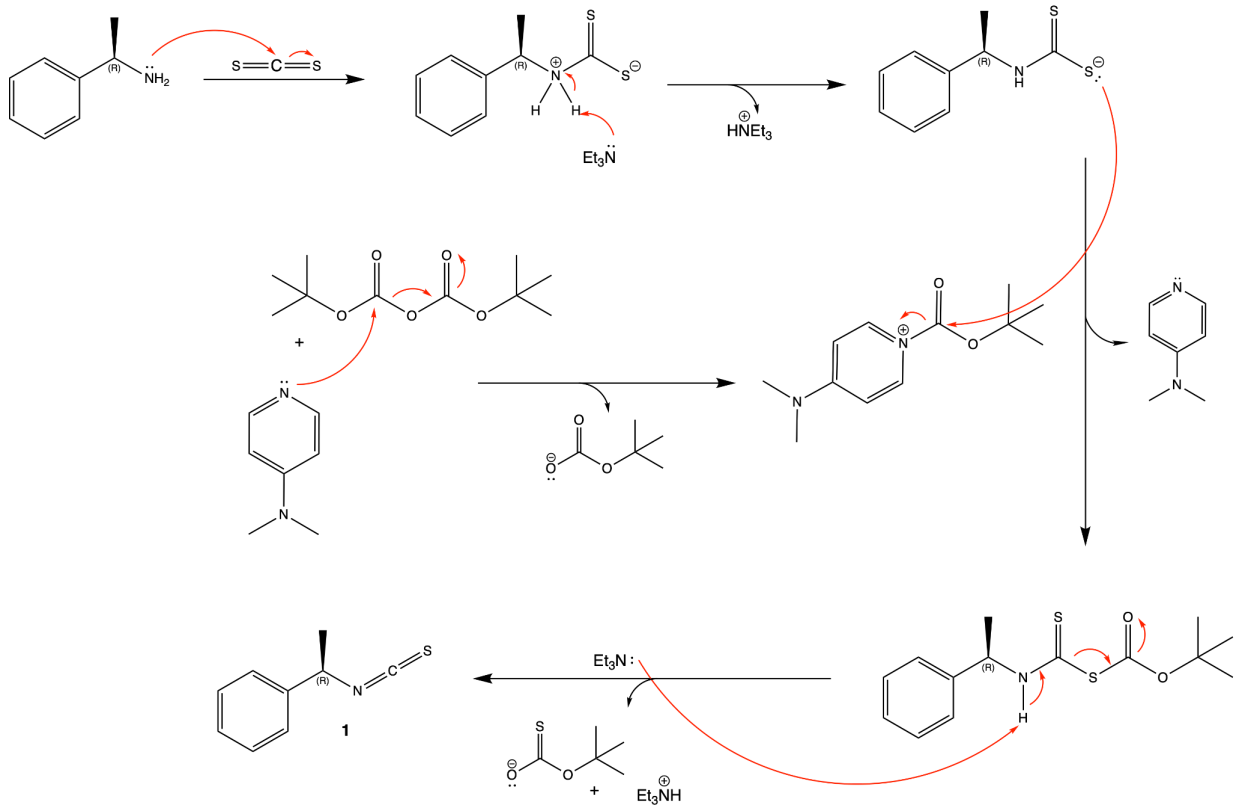


*Scheme A1. Reaction mechanism of the formation of product **1**.*

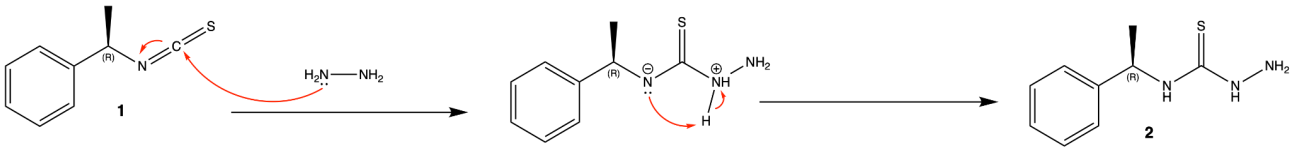


*Scheme A2. Reaction mechanism of the formation of product **2**.*

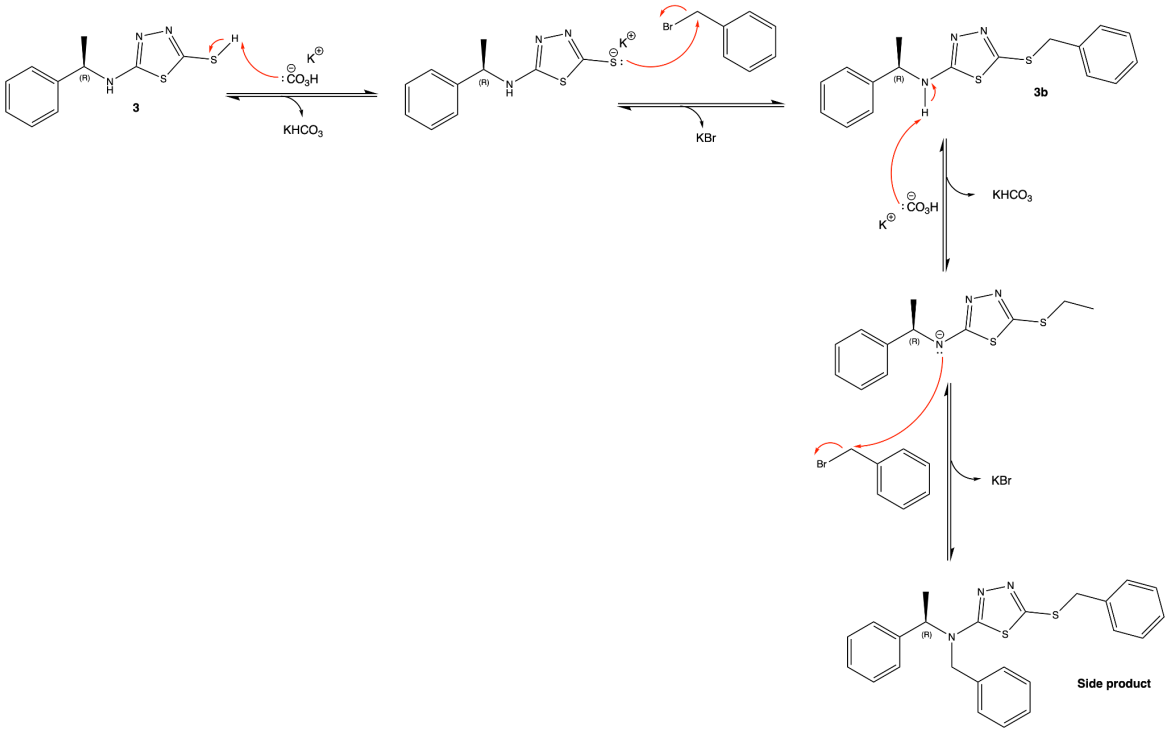


*Scheme A3. Reaction mechanism of the formation of product **3b**.*

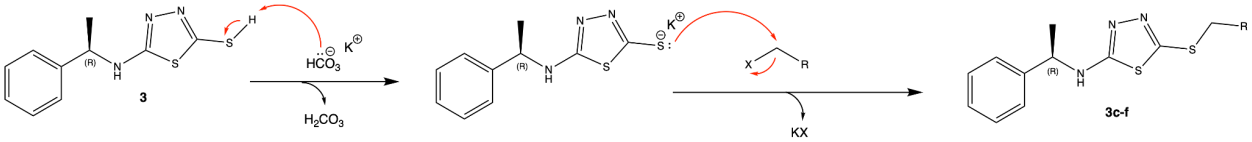


*Scheme A4. Reaction mechanism of the formation of products **3c-f**.*

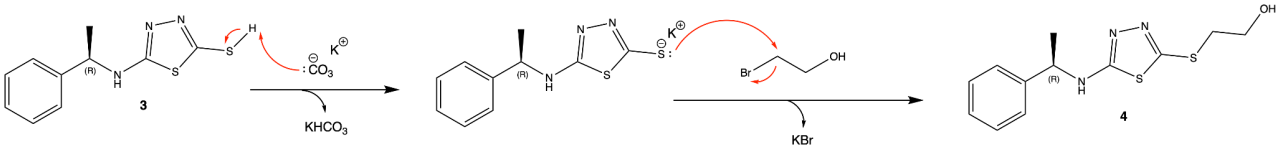


*Scheme A5. Reaction mechanism of the formation of product **4**.*

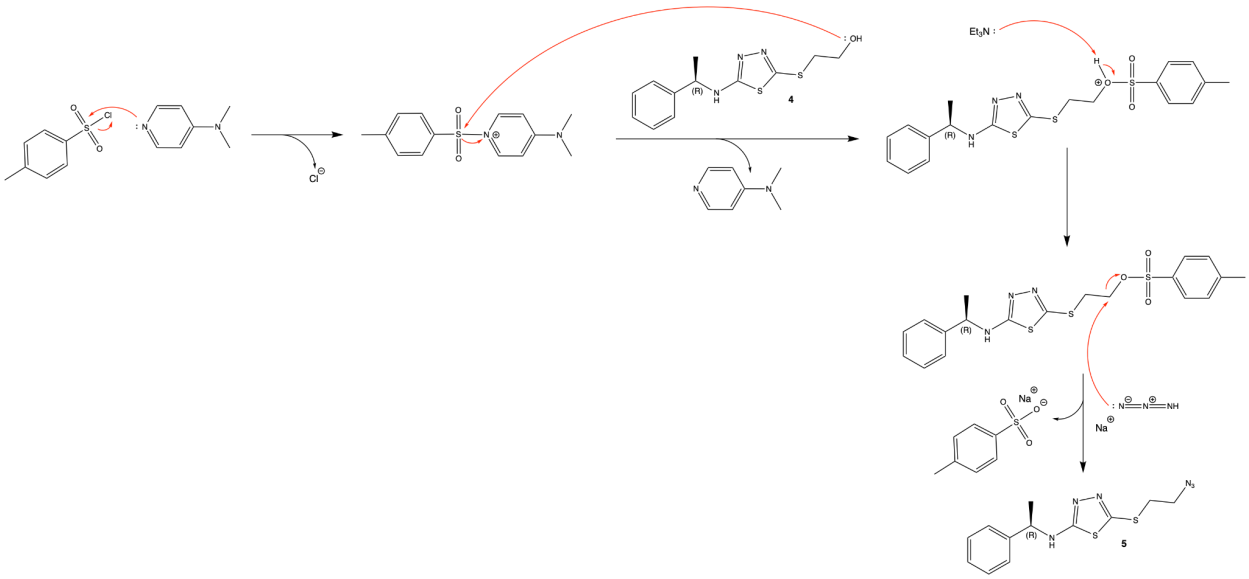

*Scheme A6. Reaction mechanism of the formation of product **5**.*

# NMR

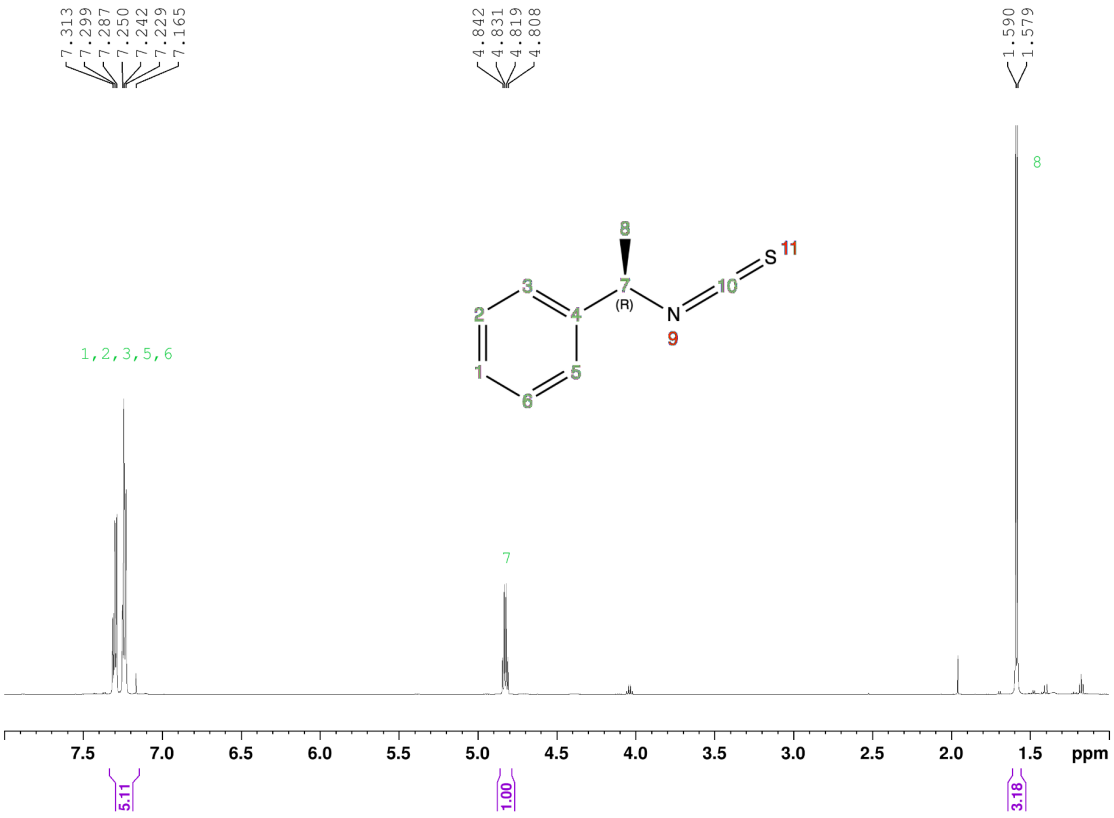


*Spectrum A1. $^{1}H$ NMR of (R)-(1-isothiocyanoethyl)benzene (**1**) in $CDCl_3$; with all the peaks assigned to protons in the molecule.*

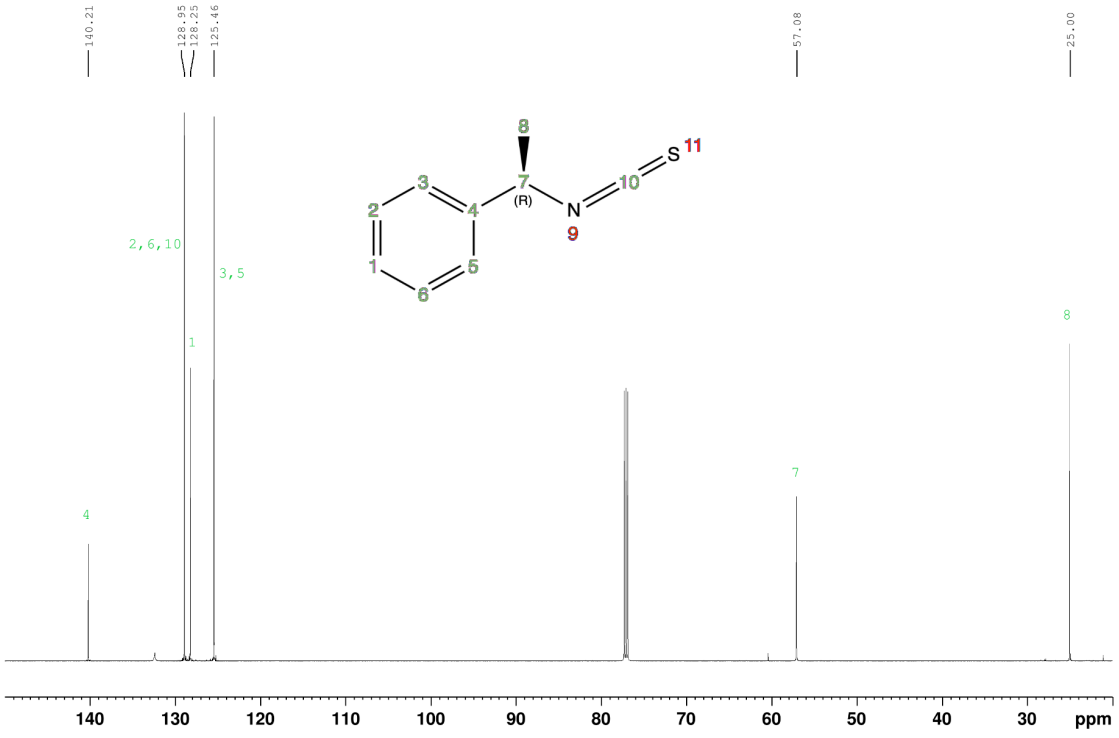


*Spectrum A2. $^{13}C$ NMR of (R)-(1-isothiocyanoethyl)benzene (**1**) in $CDCl_3$; with all the peaks assigned to protons in the molecule.*

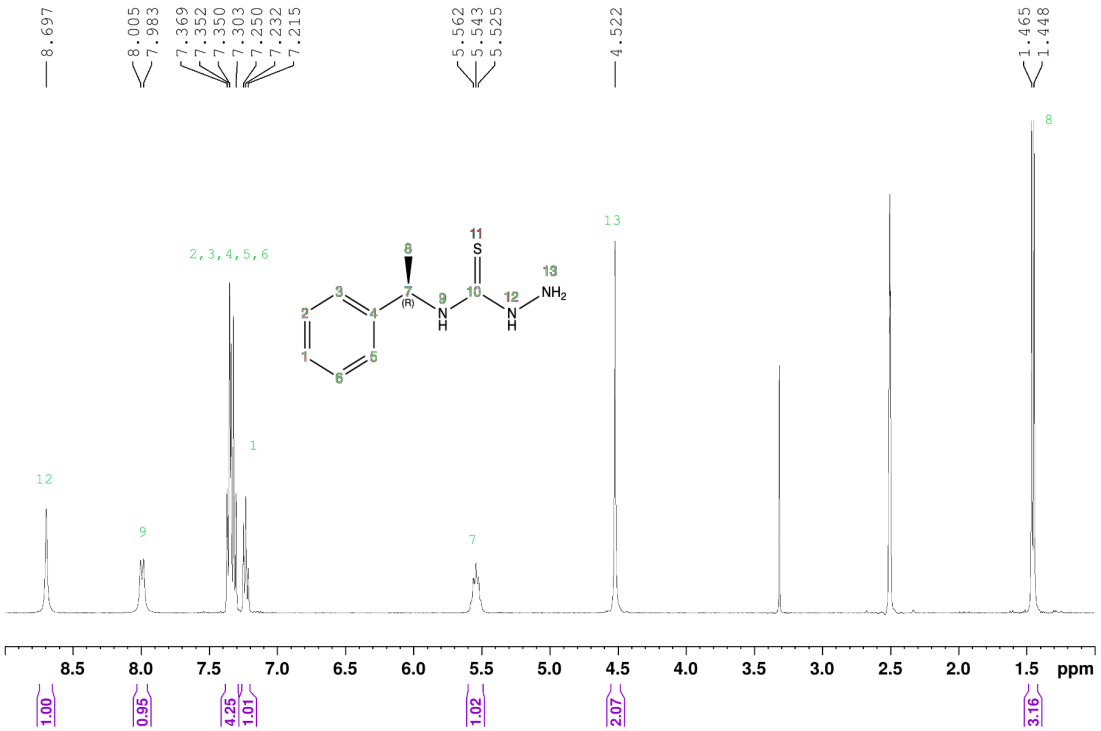


*Spectrum A3. $^{1}H$ NMR of (R)-N-(1-phenylethyl)hydrazinecarbothioamide (**2**) in DMSO-$d_6$; with all the peaks assigned to protons in the molecule.*

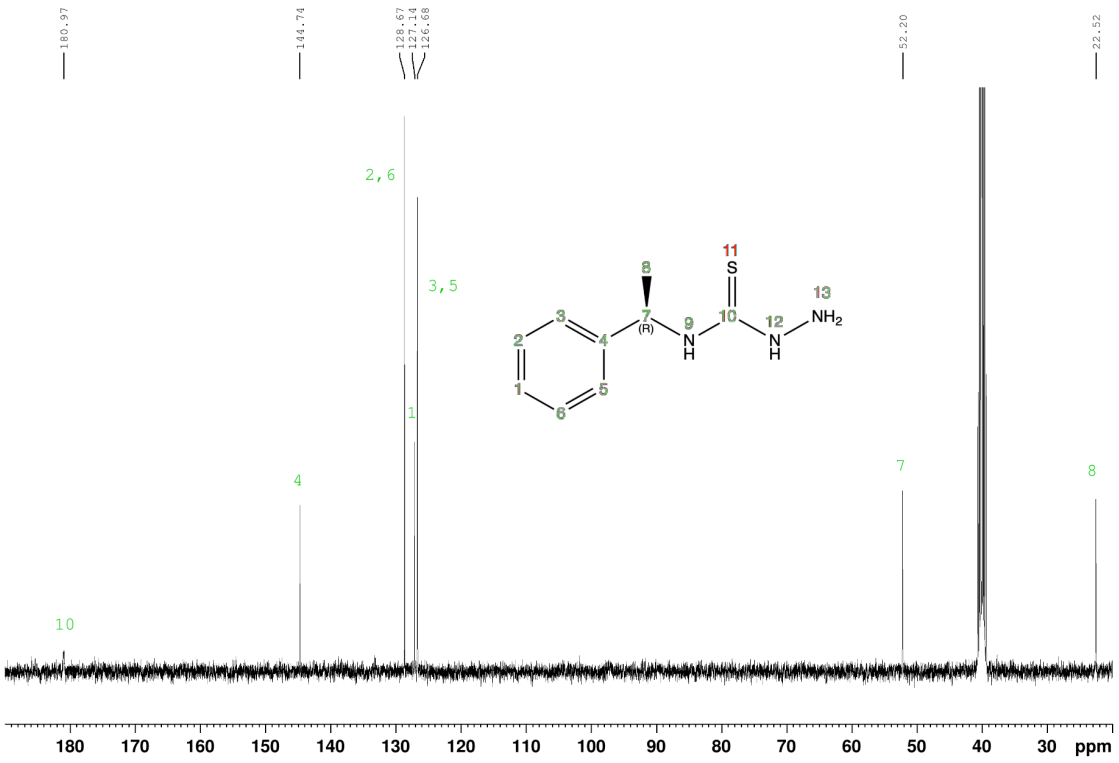


*Spectrum A4. $^{13}C$ NMR of (R)-N-(1-phenylethyl)hydrazinecarbothioamide (**2**) in DMSO-$d_6$; with all the peaks assigned to protons in the molecule.*

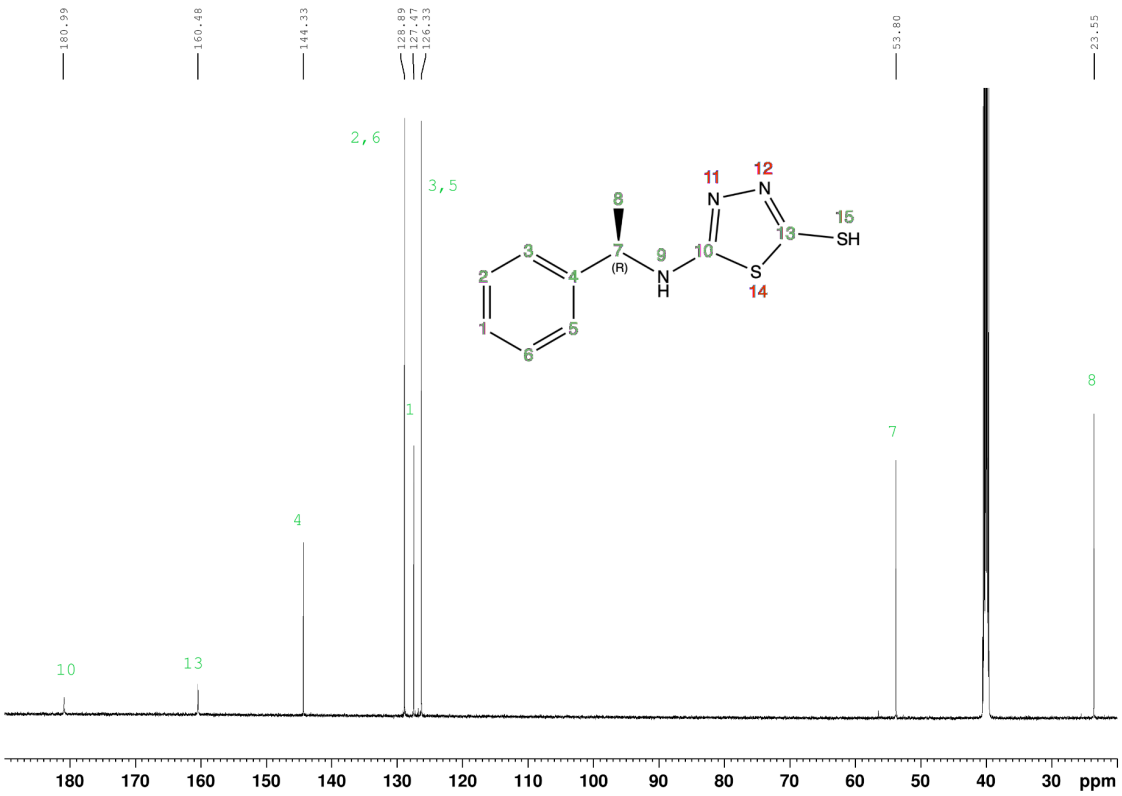


*Spectrum A5. $^{13}C$ NMR of (R)-5-((1-phenylethyl)amino)-1,3,4-thiadiazole-2-thiol (**3**) in DMSO-$d_6$; with all the peaks assigned to protons in the molecule.*

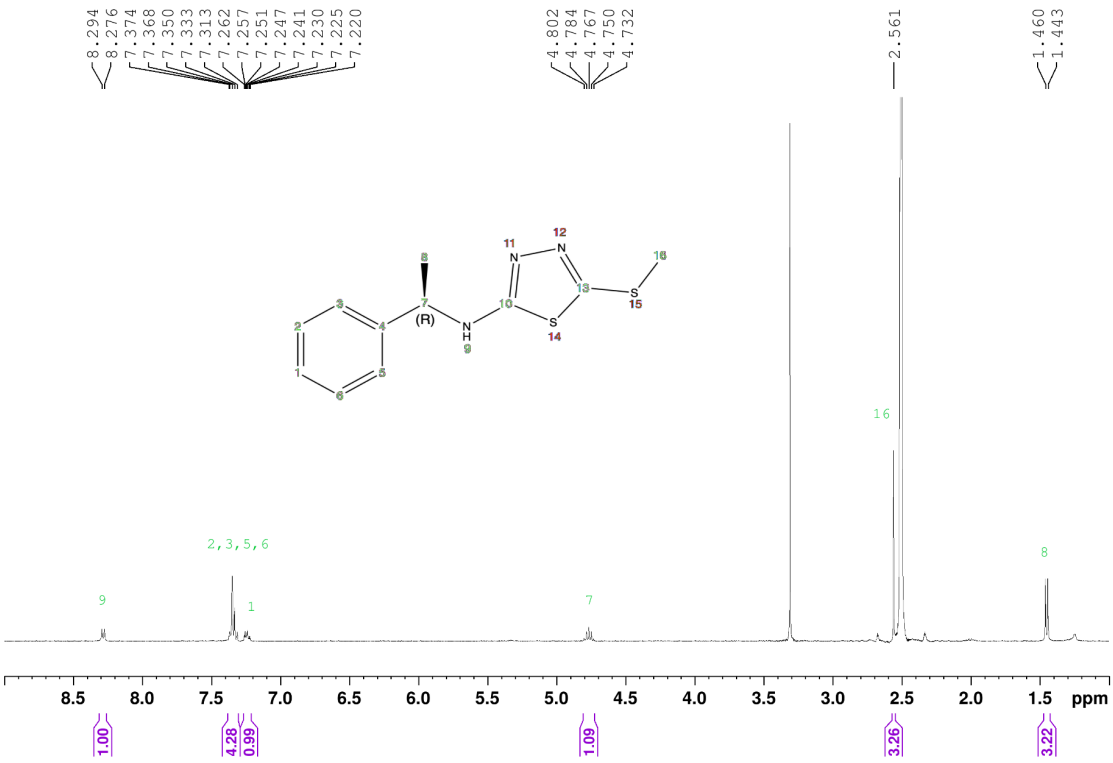


*Spectrum A6. $^{1}H$ NMR of (R)-5-(methylthio)-N-(1-phenylethyl)-1,3,4-thiodiazol-2-amine (**3a**) in DMSO-$d_6$ (some water contamination); with all the peaks assigned to protons in the molecule.*

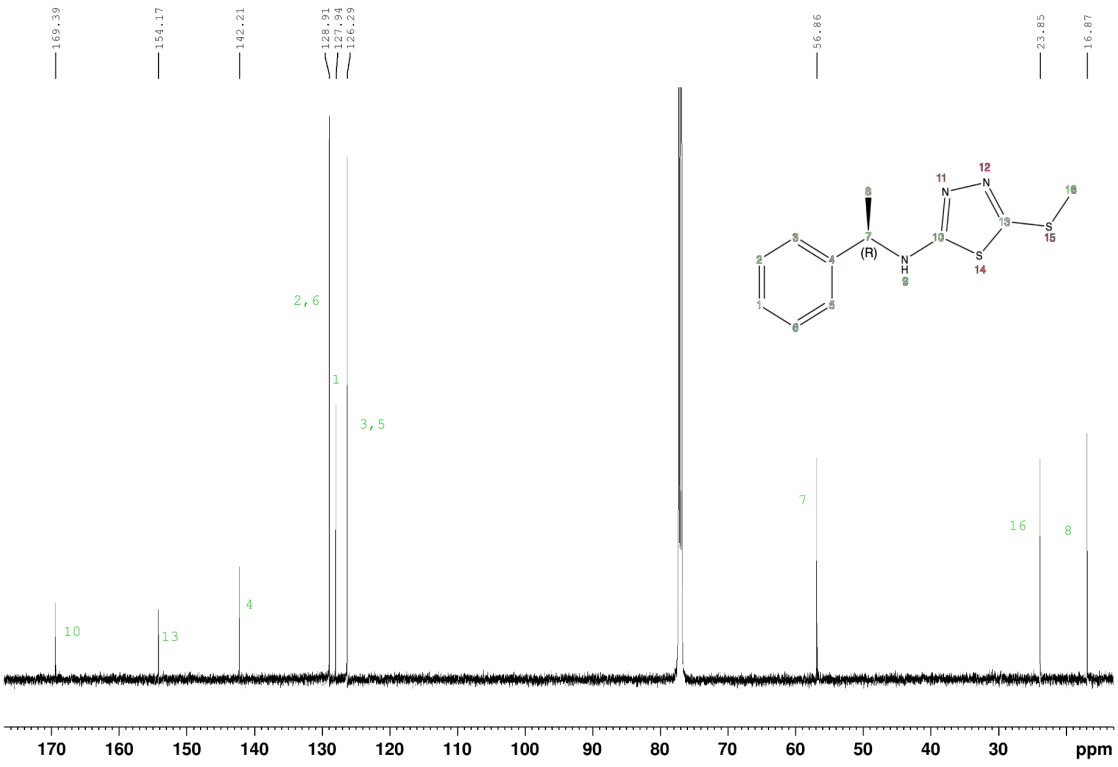


*Spectrum A7. $^{13}C$ NMR of (R)-5-(methylthio)-N-(1-phenylethyl)-1,3,4-thiodiazol-2-amine (**3a**) in $CDCl_3$; with all the peaks assigned to protons in the molecule.*

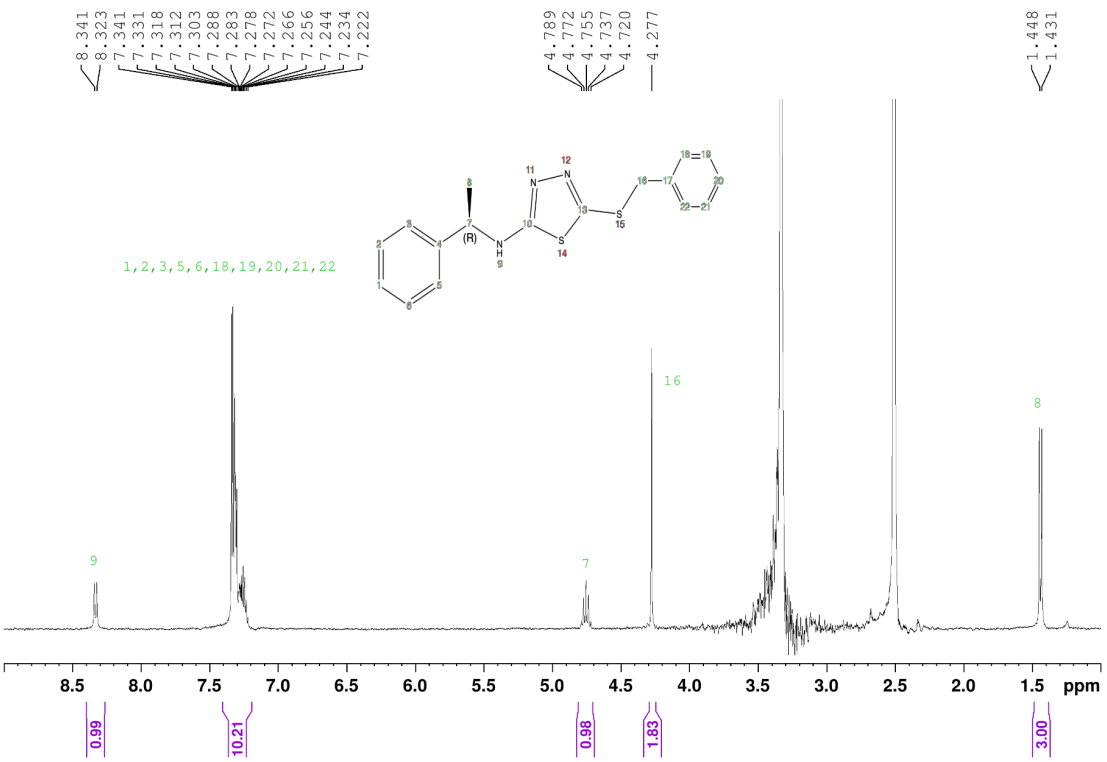


*Spectrum A8. $^{1}H$ NMR of (R)-5-(benzylthio)-N-(1-phenylethyl)-1,3,4-thiodiazol-2-amine (**3b**) in DMSO-$d_6$, (with water contamination from the solvent); with all the peaks assigned to protons in the molecule.*

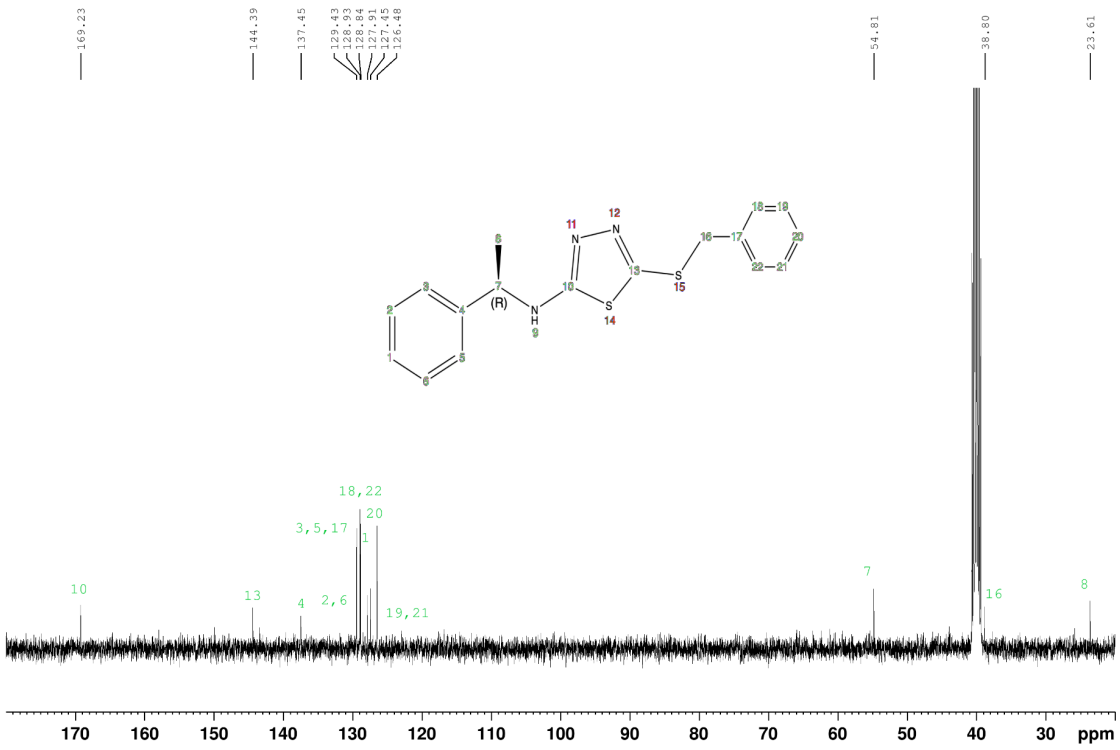


*Spectrum A9. $^{13}C$ NMR of (R)-5-(benzylthio)-N-(1-phenylethyl)-1,3,4-thiodiazol-2-amine (**3b**) in DMSO-$d_6$, (with water contamination from the solvent); with all the peaks assigned to protons in the molecule.*

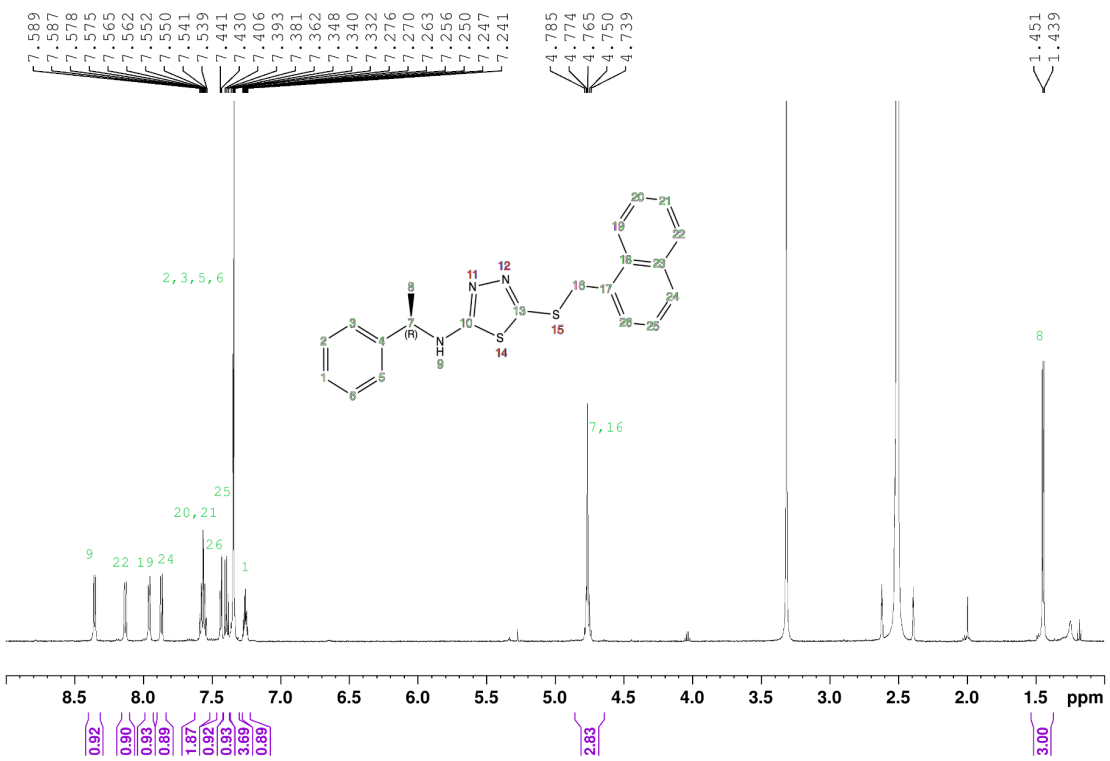


*Spectrum A10. $^{1}$H NMR of (R)-5-((naphthalen-1-ylmethyl)thio)-N-(1-phenylethyl)-1,3,4-thiadiazol-2-amine (**3c**) in DMSO-$d_6$,; with all the peaks assigned to protons in the molecule.*

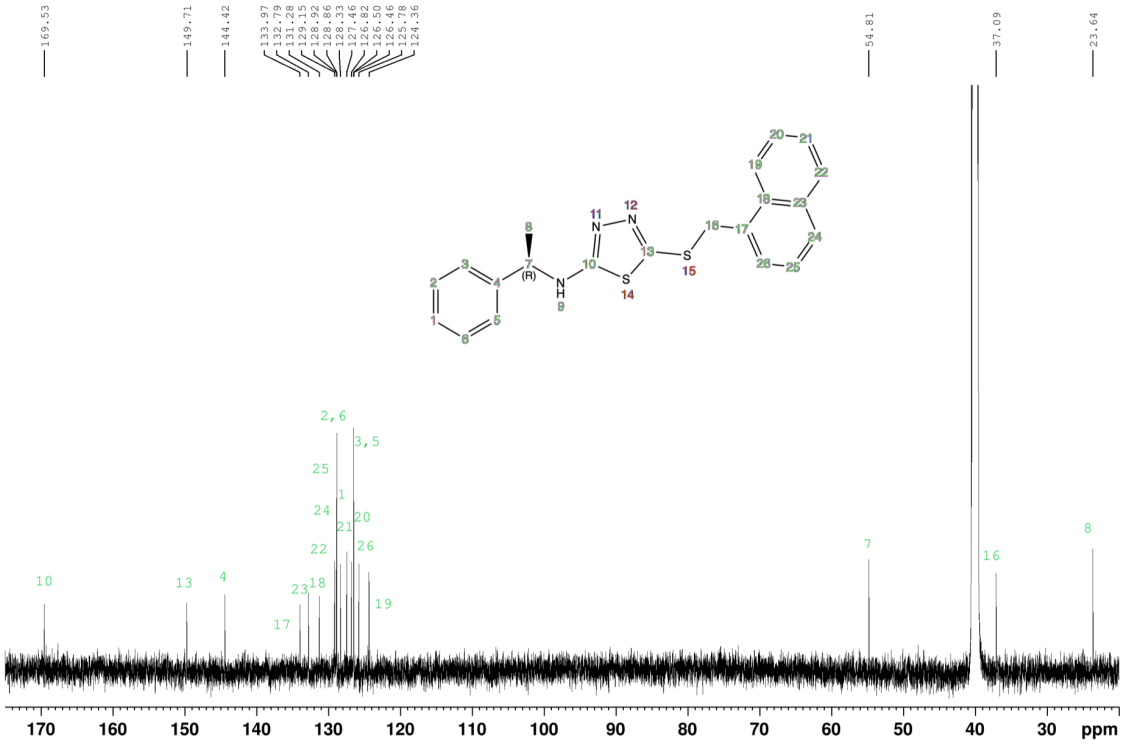


*Spectrum A11. $^{13}$C NMR of (R)-5-((naphthalen-1-ylmethyl)thio)-N-(1-phenylethyl)-1,3,4-thiadiazol-2-amine (**3c**) in DMSO-$d_6$,; with all the peaks assigned to protons in the molecule.*

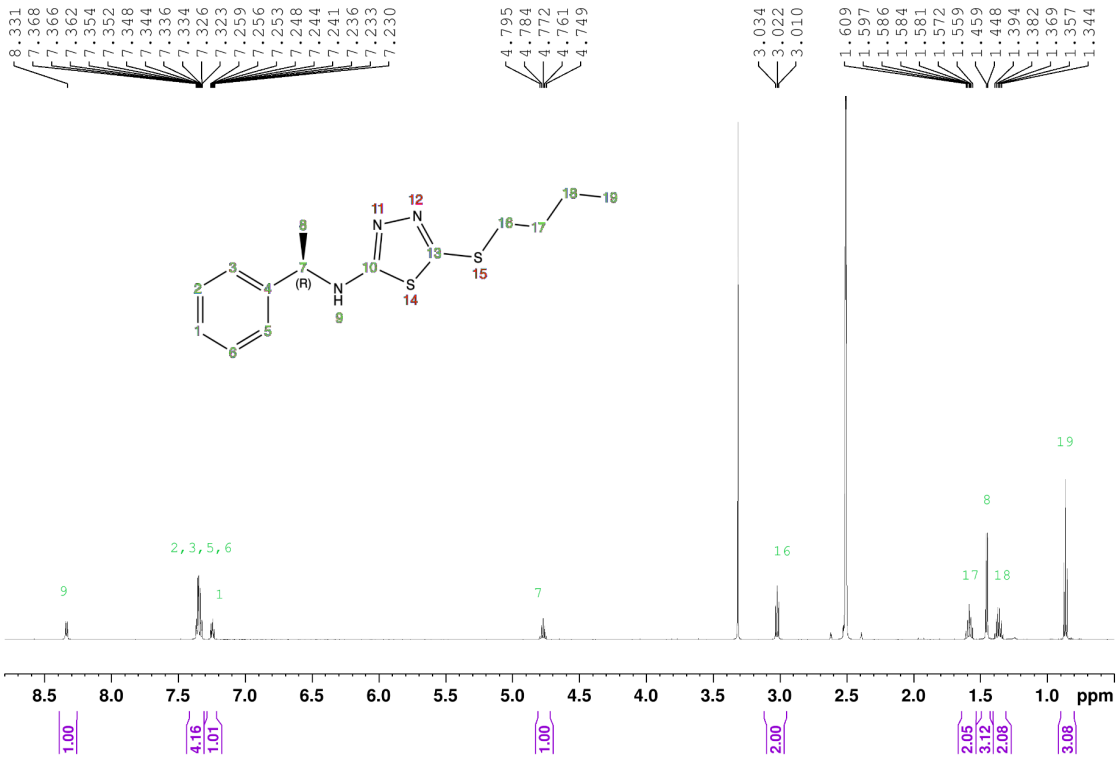


*Spectrum A12. [1]H NMR of (R)-5-(butylthio)-N-(1-phenylethyl)-1,3,4-thiadiazol-2-amine (**3d**) in DMSO-$d_6$,; with all the peaks assigned to protons in the molecule.*

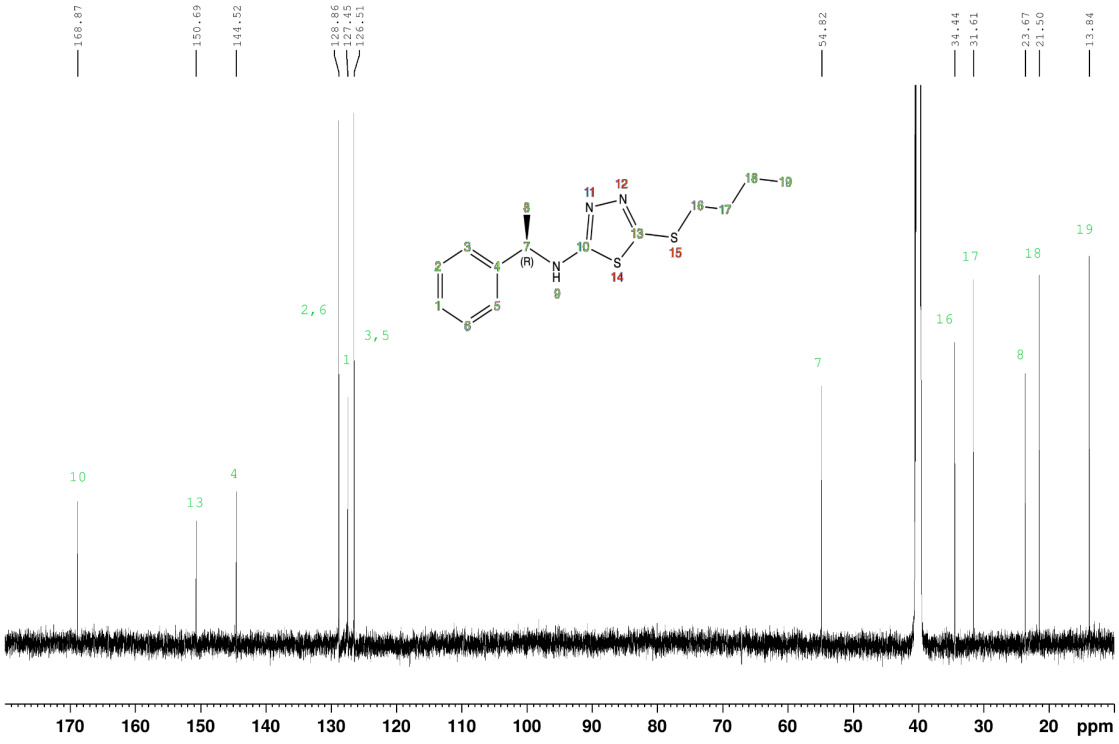


*Spectrum A13.* $^{13}$*C NMR of (R)-5-(butylthio)-N-(1-phenylethyl)-1,3,4-thiadiazol-2-amine (**3d**) in DMSO-*$d_6$*,; with all the peaks assigned to protons in the molecule.*

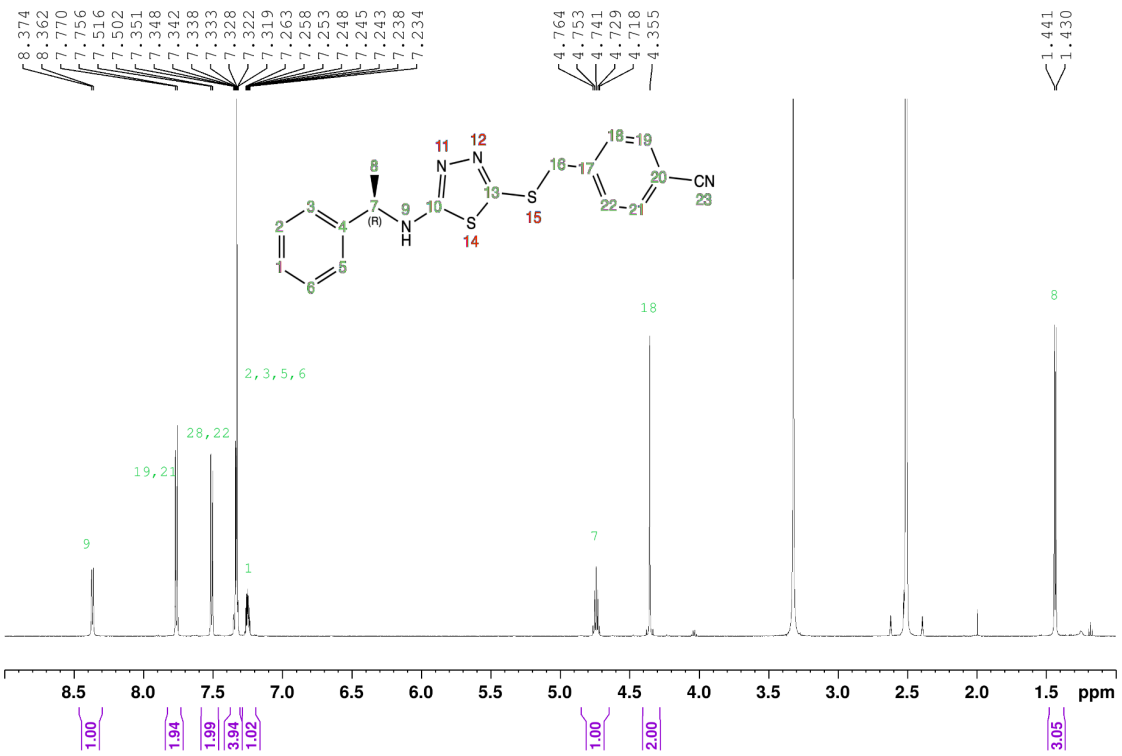


*Spectrum A14. [1]H NMR of (R)-4-(((5-((1-phenylethyl)amino)-1,3,4-thiadiazol-2-yl)thio)methyl)benzonitrile (**3e**) in DMSO-$d_6$,; with all the peaks assigned to protons in the molecule.*

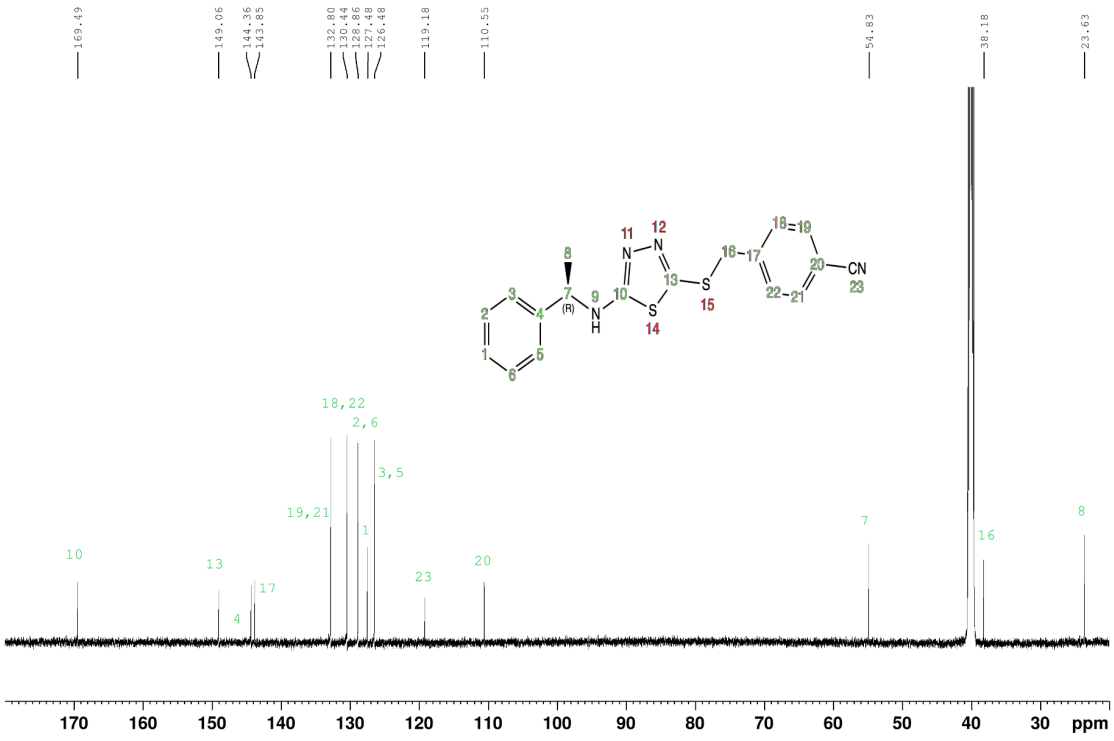


*Spectrum A15.* $^{13}$*C NMR of (R)-4-(((5-((1-phenylethyl)amino)-1,3,4-thiadiazol-2-yl)thio)methyl)benzonitrile (**3e**) in DMSO-*$d_6$*,; with all the peaks assigned to protons in the molecule.*

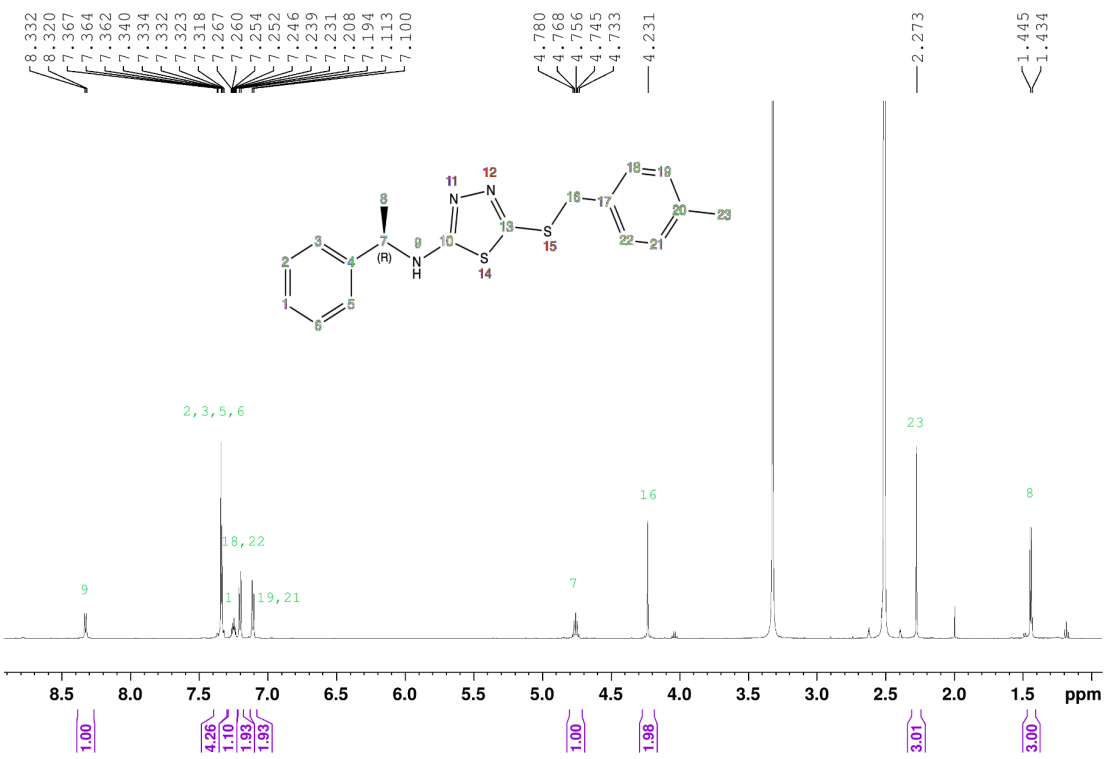


*Spectrum A16. $^{1}$H NMR of (R)-5-((4-methylbenzyl)thio)-N-(1-phenylethyl)-1,3,4-thiadiazol-2-amine (**3f**) in DMSO-$d_6$,; with all the peaks assigned to protons in the molecule.*

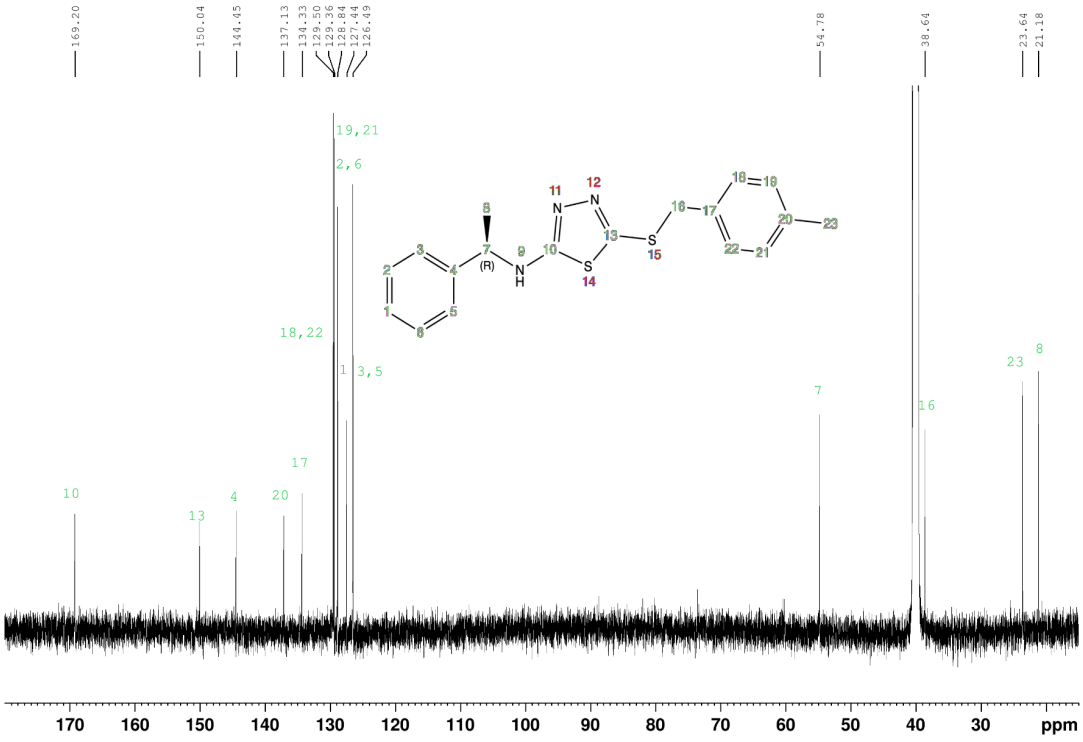


*Spectrum A17. $^{13}C$ NMR of (R)-5-((4-methylbenzyl)thio)-N-(1-phenylethyl)-1,3,4-thiadiazol-2-amine (**3f**) in DMSO-$d_6$; with all the peaks assigned to protons in the molecule.*

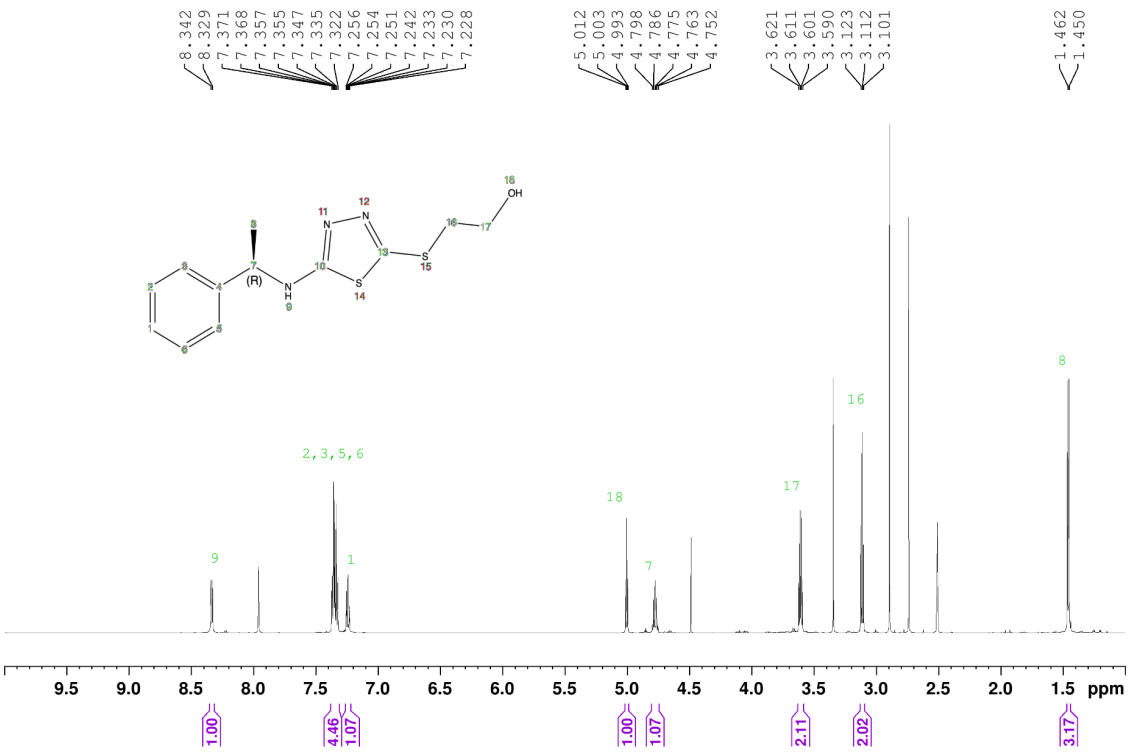


*Spectrum A18. $^{1}H$ NMR of (R)-2-((5-((1-phenylethyl)amino)-1,3,4-thiadiazole-2-yl)thio)ethan-1-ol (**4**) in DMSO-$d_6$, (with some impurities); with all the peaks assigned to protons in the molecule.*


*Spectrum A19. $^{13}C$ NMR of (R)-2-((5-((1-phenylethyl)amino)-1,3,4-thiadiazole-2-yl)thio)ethan-1-ol (**4**) in $CDCl_3$ (with some impurities); with all the peaks assigned to protons in the molecule.*

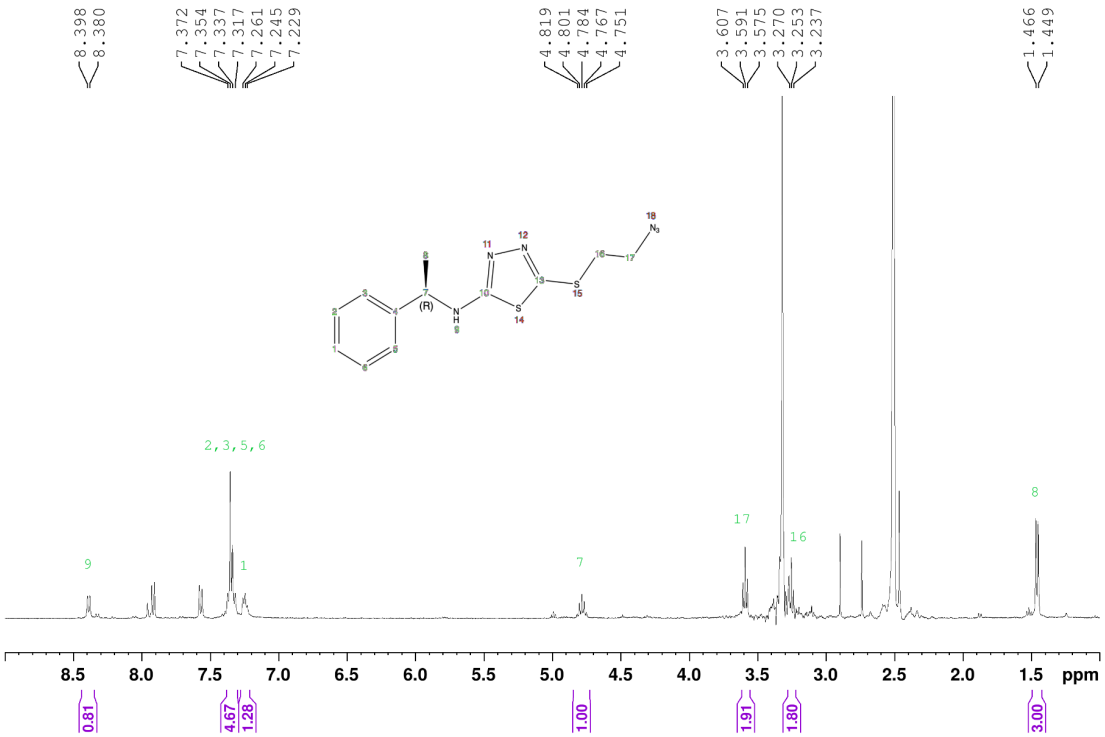


*Spectrum A20. $^{1}H$ NMR of (R)-5-((2-azidoethyl)thio)-N-(1-phenylethyl)-1,3,4-thiadiazol-2-amine (**5**) in DMSO-$d_6$ (some water contamination), (with some impurities (DMF)); with all the peaks assigned to protons in the molecule.*

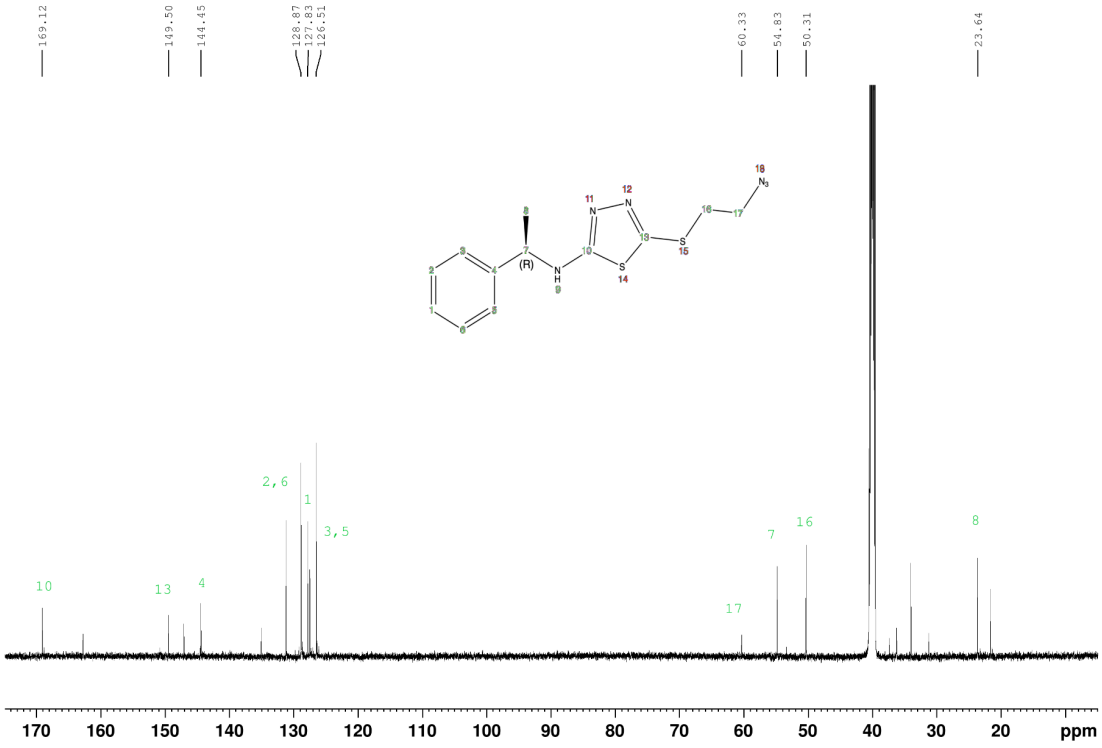


*Spectrum A21. $^{13}C$ NMR of (R)-5-((2-azidoethyl)thio)-N-(1-phenylethyl)-1,3,4-thiadiazol-2-amine (**5**) in DMSO-$d_6$, (with some impurities); with all the peaks assigned to protons in the molecule.*

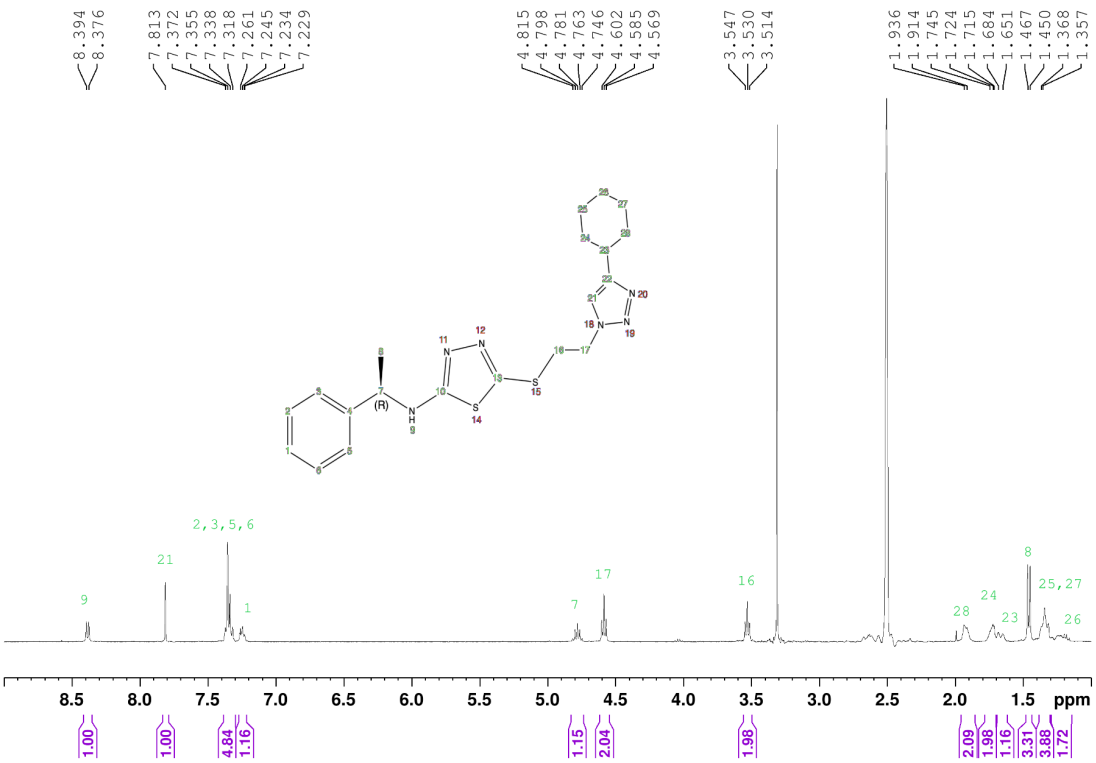


*Spectrum A22. $^{1}H$ NMR of*

*(R)-5-((2-(4-(cyclohexylmethyl)-1H-1,2,3-triazol-1-yl)ethyl)thio)-N-(1-phenylethyl)-1,3,4-thiadiazol-2-amine (**6a**) in DMSO-$d_6$ (some water contamination); with all the peaks assigned to protons in the molecule.*

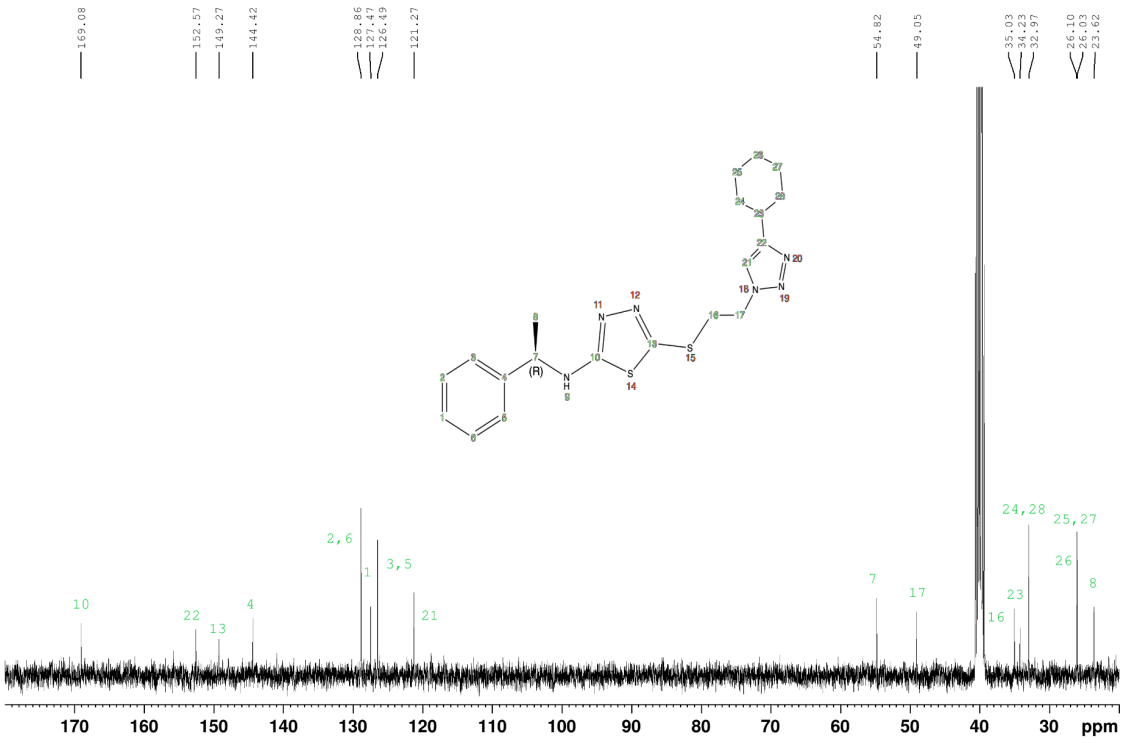


*Spectrum A23.* $^{13}$*C NMR of (R)-5-((2-(4-(cyclohexylmethyl)-1H-1,2,3-triazol-1-yl)ethyl)thio)-N-(1-phenylethyl)-1,3,4-thiadiazol-2-amine (**6a**) in DMSO-$d_6$,; with all the peaks assigned to protons in the molecule.*

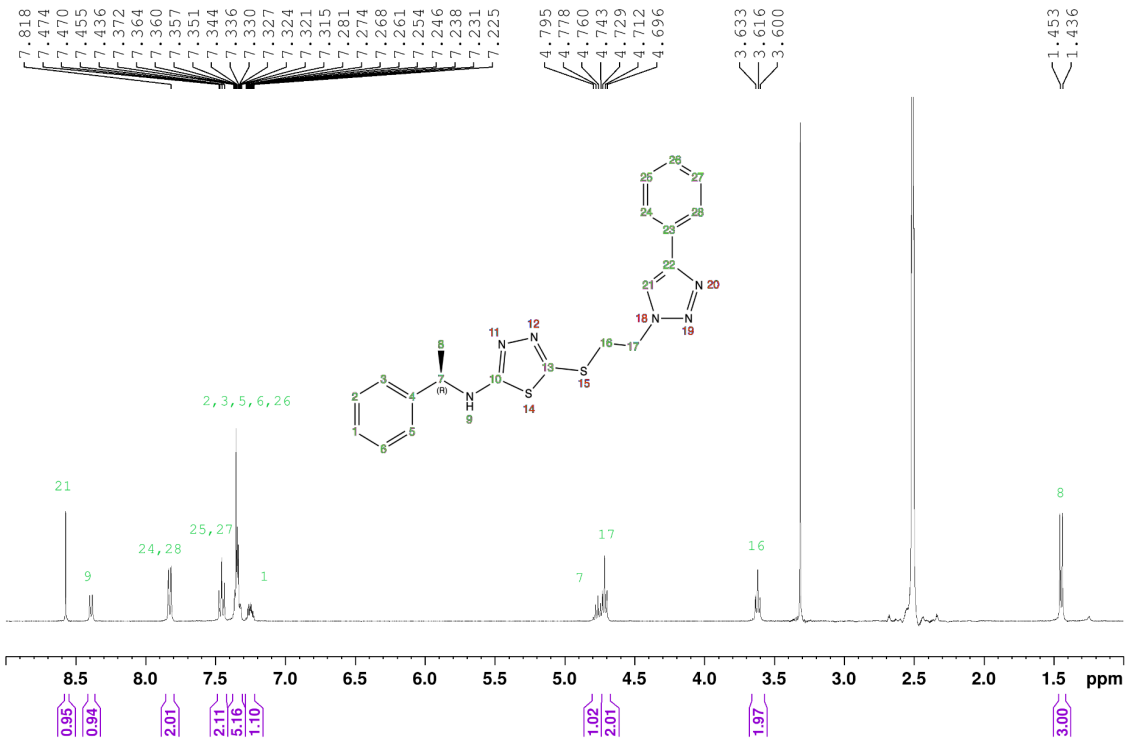


*Spectrum A24. $^{1}H$ NMR of (R)-5-((2-(4-phenyl-1H-1,2,3-triazol-1-yl)ethyl)thio)-N-(1-phenylethyl)-1,3,4-thiadiazol-2-amine (**6b**) in DMSO-$d_6$ (some water contamination); with all the peaks assigned to protons in the molecule.*

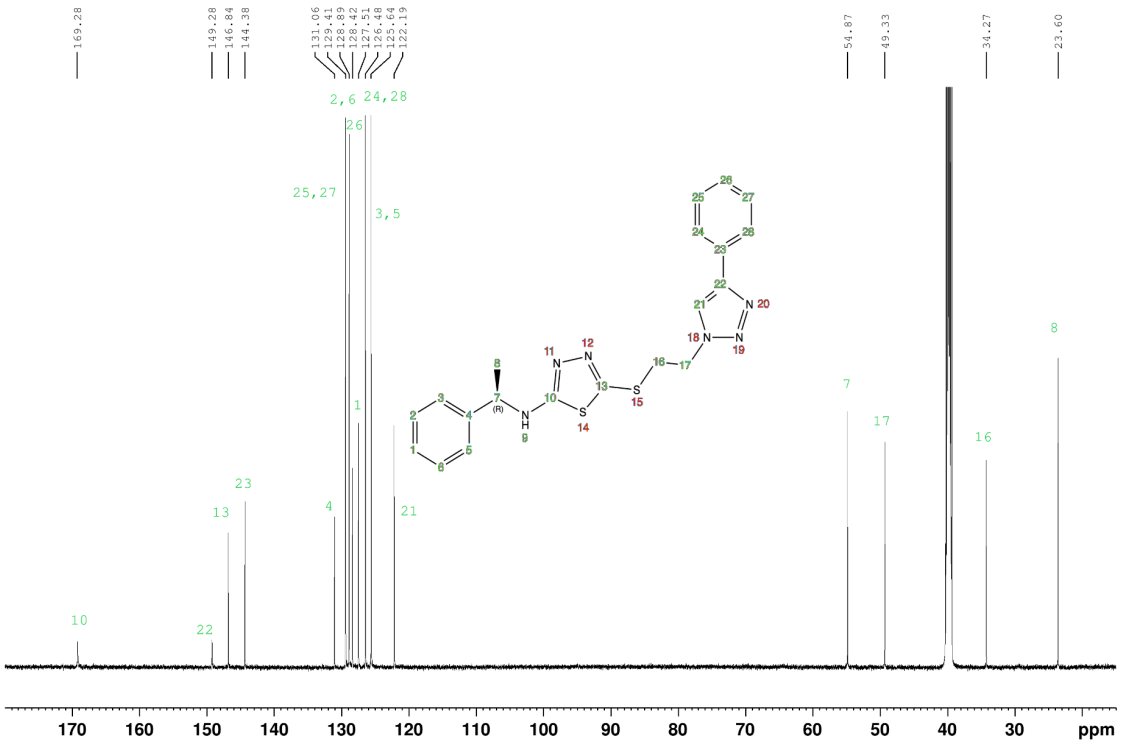


*Spectrum A25.* $^{13}$*C NMR of (R)-5-((2-(4-phenyl-1H-1,2,3-triazol-1-yl)ethyl)thio)-N-(1-phenylethyl)-1,3,4-thiadiazol-2-amine (**6b**) in DMSO-*$d_6$*,; with all the peaks assigned to protons in the molecule.*

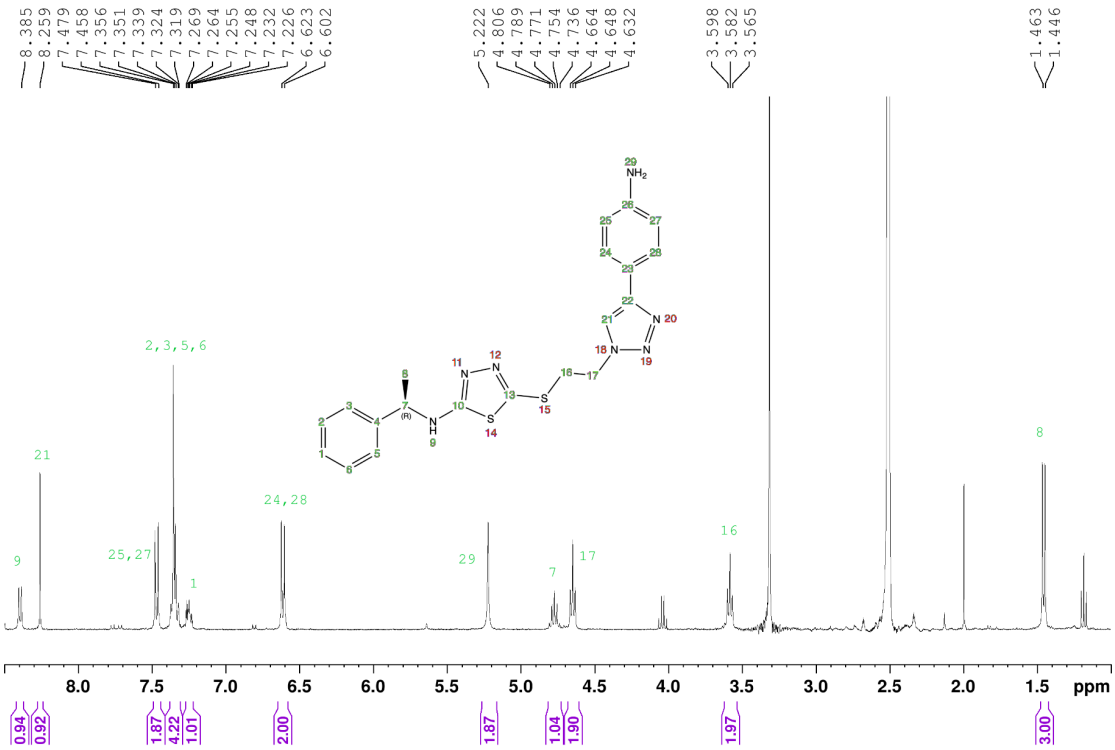


*Spectrum A26. $^{1}H$ NMR of (R)-5-((2-(4-(4-aminophenyl)-1H-1,2,3-triazol-1-yl)ethyl)thio)-N-(1-phenylethyl)-1,3,4-thiadiazol-2-amine (**6c**) in DMSO-$d_6$ (some water contamination) with some EtOAc contamination that was later evaporated; with all the peaks assigned to protons in the molecule.*

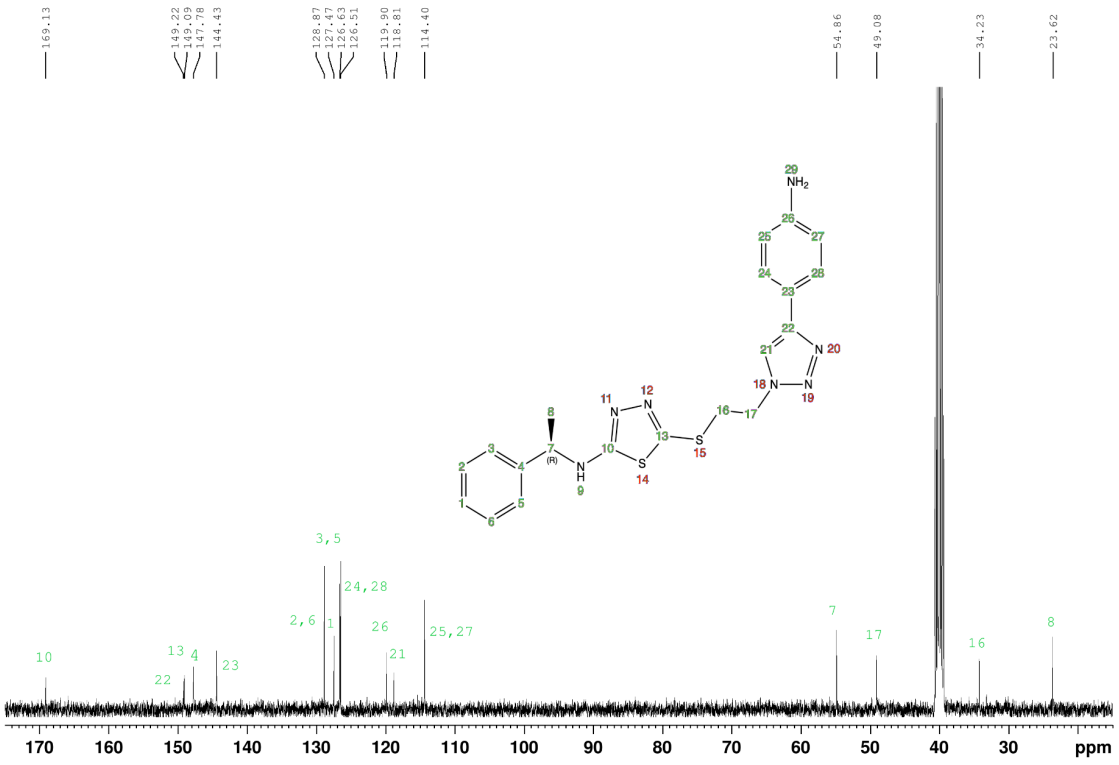


*Spectrum A27.* $^{13}$*C NMR of*
*(R)-5-((2-(4-(4-aminophenyl)-1H-1,2,3-triazol-1-yl)ethyl)thio)-N-(1-phenylethyl)-1,3,4-thiadiazol-2-amine* ***(6c)*** *in DMSO-d$_6$,; with all the peaks assigned to protons in the molecule.*

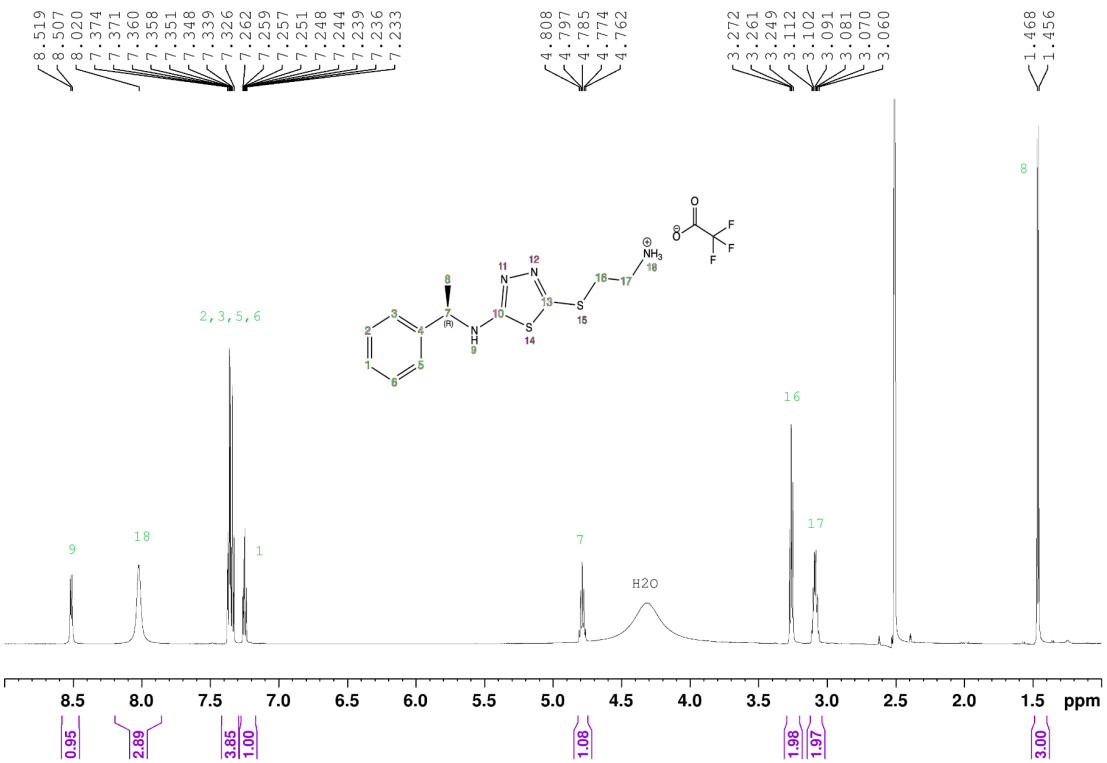


*Spectrum A28. [1]H NMR of (R)-5-((2-aminoethyl)thio)-N-(1-phenylethyl)-1,3,4-thiadiazol-2-amine as a TFA salt (**7**) in DMSO-$d_6$,; with water, with all the peaks assigned to protons in the molecule.*

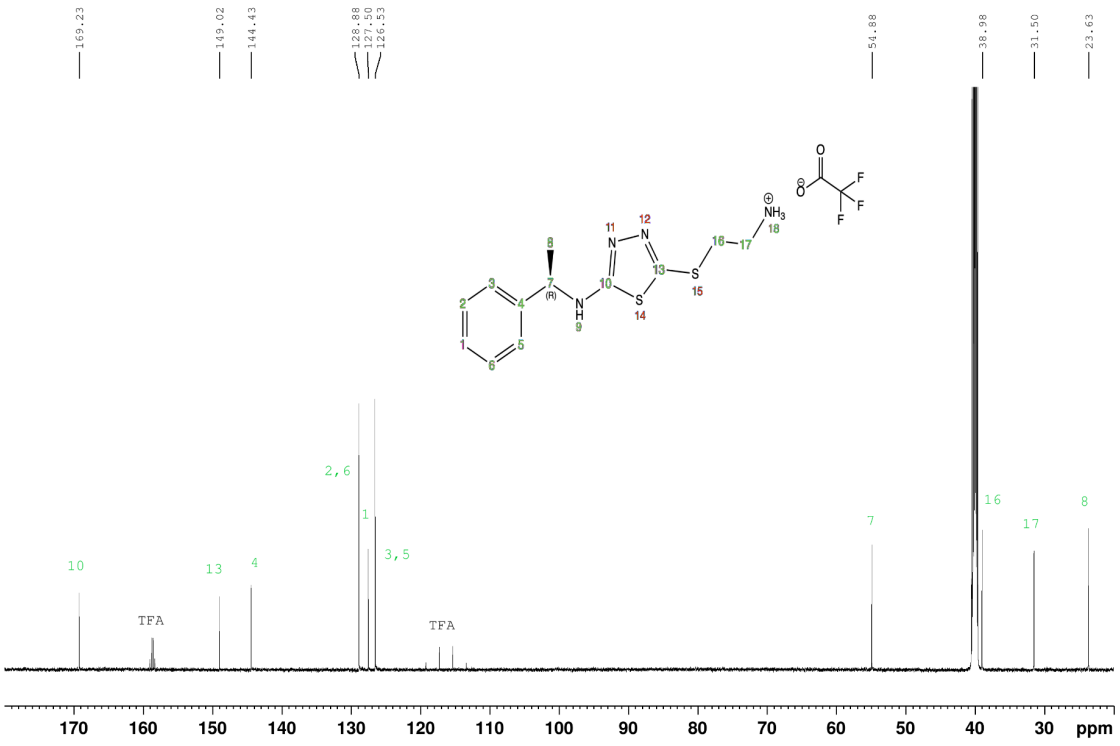


*Spectrum A29. $^{13}$C NMR of (R)-5-((2-aminoethyl)thio)-N-(1-phenylethyl)-1,3,4-thiadiazol-2-amine as a TFA salt (7) in DMSO-$d_6$,; with all the peaks assigned to protons in the molecule.*

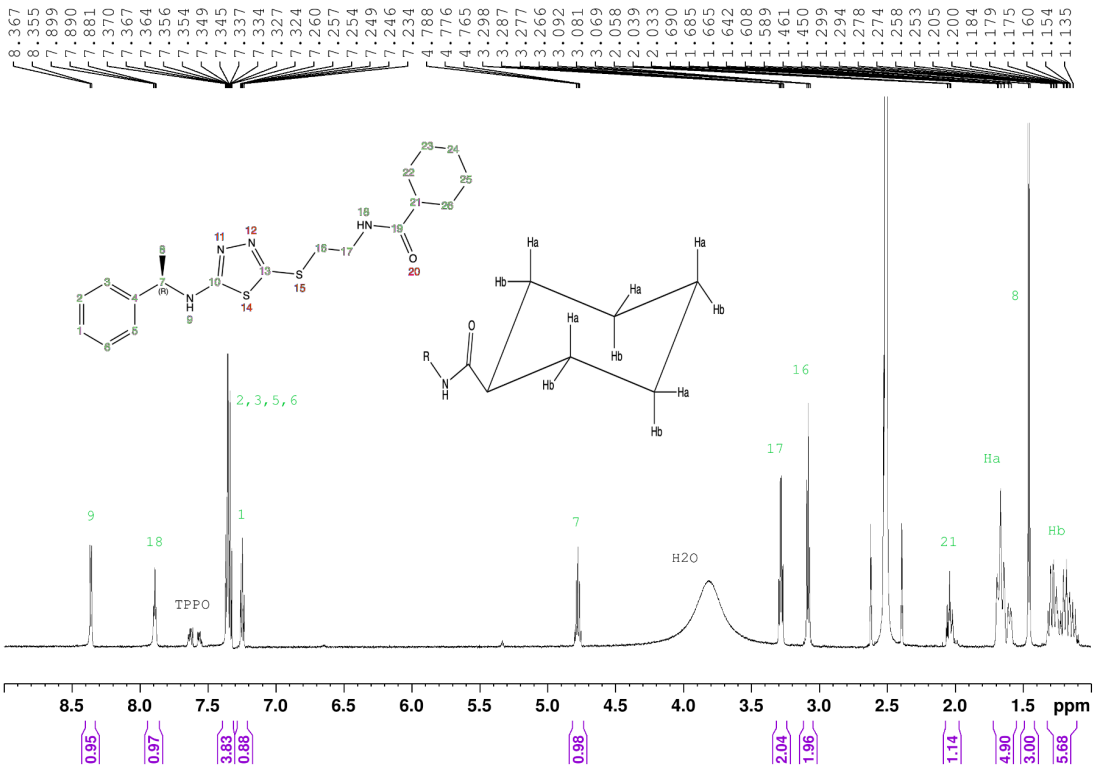


*Spectrum A30.* $^{1}$*H NMR of (R)-N-(2-((5-((1-phenylethyl)amino)-1,3,4-thiadiazol-2-yl)thio)ethyl)cyclohexanecarboxamide (**8a**) in DMSO-*$d_6$*,; with all the peaks assigned to protons in the molecule.*

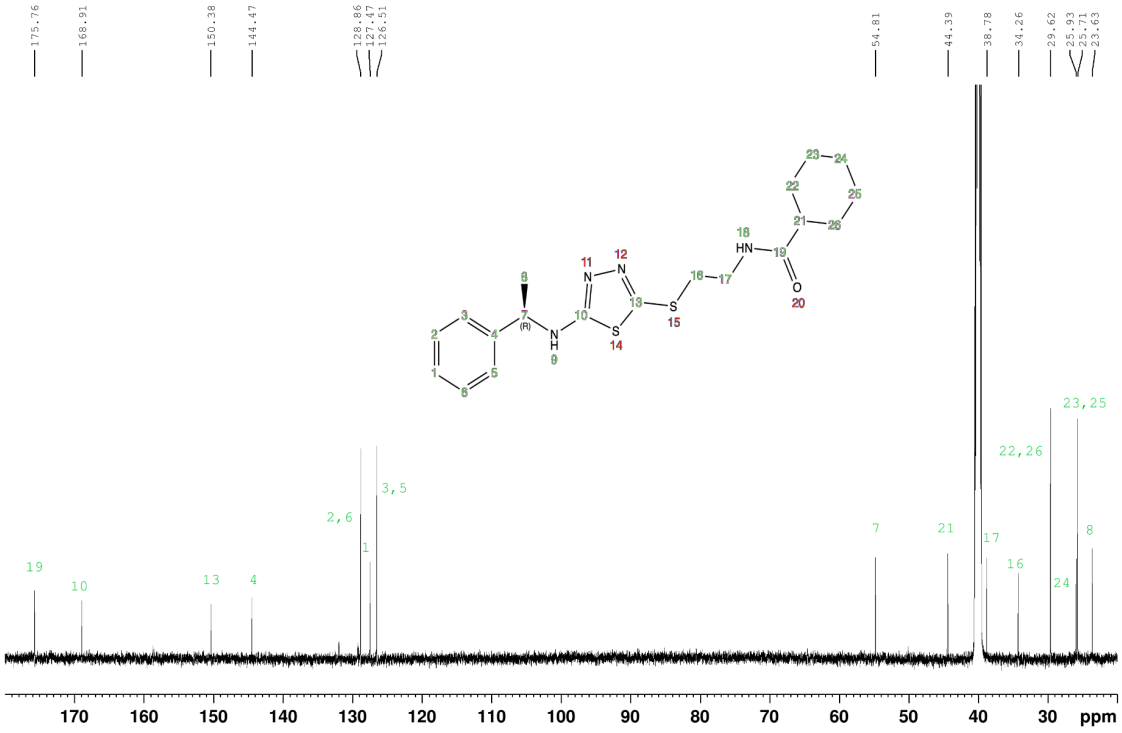


*Spectrum A31.* $^{13}$*C NMR of (R)-N-(2-((5-((1-phenylethyl)amino)-1,3,4-thiadiazol-2-yl)thio)ethyl)cyclohexanecarboxamide* ***(8a)*** *in DMSO-*$d_6$*;; with all the peaks assigned to protons in the molecule.*

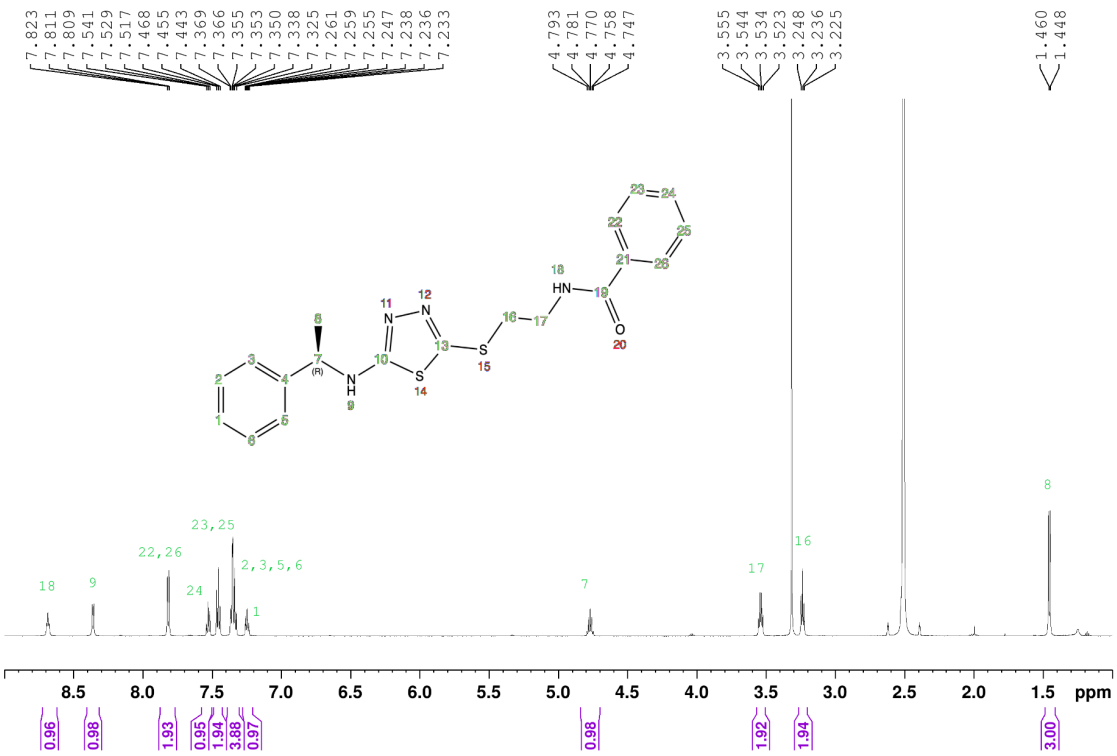


*Spectrum A32. [1]H NMR of (R)-N-(2-((5-((1-phenylethyl)amino)-1,3,4-thiadiazol-2-yl)thio)ethyl)benzamide (**8b**) in DMSO-$d_6$,; with all the peaks assigned to protons in the molecule.*

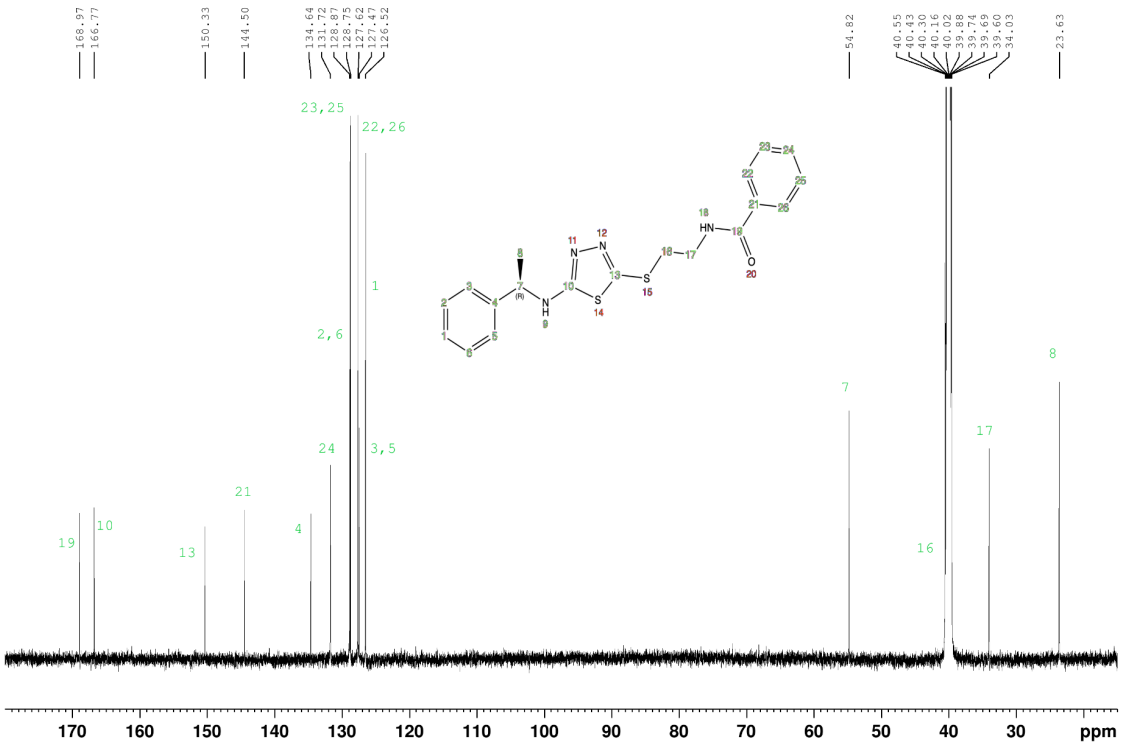


*Spectrum A33.* $^{13}$*C NMR of (R)-N-(2-((5-((1-phenylethyl)amino)-1,3,4-thiadiazol-2-yl)thio)ethyl)benzamide* ***(8b)*** *in DMSO-*$d_6$*,; with all the peaks assigned to protons in the molecule.*

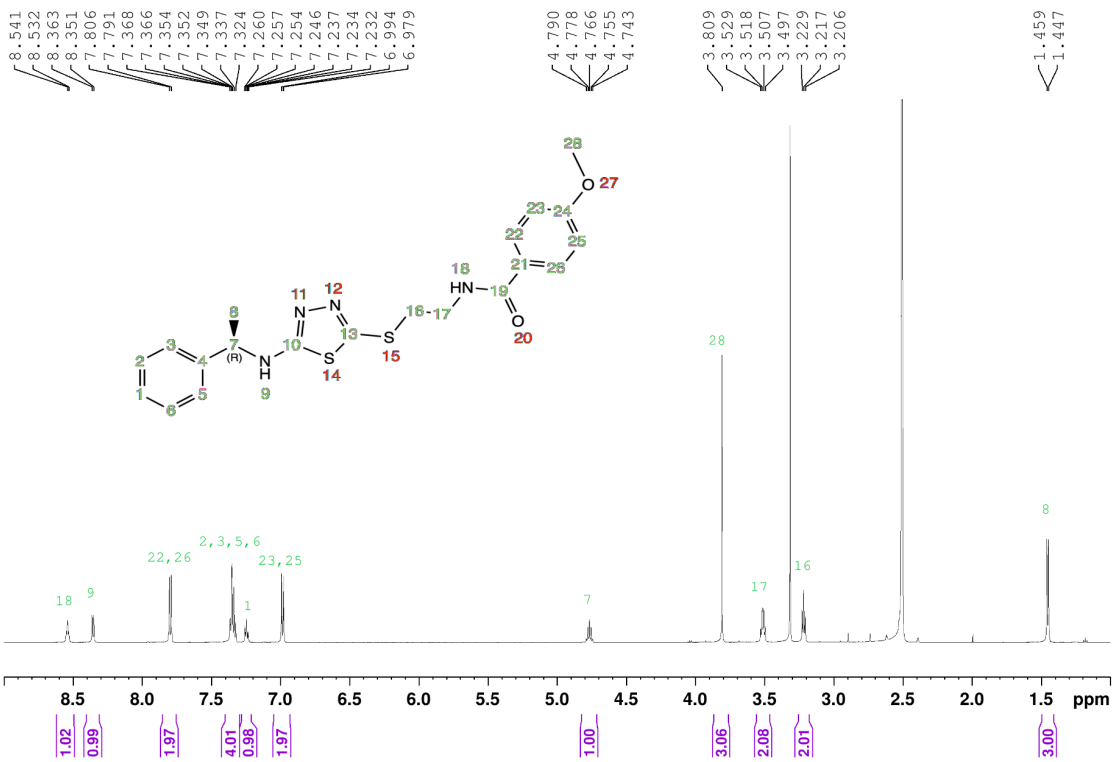


*Spectrum A34.* [1]*H NMR of (R)-4-methoxy-N-(2-((5-((1-phenylethyl)amino)-1,3,4-thiadiazol-2-yl)thio)ethyl)benzamide* ***(8c)*** *in DMSO-*$d_6$*,; with all the peaks assigned to protons in the molecule.*

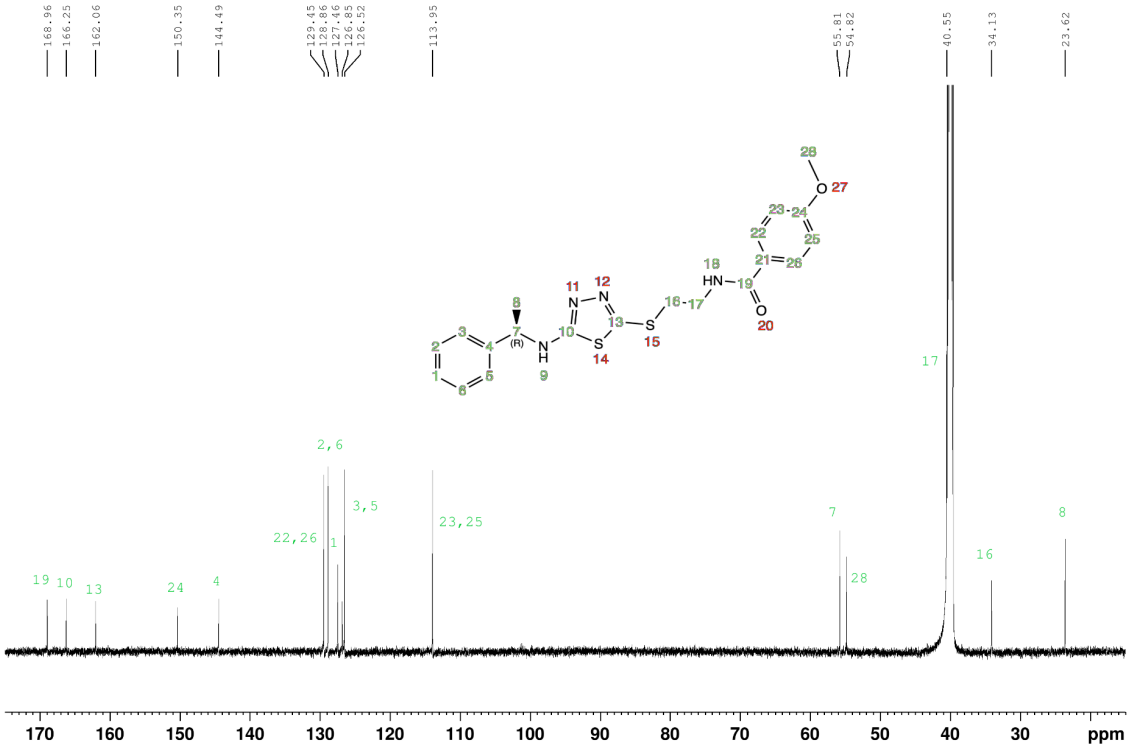


*Spectrum A35.* $^{13}$*C NMR of (R)-4-methoxy-N-(2-((5-((1-phenylethyl)amino)-1,3,4-thiadiazol-2-yl)thio)ethyl)benzamide (**8c**) in DMSO-$d_6$;; with all the peaks assigned to protons in the molecule.*